Sustainable bio-production of the platform chemical *cis,cis*-muconic acid using metabolically engineered *Amycolatopsis sp.* ATCC 39116

Dissertation

zur Erlangung des Grades

der Doktorin der Naturwissenschaften

der Naturwissenschaftlich-Technischen Fakultät

der Universität des Saarlandes

von

Nadja Barton

Saarbrücken

2024

Tag des Kolloquiums:	26.05.2025
Dekan:	Prof. Dr.-Ing. Dirk Bähre
Berichterstatter:	Prof. Dr. Christoph Wittmann Prof. Dr. Andriy Luzhetskyy
Akad. Mitglied:	Dr. Frank Hannemann
Vorsitz:	Prof. Dr. Uli Kazmaier

Publications

This work has already been partially published. It was approved by the Institute of Systems Biotechnology represented by Prof. Dr. Christoph Wittmann.

Peer-reviewed articles

Barton N, Horbal L, Starck S, Kohlstedt M, Luzhetskyy A, Wittmann C (2017) Enabling the valorization of guaiacol-based lignin: Integrated chemical and biochemical production of cis,cis-muconic acid using metabolically engineered Amycolatopsis sp ATCC 39116. *Metab Eng* 45: 200-210

Kohlstedt M, Starck S, **Barton N**, Stolzenberger J, Selzer M, Mehlmann K, Schneider R, Pleissner D, Rinkel J, Dickschat JS *et al* (2018) From lignin to nylon: Cascaded chemical and biochemical conversion using metabolically engineered Pseudomonas putida. *Metab Eng* 47: 279-293

van Duuren J, de Wild PJ, Starck S, Bradtmöller C, Selzer M, Mehlmann K, Schneider R, Kohlstedt M, Poblete-Castro I, Stolzenberger J, **Barton N,** *et al* (2020) Limited life cycle and cost assessment for the bioconversion of lignin-derived aromatics into adipic acid. *Biotechnol Bioeng* 117: 1381-1393

Weiland F, **Barton N**, Kohlstedt M, Becker J, Wittmann C (2023) Systems metabolic engineering upgrades Corynebacterium glutamicum to high-efficiency cis, cis-muconic acid production from lignin-based aromatics. *Metab Eng* 75: 153-169

Patent Applications

Wittmann C, Van Duuren J, Kohlstedt M, Stolzenberger J, Starck S, **Barton N**, Selzer M, Fritz M, De Wild P, Kuhl M, Becker J. (2020) Means and methods for lignin pyrolysis. Application No./Patent No. 16/492,476

Conference contributions

Barton N, Horbal L, Starck S, Luzhetskyy A, Wittmann C (2018, 15-18. April) Enabling the valorization of guaiacol-based lignin: Integrated chemical and biochemical production of cis,cis-muconic acid using metabolically engineered *Amycolatopsis sp.* ATCC 39116. Annual Conference of the Association for General and Applied Microbiology, Wolfsburg, Germany.

Barton N, Horbal L, Starck S, Luzhetskyy A, Wittmann C (2018, 24-28. June) Enabling the valorization of guaiacol-based lignin: Integrated chemical and biochemical production of cis,cis-muconic acid using metabolically engineered *Amycolatopsis sp.* ATCC 39116. Metabolic Engineering 12, München, Germany.

External contribution

Parts of this work were carried out by technical assistant Mirjam Selzer and the bachelor student Bianca Stephan under my supervision.
The plasmids Sset_PL13, Sset_PL20 were constructed by Mirjam Selzer, who also was involved in the conjugation to create *Amycolatopsis sp.* ATCC 39116 MA-5.
Bianca Stephan carried out cultivation experiments with *Amycolatopsis sp.* ATCC 39116 MA-2 and MA-5 using vanillate and vanillin as substrate for MA production. Furthermore, she cultivated *Amycolatopsis sp*. ATCC 39116 on agar plates, containing different sugars as sole C-source. Her work was published in the bachelor thesis "Fermentative Produktion von *cis,cis*-Muconsäure aus Vanillinsäure mithilfe von *Amycolatopsis sp.*".
Hydrothermal conversion was conducted by Sören Starck (Starck, 2020). He published this method in his doctor's thesis "Microbial production of *cis,cis*-muconic acid from hydrothermally converted lignocellulose" and provided the lignin hydrolysate and the xylose from hemicellulose (Starck, 2020).
The genetic engineering approach was developed in cooperation with Liliya Horbal from the institute of Pharmaceutical Biotechnology, Saarland University represented by Prof. Dr. Andriy Luzhetskyy.
This work was financially supported by the Bundesministerium für Bildung und Forschung (BMBF) as part of the funding programs "BioNylon" (FKZ 03V0757) and "LignoValue" (FKZ 031B0344A).

Danksagung

Allem voran gebührt mein Dank Herrn Prof. Dr. Christoph Wittmann, der mich ermutigt hat dieses Abenteuer zu wagen. Dein Vertrauen, die Ratschläge, deine Geduld und deine stets für mich offene Bürotür haben mir geholfen, durchzuhalten und mich über mich selbst hinauswachsen zu lassen. Vielen Dank und ich weiß alles wird gut!

Bei Prof. Dr. Andriy Luzhetskyy und Liliya Horbal möchte ich mich für die gelungene Zusammenarbeit bedanken, die eine effiziente genetische Veränderung von *Amycolatopsis sp.* ATCC 39116 ermöglich hat. Die Zeit bei euch hat mein molekularbiologisches Arbeiten nachhaltig geprägt.

Ganz besonders gilt mein Dank dem Bio2Nylon-Team! Sören Starck, Mirjam Selzer, Jessica Stolzenberger, Michael Kohlstedt und Joost van Duuren es war mir eine Ehre. Michel Fritz und Susanne Haßdenteutel auf euch ist immer Verlass gewesen. Vielen Dank für eure Hilfsbereitschaft und die vielen tollen Gespräche.

Auch meine Kollegen am Institut für Systembiotechnologie haben maßgeblich dazu beigetragen, dass diese Arbeit nun so vorliegt. Vielen Dank, dass ihr mich so freundlich aufgenommen habt, für die lustigen Grillabende und für gemeinsam durchwachte Nächte. Vielen Dank liebe Sarah Lisa Hoffmann für das gemeinsame Englischtraining, die besondere Zeit in China und deine lustigen Lebensgeschichten. Bei meinen Bürokolleg*innen Gideon Gießelmann, Johnathan Fabarius, Sören Starck, Susanne Schwechheimer, Muzi Tangyu und Julian Stegmüller möchte ich mich herzlich für die vielen lustigen Stunden und das ein oder andere Schokobon bedanken. Ohne euch wären die ganzen Nachtschichten unerträglich gewesen.

Nicht zuletzt gebührt mein Dank meinen Eltern und meiner Schwester. Danke, dass ihr mich bei all meinen Entscheidungen unterstützt habt und nie an mir gezweifelt habt. Danke für eure Ehrlichkeit, Hilfsbereitschaft und unseren familiären Zusammenhalt. Ohne Euch hätte ich es nicht geschafft.

Lieber Erik, ich bedanke mich für deinen Rückhalt und dafür, dass du während der langen Zeit vor allem emotional immer für mich da warst. Danke, dass du alles stehen und liegen lassen hast, um mir ins Saarland zu folgen und mich bei dem verrückten Projekt „Kind und Karriere“ unterstützt hast. Danke, dass du für uns immer ein gemeinsames Hobby suchst und es deshalb nie langweilig in unserer Ehe wird.

Table of Contents

I. Abbreviations

A. baylyi	*Acinetobacter baylyi*
apr	Apramycin
DS	Downstream
E. coli	*Escherichia coli*
g	Gravity of Earth
GC	guanine-cytosine
GC-MS	Gas Chromatography-Mass Spectrometry
Gt C	Gigatons of carbon
GusA	β-Glucuronidase
HPLC	High-Performance-Liquid-Chromatography
HTC	Hydrothermal Conversion
hyg	hygromycin
kan	kanamycin
LB	Luria-Bertani
MA	*cis,cis*-Muconic acid
Man	Mannose
mM	mmol L^{-1}
n=3	Data reflect mean values and deviations from three replicates
nal	Nalidixic acid
OD	Optical Density
PCR	polymerase chain reaction
PET	Polyethylene terephthalate
P. putida	*Pseudomonas putida*
pH	Hydrogen in concentration
rpm	Revolutions per Minute
sp.	Species
US	Upstream
USA	United States of America
X-Gluc	5-bromo-4-chloro-3-indolyl-beta-D-glucuronic acid
5-HMF	5-Hydroxymethylfurfural

II. Figure index

III. Table index

Summary

The industrial utilization of lignocellulosic biomass encompasses not only virgin plants but also waste products such as lignin from the pulp and paper industry. This work investigated the use of *Amycolatopsis sp.* ATCC 39116 for the production of *cis,cis*-muconic acid (MA), an industrial precursor for commercial plastics, from lignin-derived aromatics such as guaiacol, vanillin, and vanillate. Initially, genome editing approaches were developed to create efficient cell factories lacking muconate cycloisomerase (*catB*) genes to enable MA accumulation. The resulting strain, *Amycolatopsis sp*. ATCC 39116 MA-2, produced 3.1 g L^{-1} MA from guaiacol within 24 hours, and it was capable of producing MA from a guaiacol-rich lignin hydrolysate. Furthermore, the mutant produced MA from vanillin and vanillate, important aromatics obtained by alkaline oxidation of softwood lignin. A total of 3.2 g L^{-1} MA was produced sugar-free from vanillate, which served as substrate for growth and production. The organism was further engineered to produce MA from protocatechuate using protocatechuate decarboxylase (AroY). Finally, the ability of *Amycolatopsis sp.* ATCC 39116 to grow on lignocellulosic materials, such as xylose from hemicellulose and spent sulfite liquor, was investigated. This study provides a crucial proof-of-concept for the integrated chemical and biochemical production of MA using lignocellulosic-derived waste streams.

Zusammenfassung

Die industrielle Nutzung von Lignocellulose-basierten Materialien, wie z.B. Lignin, einem Abfallprodukt aus der Papierindustrie, ermöglicht eine nachhaltige und kostengünstige Produktion von Plattformchemikalien. In dieser Arbeit wurde gezeigt, dass *cis,cis*-Mukonsäure (MA), ein industrielles Vorprodukt für kommerzielle Kunststoffe, aus Guajakol-haltigen Lignin-Hydrolysaten gewonnen werden kann. Mithilfe neu entwickelter molekularbiologischer Methoden wurden hierfür zwei putative Mukonsäure-Cycloisomerasengene (*cat*A) aus dem Genom von *Amycolatopsis sp*. ATCC 39116 entfernt. Der daraus resultierende Stamm MA-2 produzierte innerhalb von 24 Stunden 3,1 g L^{-1} MA aus Guajakol. Darüber hinaus wurde gezeigt, dass MA auch aus Vanillin und Vanillat, die ebenfalls aus Lignin gewonnen werden können, hergestellt werden kann. Insgesamt wurden 3,2 g L^{-1} MA aus Vanillat produziert. Durch die genomische Integration der Protocatechuat-Decarboxylase (AroY) in das Genom der Mutante MA-2, war es außerdem möglich, MA aus Protocatechuat zu produzieren. Schließlich wurde die Fähigkeit des Stamms untersucht, auf Materialien wie Hemizellulose-Hydrolysaten und zuckerhaltigen Abfallströmen aus der Papierindustrie wachsen zu können. Diese Arbeit leistet einen wichtigen Beitrag zur integrierten chemischen und biochemischen Produktion von MA unter Verwendung von lignocellulosebasierten Abfallströmen und neu entwickelten Zellfabriken.

1 Introduction

Currently, the use of lignocellulosic biomass as a raw material for chemical production is gaining increasing importance (Arevalo-Gallegos et al., 2017). This approach offers a sustainable alternative to fossil resources, as it is environmentally friendly, CO_2-neutral, renewable, and does not compete with the food industry (Schutyser et al., 2018). Lignocellulosic biomass includes not only virgin plants but also agricultural, forestry, and industrial wastes, presenting an opportunity to repurpose existing lignocellulose-dependent processes, such as paper production, as sources of raw materials (Soni et al., 2018). Lignocellulose primarily consists of lignin, cellulose, and hemicellulose (Vyas et al., 2018b). The main aim of pulping is to delignify the wood while preserving the cellulose and hemicellulose fractions (Gullichsen et al., 1999). Cellulose, made up of linearly polymerized β-D-glucose molecules, is primarily used for the production of paper (Kamide, 2005). Hemicellulose, a branched heteropolymer carbohydrate, can be easily separated from woodchips through pretreatment and valorized, for example, as a substrate for the production of bio-ethanol (Hamaguchi et al., 2012). Lignin, the second most abundant polymer on this planet and the only renewable source of aromatics, remains after cellulose and hemicellulose extraction (Boudet, 1998). Large quantities of technical lignin are produced as side streams in the lignocellulose processing industry (Boudet, 1998; Bruijnincx et al., 2015). Therefore, lignin valorization offers the potential to reduce the dependence on petroleum-based aromatics (de Wild et al., 2014). However, lignin's recalcitrant nature, due to its structure of cross-linked phenolic rings, makes its use challenging, requiring aggressive fractionation and depolymerization (Schutyser et al., 2018). To utilize lignin, its complex structure must first be made bioavailable to microbes, which also need to tolerate aromatics and catalyze the desired bioconversion into value-added products such as *cis,cis*-muconic acid (MA) (Becker and Wittmann, 2019). Depolymerization strategies often result in a heterogenic mixture of aromatics (Schutyser et al., 2018b) or high concentrations of toxic compounds like guaiacol (Shen et al., 2019). Therefore, the lignin valorization process must be considered holistically, including lignin fractionation, depolymerization and microbial conversion (Becker and Wittmann, 2019). Due to these challenges, industrial lignin utilization remains an unachieved goal so far (Becker and Wittmann, 2019).

2 Objectives

The aim of this work was to enable the production of *cis,cis*-muconic acid (MA) from lignin-derived aromatics. *Amycolatopsis sp.* ATCC 39116, selected as a promising host, should be genetically engineered for efficient MA production. To achieve this, an improved deletion system should be developed that enables fast and precise genomic editing. The new approach should be applied to generate *Amycolatopsis*-based cell factories that could use guaiacol and guaiacol-rich lignin hydrolysates. The combination of these strategies should then enable the integrated chemical and biochemical production of MA using metabolically engineered *Amycolatopsis sp*. ATCC 39116. The second phase of the work should focus on the valorization of vanillin and vanillate, which can be obtained from alkaline-oxidized softwood lignin. The selected organism should be further engineered for the production of MA from protocatechuate. In the final step, the study should aim for a fully bio-based production of chemicals by investigating xylose from hemicellulose and spent sulfite liquor (SSL) as potential substrates for growth.

3 Theoretical Background

3.1 Lignocellulose as a resource

Biomass is the mass of living biological organisms, including animal- and plant-based materials, as well as bacterial or fungal biomass (Bar-On et al., 2018). The sum of biomass on earth is about 550 gigatons of carbon (1 Gt C = 10^{15} g of carbon) (Bar-On et al., 2018). Its major part is constituted by plant biomass (450 Gt C). About 90% of this fraction can be accounted to lignocellulose (Vyas et al., 2018a). Lignocellulosic biomass includes, next to virgin plants, also wastes from agricultural and forestry and industrial wastes (Soni et al., 2018). Presently, the technical processing of lignocellulosic biomass as a raw material is becoming increasingly important. There is a shift towards a more sustainable industry that relies on renewable bio-based materials instead of non-renewable petroleum-based carbon resources (Arevalo-Gallegos et al., 2017). Petroleum is finite and is becoming increasingly expensive (Arevalo-Gallegos et al., 2017). In addition, its progressive depletion has driven up prices in important sectors worldwide, including the energy and materials sectors (Arevalo-Gallegos et al., 2017). The industrial use of lignocellulosic biomass as a substrate for the production of value-added products could be a cost-effective solution, as it is cheap and renewable (Soni et al., 2018). Various industrial and agricultural processes produce large amounts of lignocellulosic waste as a low-value byproduct, which is underutilized (Soni et al., 2018). The valorization of these wastes will help to reduce environmental pollution and also create a sustainable substrate for the industry (Soni et al., 2018).

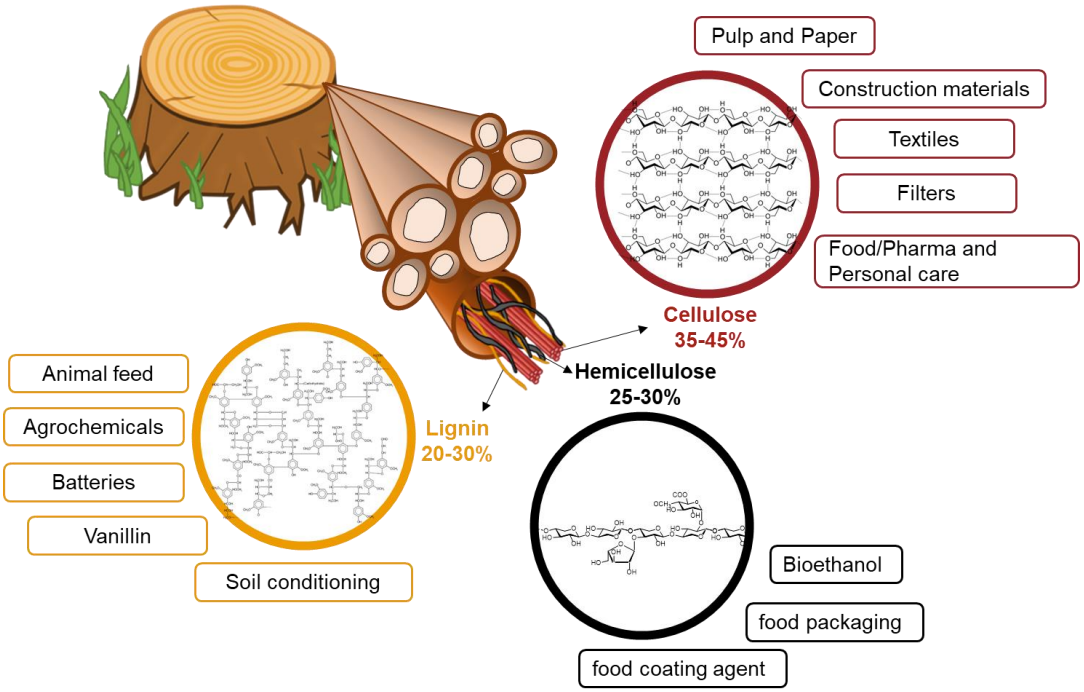

Figure 3.1: Composition of plant biomass and its industrial use. The walls of plant cells consist of cellulose, hemicellulose, and lignin. The figure is adapted from previous work (Becker and Wittmann, 2019).

However, unfortunately, lignocellulosic biomass (Figure 3.1) is a complex, highly oxygenated, and heterogeneous material that is difficult to depolymerize (Schutyser et al., 2018). It primarily consists of cellulose, lignin and hemicellulose, the prime building blocks for cell walls (Vyas et al., 2018b). Whereby, cellulose is the major constituent of the primary cell wall of green plants (about 45% of plant dry matter) and thus the most abundant organic polymer and polysaccharide on earth (Kamide, 2005). It is a straight chain polymer consisting of hundreds to many of thousands of β-1,4-glycosidically linked β-D-glucose subunits, forming cellobiose units (Kamide, 2005). These cellobiose units assemble into higher structures via hydrogen bonds and van der Waals forces (Pérez et al., 2002; Schutyser et al., 2018). Cellulose fibers are insoluble in common solvents because of the strong interaction forces (Schutyser et al., 2018). Hemicellulose is a collective term for a branched polymer consisting of a mixture of variable polysaccharides occurring in plant biomass. It contains pentoses (e.g., arabinose, xylose) and hexoses (e.g., galactose, glucose, mannose) and can account for up to 30% of plant's dry matter (Schutyser et al., 2018).

Hemicellulose is an amorphous polymer, which makes it more soluble and more sensitive to chemical attacks (Schutyser et al., 2018). Lignin is the most complex constituent of lignocellulosic biomass, which can make up over 30% of plant biomass (Abdelaziz et al., 2016). It is formed by free radical polymerization of three monolignols, namely sinapyl alcohol, coniferyl alcohol, and *para*-coumaryl alcohol and therefore called supramolecular self-assembled chaos (Achyuthan et al., 2010; Becker and Wittmann, 2019). Lignin provides stability, and rigidity, especially to wood and bark (Schutyser et al., 2018).

3.2 Lignin

Lignin is considered the second most abundant polymer on this planet (Boudet, 1998). Notably, it is the solely renewable source of aromatics (Tuck et al., 2012). The valorization of lignin therefore offers the possibility of escaping dependence on petroleum-based aromatics (de Wild et al., 2014). Lignin is an amorphous heteropolymer, i.e., a randomized network of linked aromatic monolignols (Pérez et al., 2002). They consist of guaiacyl, *para*-hydroxyphenyl, and syringyl-units (Achyuthan et al., 2010). Monolignols are mainly crosslinked by ether β-O-4 bonds (50-80%) and C-C bonds (Becker and Wittmann, 2019; Van den Bosch et al., 2018). The composition of lignin depends on the plant type and can also vary within a species (Zakzeski et al., 2010). Softwood contains up to 30% of lignin compared to hardwood (18-20%), and grass (8-20%), while it is hardly found in mosses and green algae (Abdelaziz et al., 2016). Furthermore, softwood has the largest guaiacyl content (G-type) with up to 90% (Pandey and Kim, 2011). In hardwood, the proportion of guaiacyl (G-type) and syringyl units (S-type) is about the same (Pandey and Kim, 2011). Worldwide, the amount of lignin is around 300 billion tons. In addition, around 20 billion tons are produced by plants every year (Becker and Wittmann, 2019). Furthermore, during the fractionation of biomass in lignocellulose processing industries, large quantities of technical lignin are produced as side streams (Boudet, 1998; Bruijnincx et al., 2015).

3.2.1 Pulp and paper industry as a source for lignin

In typical pulp and paper mills, large amounts of lignin are produced as by-product (Ragauskas et al., 2014). In general, the main aim of pulping is to delignify wood. This procedure should be carried out in such a way that the cellulose and hemicelluloses are retained (Hamaguchi et al., 2012). To solubilize lignin and separate it, a cooking process is conducted mechanically or chemically (Abdelaziz et al., 2016; Schutyser et al., 2018). The three major processes for delignification are the kraft process, the organosolv process, and the sulfite process (Van den Bosch et al., 2018). More than 400 million tons of paper are produced every year (Furszyfer Del Rio et al., 2022). Technical lignin, next to black liquor and other side streams, arises as a by-product of the pulping process (Rinaldi et al., 2016; Schmiedl et al., 2012). Kraft pulping alone produces around 130 million tons of lignin annually (Rinaldi et al., 2016). Most of the kraft lignin is burned, and not even 100,000 t a^{-1} of lignin is commercially utilized (Bandounas et al., 2011; Rinaldi et al., 2016).

Kraft pulping is the most common delignification method (Argyropoulos et al., 2023). In this process, wood chips are cooked together with white liquor in pressure vessels at about 160-170 °C, producing a pulp that contains dissolved organic and soluble inorganic substances (Gullichsen et al., 1999; Hamaguchi et al., 2012). The so-called white liquor is a strongly alkaline solution containing hydroxyl (OH^-) ions and hydrosulfide (HS^-) ions (Gullichsen et al., 1999). This is followed by a washing step to separate the cellulose. The washed pulp is passed on for further processing, e.g., screening, bleaching, and drying. The separated liquid, called black liquor (containing lignin and hemicellulose) is fed to the recovery line (Hamaguchi et al., 2012) (Figure 3.2 A).

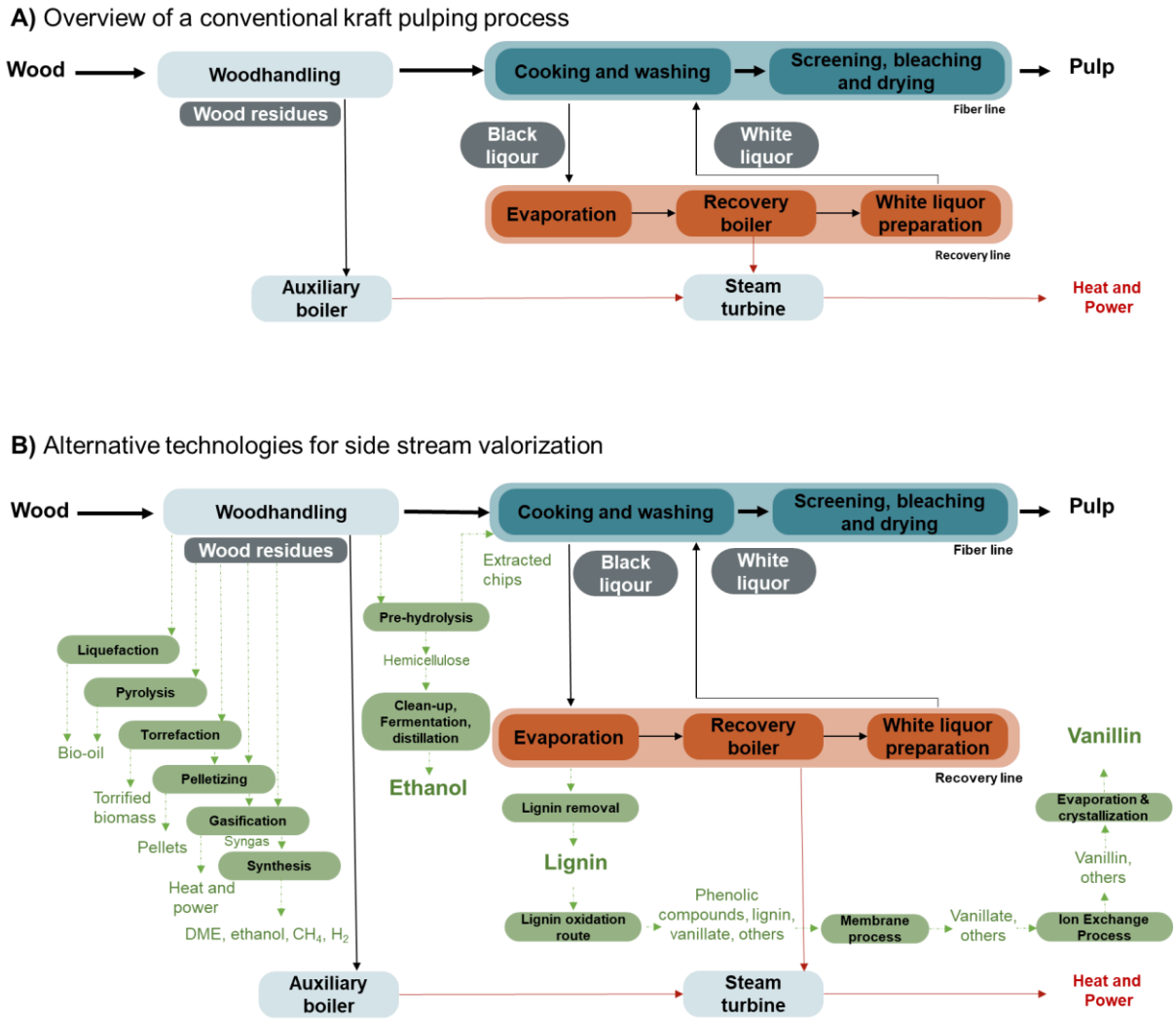

Figure 3.2: Industrial kraft pulping processes. Conventional kraft pulping with generation of pulp and energy mill (A) and advanced kraft pulping with integrated technologies for enhanced by-product valorization (B). The figure is adapted from previous work (Hamaguchi et al., 2012; Silva et al., 2009).

The recovery line is required to make the pulping process economical (Hamaguchi et al., 2012). The evaporation plant concentrates black liquor. The concentrate is then burned in the recovery boiler to regenerate the pulp chemicals. This process, in turn, generates high-pressure steam (Hamaguchi et al., 2012). The unburned fraction is mainly composed of sodium carbonate and sodium sulfide. To generate high quality white liquor, this stream is dissolved and sent to the causticizing plant (Hamaguchi et al., 2012). For economic feasibility, pulp mills must also burn the wood residues generated during wood preparation (e.g., bark, wood shavings and others) in auxiliary boilers.

The resulting high-pressure steam is used to generate heat and electricity for the mill (Hamaguchi et al., 2012). With the emergence of the global energy and environmental crisis, science is forced to apply new strategies to develop alternative technologies to valorize the side streams, e.g., the alkaline oxidation of softwood lignin (Kratzl et al., 1974; Soni et al., 2018). This industrial process already yields 3,000 tons of vanillin. Figure 3.2 B compares a normal kraft pulping process with an advanced process that incorporates alternative technologies. Such technologies will improve by-product valorization (Hamaguchi et al., 2012).

Delignification methods have different effects on lignin quality. In general, the lignocellulose pretreatment technology is divided into four categories: chemical pretreatment (kraft or sulfite pulping), solvent fractionation (organosolv process), physical pretreatment (ball milling), and biological treatment (using predominately fungi) (da Costa Sousa et al., 2009; Joseph Zakzeski, 2009). Each of these methods provides lignin of different quality and exhibits both advantages and disadvantages in terms of cost and environmental footprint (Zakzeski et al., 2010). The kraft process is the predominant process and covers a global market share of over 90% (Van den Bosch et al., 2018). Therefore, it exhibits significant infrastructure that is beneficial to the industry. Unfortunately, kraft pulping is very energy-intensive, and the entire plant relies on the combustion of lignin to generate heat for the process, limiting the supply of lignin for further utilization (Zakzeski et al., 2010). Kraft pulp supplies lignin, which contains only 1 to 3% sulfur (Van den Bosch et al., 2018). The lignin is condensed, water-insoluble, and consists only of G-type aromatics (Becker and Wittmann, 2019; Schutyser et al., 2018; Van den Bosch et al., 2018). In addition, chemical bleaching causes structural changes to the lignin, e.g., the loss of most of the native β-O-4 ether bonds (Zakzeski et al., 2010). This makes it harder to depolymerize it into monomers and a challenging feedstock for catalytic conversions to chemicals and fuels (Gierer, 1985; Schutyser et al., 2018).

The sulfite pulping treatment is conducted between pH 2 and 12 using sulfite, usually with magnesium or calcium as the counterion (Abdelaziz et al., 2016; Joseph Zakzeski, 2009). During this process, lignin becomes highly degraded with a sulfur content of 4 to 7%, and it is completely soluble in water (Becker and Wittmann, 2019; Schutyser et al., 2018; Van den Bosch et al., 2018).

The high sulfur content leads to potential problems during further processing, as there is an increased risk of catalyst poisoning (Van den Bosch et al., 2018).

A delignification method that results in a more unaltered lignin is the organosolv process (Van den Bosch et al., 2018). Wood or bagasse is crushed to extract sap or juice with various organic solvents (Johansson et al., 1987; Joseph Zakzeski, 2009). The advantage of this method is that it provides separate streams of cellulose, lignin, and hemicellulose (Nitsos et al., 2018). This allows the valorization of all components of lignocellulosic biomass (Nitsos et al., 2018). The process is generally considered environmentally friendly because it does not require harsh conditions or use sulfides (Nitsos et al., 2018; Zakzeski et al., 2010). However, the solvents and their recovery are very expensive (Zakzeski et al., 2010).

Next to hemicellulose or cellulose upgrading, lignin recovery is a promising starting point for research. The production of 130 million tons of pulp accumulates about 50 million tons of lignin annually (Boudet, 1998; Bruijnincx et al., 2015). But the unruliness and heterogeneity of industrial lignin significantly affect its further use (Beckham et al., 2016). Therefore, most of it is burned to generate electric power and heat (de Wild et al., 2014). Regarding its potential, this is highly inefficient and generates large quantities of carbon dioxide (Rinaldi et al., 2016). Research has therefore begun to focus on macromolecular applications of lignin (Schutyser et al., 2018). On a small scale, technical lignin is used as a low-value additive for gypsum and cement (Toledano et al., 2012). Furthermore, it can be used as an emulsifier, battery electrode, binding agent, or carbon fiber precursor (Figure 3.1) (Schutyser et al., 2018). A prominent example of lignin utilization is the production of the flavor vanillin by the Borregaard company (Sarpsborg, Norway) (Abdelaziz et al., 2016; Ponnusamy et al., 2018). To enable a more efficient and sustainable use of lignin, further processing is needed.

3.2.2 Lignin depolymerization

Over the past decade, there has been an increasing motivation to integrate the valorization of lignin into biorefinery systems (Schutyser et al., 2018). Hereby, the depolymerization of lignin is a key point for its valorization (Becker and Wittmann, 2019). The result of lignin depolymerization depends on the underlying mechanism of the processing method (Schutyser et al., 2018).

Successful production of chemicals from lignin requires the effective interaction of the following three important biorefinery units: lignocellulosic fractionation (e.g., delignification in pulp and paper industry), lignin depolymerization, and upgrading (Schutyser et al., 2018). Different methods have been developed for each of these aspects. While various low-value (macromolecular) applications for lignin are thinkable, a more advanced conversion of lignin into chemicals appears as a more promising possibility (Becker and Wittmann, 2019). To achieve this goal, the complex lignin structure must be made bioavailable for microbes that can catalyze the desired bioconversion. Therefore, the production of small aromatics, including phenolic monomers (e.g. guaiacol, catechol, phenol, cresol), acids (e.g. vanillate, ferulate) and aldehydes (e.g. vanillin, benzaldehyde), appears desirable (Becker and Wittmann, 2019). Admittedly, depolymerization methods are diverse and yield different spectra of monomers (Schutyser et al., 2018). In general, lignin depolymerization can be divided into base- and acid-catalyzed, reductive, oxidative, solvolytical, and thermal processes (Schutyser et al., 2018). A detailed summary of the complex topic of lignin depolymerization can be found in the reviews of van den Bosch *et al.* 2018 and Schutyser *et al.* 2018. Only certain approaches yield high fractions of phenolic monomers such as guaiacol or vanillin, which are of particular importance for the application examples of this work (Becker and Wittmann, 2019).

For thermal and chemical lignin depolymerization, two methods have emerged, namely pyrolysis and hydrolysis. During pyrolysis, lignin is heated to a high temperature in order to break down the molecular structure (De Wild et al., 2009). This is done in the absence of oxygen to prevent combustion into carbon dioxide. The formed pyrolysis vapor is condensed into lignin-rich oil. The applied temperature ranges from 400 to 800 °C (Schutyser et al., 2018). The highest monomer yields are achieved between 400 and 600 °C. Most studies report monomer yields around 10 wt% (Schutyser et al., 2018), but a selected report observed a monomer yield of 30 wt% when using softwood kraft lignin (Zheng *et al.* 2013). Notably, fast pyrolysis produces a large spectrum of monomers comprising, e.g., unsubstituted methoxyphenols, catechols, and phenols (De Wild et al., 2009). Fast pyrolysis of lignin has been studied mainly on a small scale in batch reactors, and the realization of continuous pyrolysis on a large scale has proven difficult (Schutyser et al., 2018).

Hydrolysis, also known as hydrothermal conversion (HTC), uses hot, compressed water to depolymerize lignin (Pińkowska et al., 2012; Sasaki and Goto, 2011). The temperatures used in hydrolysis range from 200-500 °C and the applied pressure can be above 300 bar (Du et al., 2013). The conversion can be carried out with subcritical or supercritical water (Pińkowska *et al*, 2012). The product stream after hydrothermal conversion is an aqueous liquid hydrolysate containing phenols and methoxylated derivates (Du et al., 2013). This method was chosen to show the entire process, from kraft pine lignin to nylon. Lignin was depolymerized in supercritical water at 395 °C for 1 hour (Kohlstedt et al., 2018), resulting in a mixture consisting mainly of catechol and phenol and minor amounts of cresols (Kohlstedt et al., 2018).

Reductive catalytic fractionation (RCF) of lignin is one of the most effective methods for converting lignin into aromatic monomers (Gu et al., 2023; Subbotina et al., 2021). This, so called “lignin-first” fractioning process combines biomass fractionation with lignin depolymerization (Renders et al., 2019). The strategy provides large amounts of aromatic monomers and selectivity compared to conventional processes (Li et al., 2023). Additional catalytic autoxidation of the obtained RCF oil, including Co/Mn/Br-based treatment, support the cleavage of carbon–carbon bonds in acetylated lignin oligomers (Gu et al., 2023). This method provides selected monomers in high yield for bioconversion, especially acetyl vanillic acid and acetyl vanillin.

In other studies, mild base-catalyzed depolymerization was investigated (Rodriguez et al., 2017). Using different process parameters (NaOH concentration, temperature) corn-stover lignin was depolymerized, and the aromatic monomers in the lignin liquor were quantified (Rodriguez et al., 2017). Interestingly, the method generated a product stream that corresponded to the “natural” aromatic composition in soil with *p*-coumarate as the dominant monomer, followed by ferulate (Shindo and Kuwatsuka, 1977). In addition, various aldehydes, e.g., vanillin, and benzoates, e.g., vanillate, were found in low concentrations (Rodriguez et al., 2017). An alternative method for depolymerization of lignin was published by Rahimi *et al.* 2014. Here, a model compound of oxidized lignin was depolymerized using a gentle treatment in aqueous formic acid, resulting in around 60 wt% of aromatic monomers. More importantly, this method produced large fractions of guaiacol.

Using aqueous formic acid at 110 °C and reducing metals such as zinc or manganese, guaiacol was obtained at 69% and 63% yield, respectively. The yield was even higher (87%) when 3 equivalents of sodium formate were added to the reaction mixture (Rahimi et al., 2014).

Biobased depolymerization of lignin is very slow due to the rigid structure of lignin (Abdelaziz et al., 2016). Depolymerization of lignin, the largest organic fraction of soil, to small aromatics is achieved in nature by microorganisms (Abdelaziz et al., 2016). The associated enzyme diversity provides an alternative to conventional depolymerization strategies (Bugg et al., 2020; Ponnusamy et al., 2018). Various enzymes work together to break down lignin, e.g., laccases, esterases, peroxidases, and cellulases (Bugg et al., 2020). White-rot fungi in particular are known to have an extensive repertoire of oxidative lignin-degrading enzymes, but they are difficult to cultivate (Janusz et al., 2017). In addition, their biosynthetic pathways underlie a complex regulation, making enzyme production a difficult undertaking (Martani et al., 2017). Furthermore, knowledge about the exact mechanisms of lignin biotransformation is currently incomplete (Rinaldi et al., 2016). It is believed that the β-*O*-4-bond, which is common in natural lignin, serves as the main target for enzymatic lignin polymerization and provides various opportunities for oxidation or oxidative cleavage (Bugg et al., 2020). The use of enzymes for lignin depolymerization has become the focus of academic attention because they are environmentally friendly, highly specific, and work under mild conditions (Bandounas et al., 2011; Salvachúa et al., 2015). However, depolymerization rates in particular are very low, and the enzymes are still expensive to produce (Abdelaziz et al., 2016). In addition, technical lignin is structurally different from natural lignin, so enzymes developed for natural lignin may have limited ability to convert technical lignin (Bandounas et al., 2011). Most enzymes prefer gentle conditions or even an acidic environment, in which the common technical lignins are difficult to dissolve (de Gonzalo et al., 2016). Consequently, there are still some hurdles to overcome before reaching industrial feasibility.

3.3 *Cis-cis* muconic acid, the premium platform chemical from lignin

Cis,cis-muconic acid (MA) is a central precursor for the production of profitable bulk chemicals (Xie et al., 2014). This di-unsaturated dicarboxylic acid can be hydrogenated to adipic acid, an important building block for industrial polyurethanes and nylons (Curran et al., 2013; Rosini et al., 2023; Xie et al., 2014). Moreover, isomerization of MA, followed by a Diels-Alder reaction with ethylene and dehydrogenation, results in terephthalic acid, one of the two constitutive monomers of the industrial polymer polyethylene terephthalate (Ravindranath et al., 1986). In addition, its reactive dicarboxylic groups and conjugated double bonds make MA itself an interesting molecule for the production of new functional chemicals, including crosslinking in composites, for example (Xie et al., 2014). The global market potential has been estimated at over $ 22 billion per annum (Sonoki et al., 2018). In addition to the *de novo* synthesis of c*is,cis*-muconic acid from glucose, it accumulates as a metabolic intermediate during the catabolism of lignin-derived aromatics (Figure 3.4) (Draths and Frost, 1994). *Cis,cis*-muconic acid accumulates when the β-ketoadipate pathway is interrupted at the step of cycloisomerase (Mizuno et al., 1988). *Cis,cis*-muconic acid has emerged as a prominent chemical, accessible by fermentation from lignin-related small aromatics, using strains of *Pseudomonas putida* KT2440 (Van Duuren, 2011), *Escherichia coli* (Zhang et al., 2015), *Saccharomyces cerevisiae* (Curran et al., 2013), *Corynebacterium glutamicum* (Weiland et al., 2023) among others.

3.4 *Amycolatopsis sp.* ATCC 39116 a potent host for the lignin industry

Amycolatopsis sp. ATCC 39116 was isolated by the Crawford group (Pometto *et al*, 1981; Sutherland, 1986) from a vanillate enriched soil in Idaho. The isolate matched in various aspects with *Streptomyces setonii,* first named by Millard and Burr in 1926 (Shinoda et al.). It is a gram-positive, aerobic, and thermophilic actinomycete (An *et al*, 2001; Park & Kim, 2003b;). *Amycolatopsis sp.* ATCC 39116 produces well-developed vegetative hyphae with branches. After a period of vegetative growth, the strain starts to produce specialized spore-bearing structures (Hopwood, 1988). Mature spore chains often bear 50 or more spores per chain (Waksman, 1953).

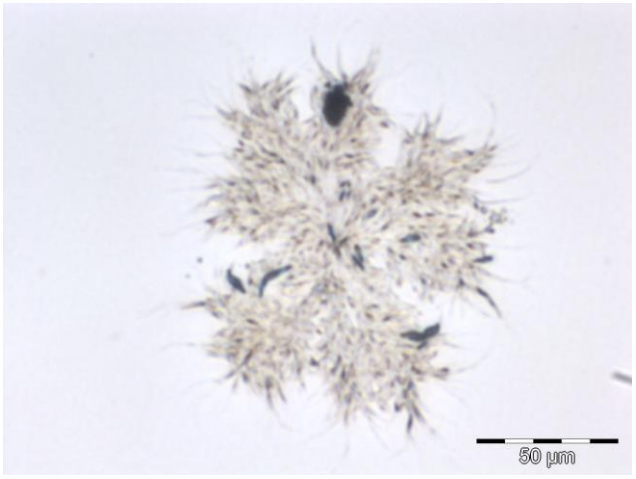

Figure 3.3: Microscopic image of *Amycolatopsis sp.* ATCC 39116 grown in GYM medium.

Interestingly, *Amycolatopsis sp.* ATCC 39116 is capable of growing on different types of sugars, such as L-arabinose, D-xylose, D-fructose, D-glucose, D-mannitol, and L-rhamnose (Shinoda et al.). The organism is already used industrially for the production of vanillin (Fleige et al., 2013).

3.4.1 *Aromatic degradation pathways*

Remarkably, *Amycolatopsis sp*. ATCC 39116 is capable of degrading lignin (Antai and Crawford, 1981). The strain was identified as one of the best lignin utilizers in a comprehensive screening of 14 bacteria with regard to their lignin depolymerizing abilities (Salvachúa et al., 2015). *Amycolatopsis sp*. ATCC 39116 exhibited the highest lignin turnover of 31% in Klason's lignin analysis under nutrient-rich culture conditions. Under nitrogen-limiting culture conditions, it was among the best five degraders (Salvachúa et al., 2015). It offers a wide variety of enzymes that degrade various small aromatic compounds such as guaiacol, catechol, and phenol (Table 3.1).

Table 3.1: Aromatic compounds that *Amycolatopsis sp.* ATCC 39116 can use for its growth.

Aromatic compounds	Reference
Benzoate	(Sutherland et al., 1981b)
Catechol	(Sutherland et al., 1981b)
Cinnamate	(Sutherland et al., 1983)
cis,cis-Muconic acid	(Sutherland et al., 1981b)
Ferulate	(Sutherland et al., 1983)
Guaiacol	(Pometto et al., 1981)
Lignin	(Antai and Crawford, 1981)
Lignocellulose	(Antai and Crawford, 1981)
p-Coumarate	(Sutherland et al., 1983)
Phenol	(Antai and Crawford, 1983)
Protocatechuate	(Sutherland et al., 1981b)
Vanillate	(Pometto et al., 1981)
Vanillin	(Sutherland et al., 1983)
Veratrole	(Sutherland, 1986)

An overview of the aromatic degradation pathways of *Amycolatopsis sp.* ATCC 39116 most relevant to this work is shown in Figure 3.4.

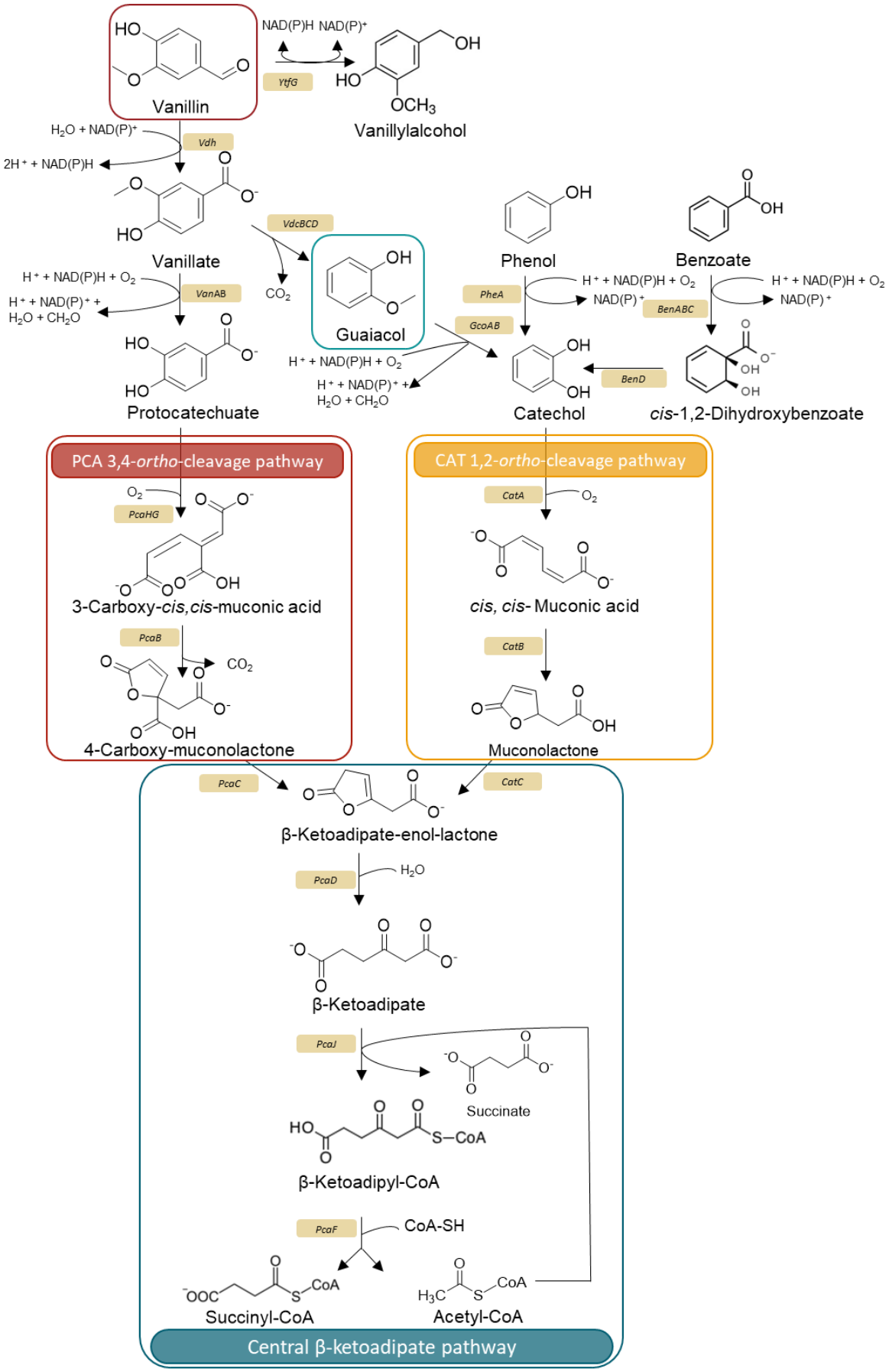
Vanillin
NAD(P)H NAD(P)+
YtfG
Vanillylalcohol
H2O + NAD(P)+
Vdh
2H+ + NAD(P)H
Vanillate
VdcBCD
CO2
Guaiacol
H+ + NAD(P)H + O2
VanAB
H+ + NAD(P)+ + H2O + CH2O
Protocatechuate
Phenol
PheA
H+ + NAD(P)H + O2
NAD(P)+
Benzoate
BenABC
H+ + NAD(P)H + O2
NAD(P)+
GcoAB
H+ + NAD(P)H + O2
H+ + NAD(P)+ + H2O + CH2O
Catechol
BenD
cis-1,2-Dihydroxybenzoate
PCA 3,4-ortho-cleavage pathway
O2
PcaHG
3-Carboxy-cis,cis-muconic acid
PcaB
CO2
4-Carboxy-muconolactone
CAT 1,2-ortho-cleavage pathway
CatA
O2
cis, cis- Muconic acid
CatB
Muconolactone
PcaC
CatC
β-Ketoadipate-enol-lactone
PcaD
H2O
β-Ketoadipate
PcaJ
Succinate
β-Ketoadipyl-CoA
PcaF
CoA-SH
Succinyl-CoA
Acetyl-CoA
Central β-ketoadipate pathway

Figure 3.4: Degradation pathways of aromatics in *Amycolatopsis sp.* ATCC 39116 funneling in the central β-ketoadipate pathway. In this study the focus was set especially on vanillin and guaiacol. Vanillin: Vanillin dehydrogenase (Vdh) (Fleige et al., 2013), oxidoreductase (YtfG) (Meyer et al., 2018). Vanillate: Vanillate-*O*-demethylase (*Van*AB) (Meyer et al., 2017) (Meyer et al., 2018), Vanillate decarboxylase (VdcBCD) (Meyer et al., 2017). Guaiacol: Guaiacol-*O*-demethylase (GcoAB) (Mallinson et al., 2018). Phenol: Phenolhydroxylase (PheA) (Antai and Crawford, 1983). Benzoate: Benzoate dioxygenase (BenABC), Benzoate diol dehydrogenase (BenD) (Park and Kim, 2003). CAT 1,2-*ortho*-cleavage pathway: Catechol-1,2-dioxygenase (CatA), *cis, cis*-Muconate cycloisomerase (CatB), Muconolactone isomerase (CatC) (Park and Kim, 2003). Protocatechuate-3,4-*ortho*-cleavage pathway: Protocatechuate-3,4-dioxygenase (PcaHG), β-Carboxy-*cis,cis*-muconate cycloisomerase (PcaB), γ-Carboxy-muconolactone decarboxylase (PcaC) (Meyer et al., 2018). Central β-ketoadipate pathway: β-Ketoadipate enol-lactone hydrolase (PcaD), β-Ketoadipate succinyl-CoA transferase (PcaIJ), β-Ketoadipyl-CoA thiolase (PcaF) (Meyer et al., 2018). The figure was adapted from Weiland et al., 2022.

Amycolatopsis sp. ATCC 39116 is able to metabolize aromatic compounds from G-type and H-type lignin into the key intermediates catechol and protocatechuate (Figure 3.4) (Becker and Wittmann, 2019). In some cases, protocatechuate can be converted into catechol, e.g., using protocatechuate decarboxylase (AroY) (Vardon et al., 2015). Both key intermediates are directed to the central β-ketoadipate pathway, which breaks them down and provides them for cell growth, secondary metabolism, and maintenance (Li and Zheng, 2020; Weiland et al., 2022).

First, key intermediates have to overcome their aromaticity by ring cleavage (Harwood and Parales, 1996). This occurs via the PCA 3,4-*ortho*-cleavage pathway and the CAT 1,2-*ortho*-cleavage pathway. On the aromatic ring, both intermediates have two hydroxyl groups adjacent to each other. Since the ring cleavage takes place between the two hydroxyl groups, it is called *ortho*-cleavage. If the fission occurs next to the hydroxyl groups, it is referred to as *meta*-cleavage.

The ring cleavage is catalyzed by the catechol-1,2-dioxygenase (CatA) respectively, by the protocatechuate-3,4-dioxygenase (PcaHG) (Harwood and Parales, 1996; Meyer et al., 2018; Park and Kim, 2003). They incorporate up to two oxygen atoms (O_2) to the organic substrate (Harwood and Parales, 1996). These so-called oxidoreductases often require metal ions, like iron, as cofactors (Fuchs et al., 2011). The aromatic ring structure is chemically stable because it contains six carbon atoms with alternating single and double carbon-carbon bonds (Kekulé, 1865). This leads to an equally distributed electron density in the ring. Because of this stability, the catechol ring fission is known to be slow.

This often leads to an accumulation of the highly toxic catechol, causing oxidative stress in the cell (Van Duuren, 2011). The gene encoding catechol-1,2-dioxygenase (*catA*) is localized in the catechol catabolic gene cluster, alongside muconate cycloisomerase (*catB*) and muconolactone isomerase (*catC*) (Park and Kim, 2003). Interestingly, the putative regulation gene c*atR* has an unusual orientation. In contrast to other organisms like *P. putida*, *catR* aligns with the orientation of the catechol operon (Park and Kim, 2003). The amino acid similarity of this gene makes it a positive catechol regulator (Rothmel et al., 1990). Catechol and 4-chlorophenol induce the *catR* gene, but benzoate does not (Park and Kim, 2003). The CatA enzyme cleaves catechol into the product *cis,cis*-muconic acid (MA). MA is further metabolized by CatB to muconolactone (Park and Kim, 2003). Interestingly, *Amycolatopsis sp.* ATCC 39116 possesses three types of *catB* genes with high sequence similarity to other catechol-degrading organisms. In the next step, muconolactone is converted to β-ketoadipate-enol-lactone by the CatC enzyme (Harwood and Parales, 1996). At this level, the PCA 3,4-*ortho*-cleavage pathway and the CAT 1,2-*ortho*-cleavage pathway jointly merge into the central β-ketoadipate pathway, which introduces β-ketoadipate-enol-lactone into the citrate cycle (Harwood and Parales, 1996). The enzymes for this conversion are encoded on the *pca* operon, namely β-ketoadipate enol-lactone hydrolase (PcaD), β-ketoadipate succinyl-CoA transferase (PcaJ) and β-ketoadipyl-CoA thiolase (PcaF) (Meyer et al., 2018; Weiland et al., 2022). The *pca*-operon is also responsible for the conversion of protocatechuate to β-ketoadipate-enol-lactone with the help of the enzymes protocatechuate-3,4-dioxygenase (PcaHG), β-carboxy-*cis,cis*-muconate cycloisomerase (pcaB) and *γ*-carboxy-muconolactone decarboxylase (PcaC) (Meyer et al., 2018; Weiland et al., 2022). In particular*, Amycolatopsis sp.* ATCC 39116 has a link between the PCA 3,4-*ortho*-cleavage pathway and the CAT 1,2-*ortho*-cleavage pathway. Vanillate can be converted into guaiacol using the vanillate decarboxylase (VdcBCD) (Meyer et al., 2017).

***O*-demethylation is crucial for lignin bioconversion**. In addition to the *p*-coumaryl alcohol subunit, lignin consists mainly of coniferyl and sinapyl subunits, which have one or two methoxy groups, respectively, on the ring structure (Achyuthan et al., 2010; Mallinson et al., 2018). To enable the oxidative cleavage of these subunits, they must first be *O*-demethylated to diols (Mallinson et al., 2018; Masai et al., 2007).

O-demethylation is a fundamental step in providing carbon from aromatic compounds and, therefore, for lignin valorization. Two well-understood *O*-demethylases are known for *Amycolatopsis sp*. ATCC 39166. The first is vanillate *O*-demethylase (VanAB), which converts vanillate to the key intermediate protocatechuate (Masai et al., 2007; Meyer et al., 2018). This enzyme allows *Amycolatopsis sp.* ATCC 39116 to introduce ferulic acid and its derivate vanillin into the central carbon metabolism (Meyer et al., 2018). VanAB is a common enzyme in many aromatics-degrading soil bacteria. A rather rare *O*-demethylase is the enzyme that catalyzes the reaction from guaiacol to catechol. Previous reports by Pometto *et al*. in 1981 first described the degradation of guaiacol to catechol in *Amycolatopsis sp*. ATCC 39116 and postulated that it was catalyzed by a cytochrome P450 enzyme. However, until recently, the enzyme has not been characterized, nor have the full gene sequences been published. Different efforts isolated the cytochrome P450-reductase genes (*gco*AB), from *Amycolatopsis sp*. ATCC 39116 (accession numbers WP_020419855.1 and WP_020419854.1), and introduced the genes via plasmid-based expression into *P. putida* KT2440 (Mallinson et al., 2018; Tumen-Velasquez et al., 2018).

c*is,cis*-Muconic acid (MA) occurs during the degradation of lignin-derived aromatics (Van Duuren, 2011). MA accumulates if the β-ketoadipate pathway is disrupted at the cycloisomerase step (*catB*) (Mizuno et al., 1988), which prevents further metabolization of c*is,cis*-muconic to muconolactone. In recent years, different microbes have been engineered for industrial production. *P. putida* KT2440 is known as a promising production host (van Duuren et al., 2011). After chemical mutagenesis, the mutant JD-1 was able to produce MA from benzoate. Further studies revealed a point mutation in *catR*, a transcriptional regulator, which shut down the entire *cat* operon (van Duuren et al., 2012). This operon carries, next to *catA* and *catC* genes, the *catB* gene encoding MA-degrading muconate cylcoisomerase (van Duuren et al., 2012). Due to a second catA2 enzyme located in the *ben* operon, the strain was now able to produce MA (van Duuren et al., 2012). A more recently discovered production host is *Corynebacterium glutamicum*. The deletion of the *catB* gene, encoding muconate cylcoisomerase, led to a MA-producer strain of *C. glutamicum ATCC 13032* (Becker et al., 2018).

3.4.2 *Molecular tools for Amycolatopsis sp. ATCC 39116*

Genetic modification of *Amycolatopsis* has generally proven slow and frustrating in the past (Dhingra et al., 2003). One of the main problems has been the low transformation efficiency and the absence of replicative plasmids (Dhingra et al., 2003). The problems with low transformation efficiency and the lack of replicative plasmids were overcome by the Steinbüchel group (Fleige and Steinbüchel, 2014; Steinbüchel, 2002).

In addition, the genome of *Amycolatopsis sp.* ATCC 39116 was sequenced in 2012, which enables the genetic modification of the organism (Davis et al., 2012). However, there are still no suitable methods for the efficient genetic engineering of *Amycolatopsis sp.* ATCC 39116 (Meyer et al., 2017). Moreover, there is a major problem with the high frequency of non-homologous DNA integration after plasmid transformation (Fleige et al., 2016). This is a known problem for actinomycetes (Kalpana et al., 1991). Numerous genetic engineering approaches have been developed for actinomycetes, but they have also reported difficulties in genetic manipulation (Siegl and Luzhetskyy, 2012). Another major problem is the low rate of homologous recombination events in the second recombineering event required to remove the plasmid backbone (Fleige et al., 2013). The required screening effort is enormous, and the duration of cultivation to force the second recombineering event is quite long (Fleige et al., 2016). The time to generate a homogenote is up to 21 days (Fleige et al., 2013). Recently, an improved deletion system was developed for *Amycolatopsis sp.* ATCC 39116 based on a suicide plasmid containing the *rspL* gene (Meyer et al., 2017). This plasmid reduces illegitimate recombination events, increases the rate of homologous recombination, reduces screening effort, and represents a highly valuable achievement. Another suitable method to reduce the screening effort in actinomycetes is the use of β-glucuronidase (GusA) as a reporter, which is encoded by *gus*A (*uidA*) and enables a blue-white screening system (Myronovskyi et al., 2011). GusA has a high specific activity and does not require cofactors. Due to its stability and its tolerance to the most commonly used chemicals and assay conditions, it provides high sensitivity (Myronovskyi et al., 2011). The reporter can be used spectrometrically (e.g., p-nitrophenyl-β-D-glucuronide), fluorimetrically (e.g., 4-methylumbelliferyl- β-D-glucuronide), chemiluminescently (e.g., 1,2-di-oxetane- β-D-glucuronide), and chromogenically for visual screening (e.g., 5-bromo-4-chloro-3-indolyl- β-D-glucuronide) (Jefferson, 1989).

Most streptomycetes do not carry the *gusA* gene, making this a simple, inexpensive, and sensitive reporter suitable for them (Myronovskyi et al., 2011). For genetic engineering of actinomycetes in general, *gusA* was set under the control of a *tipA* promoter and cloned into a suicide plasmid such as pKGLP2, which has *oriT* for conjugal transfer of DNA from *E. coli* to *Streptomyces spp.* (Bierman et al., 1992; Myronovskyi et al., 2011). The suicide plasmid was constructed specifically for gene inactivation and contains a second antibiotic resistance gene in addition to the reporter flanked with *loxP* sites for subsequent removal from the genome. The combination of the reporter and the resistance gene ensures that nearly 100% of white clones contain the inactivated gene (Myronovskyi et al., 2011). For *Amycolatopsis sp.* ATCC 39116 the reporter gene *gusA* was also tested. To facilitate screening, it was set under control of the *ermE* promoter and cloned into the plasmid p6sui, linearized with NheI/DraI (Fleige et al., 2016). This plasmid is based on p6apra, which was previously patented as an *E. coli-Amycolatopsis* shuttle vector (Fleige and Steinbüchel, 2014). After plasmid transfer, which was performed by direct transformation of mycelia, apramycin-resistant clones with glucuronidase activity were observed (Fleige et al., 2016). Unfortunately, transformants lacking the deletion construct were also detected. Therefore, they decided to improve the deletion system and use the *rspL* gene instead of *gusA* for further studies (Meyer et al., 2017).

4 Material and Methods

4.1 Strains and plasmids

Amycolatopsis sp. ATCC 39116 was purchased from the ATCC (Manassas, USA). *E. coli* DH5α (Thermo Fisher Scientific, Waltham, USA) was used for plasmid assembly and plasmid maintenance. *E. coli* ET12567 was used as a donor to transfer integrative plasmids to *Amycolatopsis sp*. ATCC 39116 (Kieser et al., 2000). Strains were stored in 30% glycerol stocks at -80°C.

Plasmids and Primer were designed using Clone Manager Professional 9 (Sci Ed Software, Denver, USA). For gene deletion and genomic modification of *Amycolatopsis sp*. ATCC 39116, the plasmid pKG1132 (Myronovskyi et al., 2011) was used (Figure 8.1). All plasmids and strains used in this work are listed in Table 4.1 and Table 4.2.

Table 4.1: Bacterial strains used in this work.

Strains	Description	Reference
Amycolatopsis sp. ATCC 39116	wild-type	ATCC Manassas, USA (Antai and Crawford, 1981)
Amycolatopsis sp. ATCC 39116 MA-1	*ΔcatB- 9302::hyg^R*	This study
Amycolatopsis sp. ATCC 39116 MA-2	*ΔcatB-9302::hyg^R, ΔcatB-18510*	This study
Amycolatopsis sp. ATCC 39116 MA-3	*ΔcatB-9302::hyg^R, ΔcatB-18510, ΔcatB-1440::Pcat_catA-18515*	This study
Amycolatopsis sp. ATCC 39116 MA-4	*ΔcatB-18510*	This study
Amycolatopsis sp. ATCC 39116 MA-5	*ΔcatB-9302::hyg^R, ΔcatB-18510, ΔpcaG-37543::aroY*	This study
E. coli ET12567	*dam-13::Tn9, dcm-6, hsdM, hsdS,* pUZ8002	(Kieser et al., 2000; MacNeil et al., 1992)
E. coli DH5α	*F- Φ80lacZΔM15 Δ(lacZYA-argF) U169 recA1 endA1 hsdR17(rk-, mk+) phoA supE44 thi-1 gyrA96 relA1 λ-*	Thermo Fisher Scientific, Waltham, USA
E. coli GB2005	*derived from DH10B by deleting fhuA, ybcC and recET*	(Wang et al., 2017)

Table 4.2: Plasmids used in this work.

Plasmids	Description	Reference
pKG1132	*gus*A *Am*^{R}	(Myronovskyi et al., 2011)
pKHint31	*hyg*^{R}	(Myronovskyi et al., 2014)
Sset_PL4	pKG1132 derivative, helper plasmid 2.5 *kbp US- catB-9302-DS* 2.5 *kbp*	This study
Sset_PL6	pKG1132 derivative, *Δcat*B-*9302::hyg*^{R}	This study
Sset_PL12	pKG1132 derivative, *Δcat*B-*18510*	This study
Sset_PL13*	pKG1132 derivative, *ΔcatB-1440::Pcat_catA-18515*	This study
Sset_PL20*	pKG1132 derivative, *ΔpcaG-37543::aroY*	This study

*Designed and constructed by Mirjam Selzer (Saarland University)

Genes of interest to be engineered in this work were identified from the genome of *Amycolatopsis sp*. ATCC 39116 (Caspi et al., 2010; Davis et al., 2012; Karp et al., 2010) (Table 4.3).

Table 4.3: Genes considered for genetic engineering of *Amycolatopsis sp.* ATCC 39116.

Gene	Biocyc entry	Accession ID	Length [bp]	Description
catB-9302	AATC3_020100009302	G10GW-1735	1278	Putative muconate lactonizing enzyme
catB-1440	AATC3_020100001440	G10GW-198	1128	Putative muconate lactonizing enzyme
catB-18510	AATC3_020100018510	G10GW-3575	1104	Putative muconate lactonizing enzyme
catA-18515	AATC3_020100018515	G10GW-3576	846	Catechol 1,2-dioxygenase
pcaH-37538	AATC3_020100037538	G10GW-7404	744	Protocatechuate 3,4-dioxygenase subunit beta
pcaG-37543	AATC3_020100037543	G10GW-7405	546	Protocatechuate 3,4-dioxygenase subunit alpha
gcoA-11764	AATC3_020100011764	G10GW-2225	1224	Cytochrome P450 monooxygenase
gcoB-11759	AATC3_020100011759	G10GW-2224	1005	Cytochrome P450 reductase

To enable the conversion of protocatechuate into catechol, the gene *aroY*, encoding protocatechuate decarboxylase (ECL_01944), was inserted (Curran et al., 2013). The protocatechuate decarboxylase was isolated from *Enterococcus cloacae* ATCC 13047 (DSMZ, Braunschweig, Germany).

4.2 Chemicals

Chemicals were obtained from Difco Laboratories (Detroit, MI, USA), Becton Dickinson (Franklin Lakes, NJ, USA), Merck (Darmstadt, Germany), Roth (Karlsruhe, Germany), Sigma Aldrich (Taufkirchen, Germany) and VWR International GmbH (Hannover, Germany), respectively, if not stated otherwise.

4.3 Media

For the preparation of media, only demineralized water was used. To solidify the medium, 20 g L^{-1} agar was added. Culture media and stock solutions were sterilized at 121 °C and 1 bar for 45 min or by filtration (0.2 µm).

4.3.1 Media for genetic engineering

E. coli was cultivated in standard liquid or solid LB-medium (Table 4.4). In the case of *E. coli* ET12567, the medium was additionally amended with 50 µg mL^{-1} kanamycin to maintain the fertilization plasmid. *Amycolatopsis sp*. ATCC 39116 was grown in liquid GYM medium (Table 4.4). To enhance sporulation and screening, a solid GYM medium was used. For the cultivation of strains possessing pKG1132 or derivates, the medium was supplemented with 50 µg mL^{-1} apramycin.

During the conjugation process, apramycin (50 µg mL^{-1}), hygromycin (50 µg mL^{-1}) or nalidixic acid (100 µg mL^{-1}) was added as required. For blue-white screening, the agar was supplemented with 5-bromo-4-chloro-3-indolyl-beta-D-glucuronic acid (X-Gluc 50 µg mL^{-1}) (Myronovskyi et al., 2011).

Table 4.4: Composition of growth media used during genetic engineering.

Media	Compound	Concentration [g L^{-1}]	Comment
LB-medium	NaCl	5.0	Sterilized by autoclaving
	Tryptone	10.0	pH adjusted to 7.0
	Yeast extract	5.0	
GYM-medium	Glucose	4.0	Sterilized by autoclaving
	Yeast extract	4.0	pH adjusted to 7.2
	Malt extract	10.0	*Only used in solid medium
	$CaCO_3$*	2.0	

4.3.2 Media for growth and production studies

The minimal media used for growth and production studies on aromatics (Table 4.5) and aromatics plus sugar (Table 4.6) was modified from a previous recipe (Sutherland, 1986). Before use, they were freshly prepared from sterile stock solutions.

In several experiments, the medium contained spent sulfite liquor ultrafiltration permeate (SSL UF, Borregaard, Snarpsborg, Norway) at a level of 10%. The concentrations of sugars contained in this SSL are measured via HPLC and are shown below (Table 4.6).

Table 4.5: Minimal medium for growth and production studies on aromatic substrates. Cultivations were carried out in MM with and without glucose, plus one additional aromatic compound. The medium was freshly prepared from concentrated stocks. The initial level of the aromatics in the main culture differs between 5 and 75 mM, depending on the experiment. While pre-cultures, grown for a short time of 24 h to raise exponentially growing cells, contained only 10% of the amount.

Stock solution		Compound	Concentration	Comment
Buffer	5x	KH_2PO_4	11.4 g L^{-1}	Sterilized by autoclaving pH adjusted to 7.4
		Na_2HPO_4·	5.0 g L^{-1}	
		$(NH_4)_2SO_4$	15.0 g L^{-1}	
Trace-elements	100x	$ZnSO_4 \cdot 7H_2O$	200.0 mg L^{-1}	Sterilized by filtration
		$MnCl_2 \cdot 4H_2O$	122.2 mg L^{-1}	
		$CoCl_2 \cdot 6H_2O$	40.0 mg L^{-1}	
		$Na_2MoO_4 \cdot 2H_2O$	20.0 mg L^{-1}	
		$CuSO_4 \cdot 5H_2O$	20.0 mg L^{-1}	
EDTA	1000x	Na_2H_2-EDTA$\cdot 2H_2O$	12.7 g L^{-1}	Sterilized by filtration
Salt 1	1000x	NaCl	200.0 g L^{-1}	Sterilized by filtration
Salt 2	1000x	$MgCl_2 \cdot 6H_2O$	200.0 g L^{-1}	Sterilized by filtration
Salt 3	1000x	$CaCl_2$ $2H_2O$	50.0 g L^{-1}	Sterilized by filtration
Iron	1000x	$FeCl_3$ $6H_2O$	7.0 g L^{-1}	Sterilized by filtration
C-source	pure	Guaiacol	9.095 mol L^{-1}	Not sterilized
	250 mM	Catechol	27.5 g L^{-1}	Not sterilized
	250 mM	Methyl-catechol	31.1 g L^{-1}	Not sterilized
	200 mM	Benzoate	24.2 g L^{-1}	Not sterilized
	250 mM	*o*-Cresol	27.0 g L^{-1}	Not sterilized
	pure	*m*-Cresol	9.560 mol L^{-1}	Not sterilized
	200 mM	*p*-Cresol	27.0 g L^{-1}	Not sterilized
	250 m	Phenol	23.5 g L^{-1}	Not sterilized
	pure	Toluol	9.409 mol L^{-1}	Not sterilized
	200 mM	*p*-Coumarate	32.8 g L^{-1}	Not sterilized
	500 mM	*cis*, *cis*- Muconic acid	71.1 g L^{-1}	Not sterilized
	65 mM	Vanillin	10 g L^{-1}	Not sterilized
	65 mM	Vanillate	10.9 g L^{-1}	Not sterilized
	81 mM	Protocatechaute	12.5 g L^{-1}	Not sterilized
	100x	Glucose H_2O	550.0 g L^{-1}	Sterilized by autoclaving

Table 4.6: Medium for growth studies on various sugars. Cultivations were carried out in MM containing only one sugar, a combination of sugars, or SSL as substrate for growth. In some cases, aromatics were added. The medium was freshly prepared from concentrated stocks.

Stock solution		Compound	Concentration	Comment
Buffer	10x	MOPS	209.26 g L^{-1}	Sterilized by autoclaving pH adjusted to 7.2
Trace-elements	100x	$ZnSO_4 \cdot 7H_2O$	200.0 mg L^{-1}	Sterilized by filtration
		$MnCl_2 \cdot 4H_2O$	122.2 mg L^{-1}	
		$CoCl_2 \cdot 6H_2O$	40.0 mg L^{-1}	
		$Na_2MoO_4 \cdot 2H_2O$	20.0 mg L^{-1}	
		$CuSO_4 \cdot 5H_2O$	20.0 mg L^{-1}	
P-source	100x	K_2HPO_4	23.0 g L^{-1}	Sterilized by filtration
EDTA	1000x	Na_2H_2-EDTA$\cdot 2H_2O$	12.7 g L^{-1}	Sterilized by filtration
Salt 1	1000x	NaCl	200.0 g L^{-1}	Sterilized by filtration
Salt 2	1000x	$MgCl_2 \cdot 6H_2O$	200.0 g L^{-1}	Sterilized by filtration
Salt 3	1000x	$CaCl_2$ $2H_2O$	50.0 g L^{-1}	Sterilized by filtration
C-source	pure	Guaiacol	9.095 mol L^{-1}	Not sterilized
	65 mM	Vanillin	10 g L^{-1}	Not sterilized
	65 mM	Vanillate	10.9 g L^{-1}	Not sterilized
	10x	L-Arabinose	50.0 g L^{-1}	Sterilized by autoclaving
	100x	D-Galactose	500.0 g L^{-1}	Sterilized by autoclaving
	10x	D-Mannose	50.0 g L^{-1}	Sterilized by autoclaving
	10x	L-Rhamnose	50.0 g L^{-1}	Sterilized by autoclaving
	100x	D-Xylose	500.0 g L^{-1}	Sterilized by autoclaving
	100x	Glucose H_2O	550.0 g L^{-1}	Sterilized by autoclaving
10 % SSL	8.8 %	Glucose	~4.5 g L^{-1}	Not sterilized (SSL UF, Borregaard, Snarpsborg, Norway) Concentrations were measured using HPLC
	27.7 %	D-Mannose	~9 g L^{-1}	
	5.3 %	D-Galactose	~3 g L^{-1}	
	0.6 %	L-Rhamnose	~0.3 g L^{-1}	
	12.1 %	D-Xylose	~6 g L^{-1}	
	2.5 %	L-Arabinose	~1.5 g L^{-1}	

4.4 Genetic engineering of *Amycolatopsis sp.* ATCC 39116

The molecular methods used are based on standard protocols (Becker et al., 2013; Kieser et al., 2000; Myronovskyi et al., 2011). The genetic engineering of *Amycolatopsis sp*. ATCC 39116 was based on homologous recombination (Myronovskyi et al., 2011). Typically, 2,500 bp long flanking regions were used to enable the recombination process.

Briefly, plasmids were assembled *in vitro*, transformed into *E. coli* DH5α (heat shock), amplified, isolated, transformed into *E. coli* ET12567 (electroshock), and then transferred into *Amycolatopsis sp.* ATCC 39116 using conjugation. Finally, a blue-white screening system was used to distinguish between wild-type and mutant clones. Appendix Table 8.1. provides the primers used for plasmid construction, screening, and sequencing.

4.4.1 Isolation of nucleic acids

Genomic DNA was isolated using the GeneElute TM Kit according to the manufacturer's instructions (Sigma Aldrich, Taufkirchen, Germany). To improve PCR results, the genomic DNA from *Amycolatopsis sp.* ATCC 39116 was digested with *Eco*RV, followed by purification using the Wizard ® SV Gel and PCR Clean-Up System (Promega, Fitchburg,WI, USA).

Plasmid preparation was conducted using the QIAprep Spin Miniprep (Qiagen, Hilden, Germany). All nucleic acids were eluted with pre-warmed demineralized water (65 °C) and stored at -20 °C. DNA concentration was determined spectrophotometrically (NanoDrop ® 1000, Thermo Fisher Scientific, Waltham, MA, USA).

4.4.2 Amplification of nucleic acids

PCR (Mullis et al., 1986) was performed for the amplification of nucleic acids and strain validation. PCR was carried out in the Tgradient thermocycler (Analytik Jena AG, Jena, Germany) using a polymerase master-mix, DMSO, DNA as a template, and sequence specific primers (Table 8.1). The amplification of nucleic acids and the attachment of homologous overhangs were performed using the Phusion High-Fidelity Polymerase master mix with GC buffer (Thermo Fisher Scientific, Waltham, MA, USA).

To analyze competent *E. coli* cells, colony PCR was performed. For this purpose, colonies growing on an agar plate were picked with a toothpick and added to the PCR master mix, which also contained the primers 43 and 44 (Table 8.1). The primers bound upstream and downstream of the multiple cloning site. Strain verification was carried out using the Phire Hot Start II PCR master mix (Thermo Fisher Scientific, Waltham, MA, USA). PCR was carried out using the following temperature profile:

Table 4.7: Standard PCR-program.

Number of cycles	Temperature [°C]	Time [s]
1 x	98	120
30 x	98	30
	X	30
	72	XX
1 x	72	420
1 x	4	Pause

X = Annealing-temperature determined by Wallace's rule; XX = 30 s kb^{-1} Phusion HighFidelity Polymerase or 10 to 15 s/kb using Phire Hot Start II PCR

The PCR products obtained were purified using the Wizard ® SV Gel and PCR Clean-Up System (Promega, Fitchburg, WI, USA). All nucleic acids were eluted from the columns with pre-warmed 65 °C demineralized water. The DNA concentration was determined spectrophotometrically (NanoDrop ® 1000, Thermo Fisher Scientific, Waltham, MA, USA). The PCR products were then analyzed by agarose gel electrophoresis and stored at -20 °C until further use.

4.4.3 Assembly of nucleic acids

For plasmid construction, nucleic acids were assembled *in vitro* (Gibson et al., 2009). The inserts were assembled with a linearized vector using 20 bp homologous overhangs. To create these overhangs, the forward and reverse gene priming sequences were fused at their 5′ ends to a 20-nucleotide long sequence homologous to the neighboring target fragment.

The reaction mixture for the assembly, prepared in-house, contained 157.5 mM Tris·HCl (pH 7.5), 15.75 mM $MgCl_2$, 0.3 mM dNTPs, 15.75 mM DTT, 42 mg μL^{-1} PEG-800, 0.6 mg μL^{-1} NAD, 4 U μL^{-1} Taq Ligase (Thermo Fisher Scientific, Waltham, MA, USA), 25 mU μL^{-1} Phusion High-Fidelity DNA Polymerase (Thermo Fisher Scientific, Waltham, MA, USA), and 7.5 mU μL^{-1} T5 exonuclease (Epicentre, Madison, USA) (Rohles et al., 2016). The master mix was stored in 15 µL aliquots at -20 °C.

Firstly, the vector pKG1132 was linearized using *Eco*RV (FastDigest, Thermo Fisher Scientific, Waltham, MA, USA). Vector and PCR fragments were added to the master mix in a 1:3 vector insert ratio and made up to 5 µL with sterile demineralized water. The reaction mixture was stored at 50 °C for 1 hour. Then 5 µL were transformed into *E. coli* DH5α by heat shock. Assembled plasmids were isolated (Section 4.4.1) and further analyzed by enzymatic digestion and sequencing (LightRun, Eurofins Genomics Germany GmbH, Ebersberg, Germany).

4.4.4 Enzymatic digestion

For the linearization of vectors and the validation of plasmids, enzymatic digests were performed using FastDigest enzymes from Thermo Fisher (Waltham, MA, USA). For analytical digestions, 200 ng plasmid DNA was used. To obtain a sufficient amount of linearized vector for the assembly, 10 µg of plasmid was digested overnight at 37 °C and subsequently purified (Wizard ® SV Gel and PCR Clean-Up System, Promega, Fitchburg,WI, USA). Enzymatic digests were analyzed by gel electrophoresis.

4.4.5 Gel electrophoresis

Amplified, digested, and linearized DNA was analyzed by electrophoretic separation in a 1% agarose gel. For preparation, 5 g of agarose was dissolved in a boiling 1xTAE solution. The gel was poured and subsequently run in an Owl D2 system (Thermo Scientific, Marietta, OH, USA) with 1x TAE buffer at 120 V (PowerPac TM 300 BioRad Laboratories, Hercules, CA, USA). Before loading, samples were prepared in a ratio of 1:10 with OrangeG loading dye (Table 4.8). To estimate the size of DNA fragments, the O'GeneRulerTM 1 kb DNA ladder (ready-to-use, Fermentas, St. Leon-Roth, Germany) was used. After electrophoresis, gels were incubated in a 2.5 mg L^{-1} ethidium bromide bath. The stained gel was analyzed under UV light (ChemiDoc XRS+ System, BioRad Laboratories, Hercules, CA, USA).

Table 4.8: Composition of buffers used for gel electrophoresis.

Buffer	Concentration	Compound
1x TAE	0,04 M 0,02 M 1,00 mM	Pufferan® Tris Acetic acid EDTA- Na_2
10x Orange G	20 g 100 mg	Sucrose OrangeG ad 50 mL H 2 O

4.4.6 Transformation

Heat-shock-competent *E. coli* DH5α cells were generated by $CaCl_2$ treatment (Inoue et al., 1990). For transformation, 50 µL of competent cells were mixed with 1 µL of plasmid DNA or 5 µL of assembly solution and incubated on ice for 30 minutes. Heat shock was performed at 45 °C for 45 seconds (Thermomixer, Eppendorf, Hamburg, Germany). The cells were chilled on ice for 5 minutes, then mixed with 950 µL of sterile LB medium and incubated at 37 °C and 900 rpm for 1 hour. For selection purposes, the mixture was plated on LB^{apr} agar and incubated for 24 hours at 37 °C. The following day, agar plates were examined for colony formation. The recombinant *E. coli* colonies were further analyzed by PCR or enzymatic digestion.

For transformation *of E. coli* ET12567, electroporation was performed. Cells were grown overnight in 15 mL of LB medium containing kanamycin and apramycin. The overnight culture was transferred to a 500 mL shake flask containing 35 mL of fresh medium and incubated at 37 °C for 3 hours. Cells were then harvested by centrifugation (5,000 x *g*, 10 min, 4 °C), washed with 2 mL of ice-cold sterile water, and aliquoted into sterile Eppendorf tubes. Cells were centrifuged at 2,700 x *g* for 1 minute again and washed with 1.5 mL of ice-cold water. After a further round of centrifugation, the supernatant was discarded and cells were suspended in 1.5 mL of ice-cold 10% glycerol and centrifuged again. Finally, cells were suspended in 100 µL of ice-cold 10% glycerol. Then, 1 µg plasmid DNA was pipetted to the cell aliquots. The electroporation was carried out at 2 kV, 400 Ω and 25 µF, using a MicroPulser electroporator (BioRad Laboratories, Hercules, CA, USA). Subsequently, 900 µL of pre-warmed LB medium was added, and cells were incubated at 37 °C and 550 rpm for 1.5 h (Thermomixer, Eppendorf, Hamburg, Germany).

For selection purposes, cell suspension was plated on $LB^{apr + kan}$ agar. Plates were incubated for 24 hours at 37 °C. For verification, obtained *E. coli* colonies were further analyzed by enzymatic digestion, or PCR.

4.4.7 Conjugation

Amycolatopsis sp. ATCC 39116 was modified using homologous recombination (Myronovskyi et al., 2011). Therefore, non-replicative plasmids with 2,500 bp long flanking regions were transformed into the microbe using conjugation. The cloning host *E. coli* ET12567/pUZ8002 is a methylation defective cloning host, used for conjugal transfer of DNA from *E. coli* to Streptomyces (MacNeil et al., 1992).

First, *Amycolatopsis sp.* ATCC 39116 (recipient) was grown on GYM agar for about 3 days at 30 °C to generate spores. Competent *E. coli* ET12567 (donor) was grown on $LB^{apr + kan}$ agar overnight at 37 °C. Agar plates were overlaid with 5 mL of liquid GYM medium, and cells and spores were removed with a plastic inoculating loop. The supernatant was transferred into sterile Eppendorf tubes. For conjugation, 1.5 mL suspensions of both the donor and recipient were mixed. This mixture was spread on GYM agar plates and kept at 30 °C for 14 hours. To generate a selection pressure and remove *E. coli,* the overgrown agar plates were then overlaid with a mixture of liquid GYM and 10 µL each of nalidixic acid and apramycin. Agar plates were incubated for additional two days at 37 °C. Then, new colonies were transferred onto fresh $GYM^{apr + nal}$ agar. After 24 hours of incubation at 37 °C, cells were further analyzed by blue-white screening. To improve efficiency, a hygromycin resistance gene (Sset_PL6) was introduced in *Amycolatopsis sp*. ATCC 39116 and hygromycin was used to get rid of *E. coli* ET12567 instead of nalidixic acid.

4.4.8 Blue-white screening

After the first recombineering event in *Amycolatopsis sp*. ATCC 39116, a blue-white screening system was used to distinguish between wild-type (white) and mutant clones (blue). For this purpose, 3 µL of X-Gluc was pipetted onto newly grown colonies and incubated at 30 °C for 20 min (Myronovskyi et al., 2011). The evaluation was based on the resulting color. If the plasmid integration was successful, the colony turns blue, otherwise, it remains white. To force the second recombineering event, a blue colony was grown at 30 °C for 24 h in liquid GYM medium without selection pressure.

Cells were then plated on GYM$^{X\text{-}Gluc}$ agar and incubated overnight at 37 °C. The differentiation between mutants and wild types was carried out using colony PCR. For this purpose, white colonies were examined for the desired mutation. This was done using two specific primers that bound upstream and downstream of the target mutation.

4.4.9 Construction of the plasmid pKG1132 for genomic modifications

To simplify the genetic engineering *of Amycolatopsis sp*. ATCC 39116, a blue-white screening with GusA (UidA) was established (Myronovskyi et al., 2011). Therefore, a DNA fragment, containing the β-glucuronidase gene (*gusA*, NP_416134 from *E. coli*) under the control of the *tipA* promoter, was amplified and digested with BglII (Murakami et al., 1989). The *tipA* promoter is a leaky promoter in streptomyces (Myronovskyi et al., 2011). Subsequently, this fragment was cloned via ligation into the BglII site of pKC1132 (Bierman et al., 1992). The plasmid was designated pKG1132 (Figure 8.1) (Bierman et al., 1992; Myronovskyi et al., 2011).

4.4.10 Construction of the deletion mutant Amycolatopsis sp. ATCC 39116 MA-1

Deletion of *catB*-9302 was achieved by a simultaneous integration of a hygromycin resistance gene into the *catB*-9302 locus and deletion of *catB*-9302. To construct this particular plasmid, the entire locus of *catB*-9302 plus 2,500 bp upstream and downstream was amplified using primers Sset_PR1 and Sset_PR2. This fragment was cloned into the EcoRV site of pKG1132 by blunt end ligation using a T4 DNA ligase (Thermo Fisher, Waltham, MA, USA). The new plasmid Sset_PL4 was transformed into *E. coli* GB2005 cells. In the next step, the *catB*-9302 gene was replaced with the hygromycin resistance gene using ET recombination (Zhang and Buchholz, 1998). For this purpose, the hygromycin resistance gene was amplified from the pKHint31 plasmid and fused with 50 bp overhangs that are homologous to the upstream and downstream flanking regions of *catB*-9302 (Sset_PR13 and Sset_PR14). To remove the resistance gene later, additional recombinase recognition sites located upstream and downstream of the resistance gene on pKHint31 were amplified, too (Siegl and Luzhetskyy, 2012). In the next step, the linear selection marker with 50 bp homologous overhangs was transformed into *E. coli* GB2005, already possessing the target plasmid Sset_PL4. In addition to the description in Section 4.4.6, the cells were induced with l-arabinose after 2 hours to express the lambda red recombinase.

After electroporation, cells were plated on LB^{hyg} agar. The new plasmid was named Sset_PL6 (Figure 8.2) and verified by sequencing (LightRun, Eurofins Genomics Germany GmbH, Ebersberg, Germany). This plasmid was used for homologous recombination in the wild-type strain *Amycolatopsis sp.* ATCC 39116. In further conjugations, the hygromycin resistance was used to remove the helper strain *E. coli* ET12567.

4.4.11 Construction of Amycolatopsis sp. ATCC 39116 mutants in general

Genetic modification relied on homologous recombination, using the integrative plasmid pKG1132 (Figure 8.1), which is non-replicative in *Amycolatopsis sp.* ATCC 39116. To construct a deletion plasmid, 2,500 bp upstream and downstream of the target gene were amplified by PCR using primer pairs with 20 bp long overhangs for assembly (Table 8.1). Between the upstream and downstream flanking regions, the translational start codon of the target gene was left adjacent to the stop codon. In the case of integration of the *catA*-18515 gene and *aroY* gene, the gene sequence was inserted between the flanking regions. The fragments were assembled into the EcoRV site of pKG1132. The assembled plasmids (Appendix 8.2) were further analyzed by enzymatic digestion and sequencing (LightRun, Eurofins Genomics Germany GmbH, Ebersberg, Germany).

4.5 Low-temperature hydrothermal conversion of lignin

In several experiments the medium contained lignin hydrolysate. To obtain this hydrolysate, 5 g of lignin (IndulinAT, S3Chemicals, Bad Oeynhausen, Germany) was suspended in 250 mL of deionized-water and then hydrolyzed in a sealed 500 mL stirred stainless steel pressure vessel (4575A, Parr Instruments, Moline, IL, USA). The speed of the stirrer was adjusted to 400 rpm. The reactor was purged five times with nitrogen gas. Subsequently, the reactor was heated up to 330 °C and 130 bar, 350 °C and 165 bar, or 370 °C and 210 bar. After reaching the desired temperature, hydrothermal conversion was conducted for 20 minutes. After the time had elapsed, an internal cooling coil with cold water (8 °C) and a fan were used to cool down the reactor (80 °C).

Before the reactor was opened, it was flushed 3 times with nitrogen. The depolymerized lignin was freed from debris using centrifugation (10,000 × g, 5 min), and the resulting supernatant (250 mL) was concentrated using steam distillation. Distillation was carried out for 3 h in a 500 mL flask, which was stored in an oil bath (120 °C) and linked to a water-cooled Liebig condenser. Tap water (8 °C) was used as cooling liquid. The hydrolysis process was conducted by Sören Stark from Saarland University (Starck, 2020).

4.6 Hydrothermal hemicellulose conversion

Hemicellulose (Bolise Co., Ltd., Xiamen, China) was suspended in deionized water and hydrolyzed at 200 °C in a 500 mL stirred (400 rpm) stainless steel pressure vessel (4575A, Parr Instruments, Moline, IL, USA). The reactor was purged five times with nitrogen gas. At the end of the selected reaction time, the reactor was cooled down. For this purpose, an internal cooling coil with cold water (8 °C) and a fan were used. The reactor was emptied at 85 °C. The obtained hydrolysate was centrifuged to remove debris (10,000 x g, 5 min, room temperature). To remove furfural from the supernatant, steam distillation was used. For this purpose, the supernatant was poured into a 500 mL distillation flask. It was then stored in an oil bath at 130 °C and linked to a water-cooled Liebig condenser. Tap water (8 °C) was used as a cooling liquid. Distillation was continued for 30 min. The distillate contained furfural. The conversion was conducted by Sören Stark from Saarland University (Starck, 2020).

4.7 Cultivation of *Amycolatopsis sp.* ATCC 39116

Amycolatopsis sp. ATCC 39116 was grown in baffled shake flasks with either minimal or GYM liquid medium, with a 10% filling volume for each. Sterile glass beads were added until the bottom was completely covered (≈5 mm, Sigma Aldrich, Taufkirchen, Germany). An inoculation loop with cell material from a one-day incubated plate culture (37 °C) was used to inoculate the pre-culture. The pre-culture was incubated for 24 hours at 37 °C. Then cells were harvested (5 min, 8,000 ×*g*, room temperature) during the exponential growth phase and used for inoculation. The main cultures were carried out in triplicate at 37 °C (if it not stated otherwise), and with a shaking frequency of 230 rpm on an orbital shaker (Multitron, Infors AG, Bottmingen, Switzerland). The humidity control has been set to 85% relative humidity.

4.8 Fed-batch production of MA in lab-scale bioreactors

The genetically engineered MA producer strain was tested in a fed-batch process to determine its production efficiency. The cultivation was carried out in 250 mL bioreactors (SR0700ODLS, DASGIP AG) at 37 °C using the CWD4 bio-block (DASGIP AG, Jülich, Germany). The pH was measured using a pH electrode (Mettler Toledo, Giessen, Germany) and kept constant at 7.2 ± 0.1 by automatic addition of 6 M NaOH (MP8 pump system, Eppendorf, Hamburg, Germany). The pO_2 was monitored with a pO_2 electrode (Hamilton, Höchst, Germany) and kept above 30% of saturation by adjusting the aeration rate and the stirrer speed. Initially, the batch contained 100 mL of minimal medium with 5 mM guaiacol and 6 g L^{-1} glucose. For inoculation, cells were prepared as described above. During the feeding phase, guaiacol from a non-sterile, pure feed (9 M) was added repeatedly after it had been consumed by the cells. The guaiacol content was determined by HPLC during cultivation. For data acquisition and process operations, DASGIP control software (DASGIP AG) was used.

4.9 Cell concentration

The cell concentration was measured spectrophotometrically (UV-1600PC spectrometer, Radnor, PA, USA) as optical density at 600 nm.

4.10 GC-MS analysis of metabolites

To examine the transformation of *o*-cresol, the labeling pattern of muconic acid and its derivates was analyzed after derivatization into t-butyl-dimethylsilyl derivates (Becker et al., 2013). To do this, nitrogen gas was used to dry 100 µL of culture supernatant. This was then mixed with 50 µL of di-methylformamide (0.1% pyrimidine) and 50 µL of N-methyl-N-tert-butyldimethylsilyltrifluoracetamid (Macherey and Nagel, Düren, Germany) and incubated for 30 minutes at 80 °C. Then, the derivatives were analyzed by GC-MS (GC/MS 7890A, 5975C quadrupole detector, Agilent Technologies, Santa Clara, CA, USA) (Lange et al.,2017).

4.11 Quantification of aromatics, *cis,cis*-muconic acid and its derivatives

Aromatics and MA were analyzed and quantified by HPLC (1260 Infinity, Agilent, Waldbronn, Germany). A reversed phase column (Nucleodur C18 Isis, 3 µm, Macherey Nagel, Düren, Germany), a gradient of 0.025% H_3 PO_4 (Eluent A) and acetonitrile (Eluent B) at 25 °C and a flow rate of 1 mL min^{-1} were used to separate the analytes. Two different gradients were used, depending on the analytes of interest (Table 4.10, Table 4.12). Analytes were determined by UV absorption at compound specific wavelengths (Table 4.9,

Table 4.11). External standards were used for quantification. 2-Methyl-MA, which was produced from *o*-cresol in some experiments, did not interfere with the analytes listed in Table 4.9.

Table 4.9: Aromatic compounds that can be separated with gradient A.

Compound	wavelength [nm]	Retention time [min]
cis-,cis-Muconic acid	260	3.2
Catechol	210	3.9
Phenol	210	5.6
Guaiacol	210	6.2
o-Cresol	210	7.4

Table 4.10: Gradient A used in this work.

Time [min]	Eluent A [%]	Eluent B [%]
0.0-13.8	100-31	0-69
13.8-14.3	31-0	69-100
14.3-17.3	0	100
17.3-17.8	0-100	100-0
17.8-24.0	100	0

Table 4.11: Aromatic compounds that can be separated with gradient B.

Compound	wavelength [nm]	~Retention time [min]
cis-cis-Muconic acid	260	4.2
Protocatechuate	210	3.9
Catechol	210	4.5
cis-trans-Muconic acid	260	5.2
4-Hydroxybezoate	260	5.4
Vanillic acid	220	6.3
Caffeic acid	325	6.6
Vanillin	230	7.5
p-Coumarate	325	8.2
Guaiacol	210	8.7
Ferulic acid	325	8.8
Phenol	210	9.1
Benzoic acid	230	9.9
o-Cresol	210	11.3

Table 4.12: Gradient B used in this work.

Time [min]	Eluent A [%]	Eluent B [%]
0.0-1.0	99	1
1.0-13.8	99-67	1-33
13.8-14.3	67-0	33-100
14.3-17.3	0	100
17.3-17.8	0-99	100-1
17.8-24.3	99	1

4.12 Quantification of sugars

Separation of glucose, xylose, mannose, arabinose, and galactose was performed by isocratic HPLC (1260 Infinity Series, Agilent) and carried out on an Aminex HPX-87H column (300 × 7.8 mm; Bio-Rad) at 85 °C (Starck, 2020). Deionized water was used as mobile phase (flow rate, 0.5 mL min^{-1}). Because of co-elution, rhamnose concentration could only be determined if the sugar was present alone. The detection was performed via refraction index analysis at 55 °C. For quantification, external standards were used.

4.13 Enzymatic activity of the catechol oxygenase

The properties and activity of the catechol-dioxygenase (CatA-18515), were studied by an enzyme assay (Jimenez et al., 2014). For this purpose, cells were grown in minimal medium. During exponential growth, cells were harvested by centrifugation (5 min, 8,000× g, room temperature), washed in 60 mM Tris-HCL-buffer (pH 8.2) and disrupted in a ribolyzer (Precellys-24, PeqLab, Hannover, Germany), using pre-packed lysis tubes (0.1 mm silica spheres, Lysing Matrix B, MP Biomedicals, Heidelberg, Germany). Cells were destroyed in three intervals (3 × 30 s, 6 ms^{-1}), with 1 min breaks on ice in between. The cell debris was then removed and proteins quantified as previously described in Becker *et al.*, 2009. The reaction mixture for enzymatic analysis contained 100 µL mL^{-1} crude cell extract, 30 mM Tris-HCl buffer (pH 8.2) and 20 µM catechol. In further experiments, catechol was substituted by equimolar amounts of 3- and 4-methyl catechol. Negative controls were carried out without substrate and cell extract, respectively. The reaction was monitored by absorbance measurement at 260 nm (Specord 40; Analytik Jena, Jena, Germany). The observed increase in absorption reflected the accumulation of MA (ε = 16,800 M^{-1} cm^{-1}) (Jimenez et al., 2014). When studying the conversion of methylated derivatives, the same extinction coefficient was considered.

5 Results

5.1 *Amycolatopsis sp*. ATCC 39116 utilizes guaiacol-rich lignin hydrolysates

Initial studies aimed to evaluate *Amycolatopsis sp*. ATCC 39116 with respect to its natural potential to utilize aromatics as sole carbon source, grow on aromatic-rich lignin hydrolysates and natively accumulate *cis,cis*-muconic acid.

5.1.1 Aromatic substrate spectrum of the wild-type

The wild-type *Amycolatopsis sp.* ATCC 39116 was grown in minimal medium on different aromatics intended to reflect aromatics from waste products of the pulp and paper industry. Consistent with previous work (Pometto et al., 1981; Sutherland, 1986; Sutherland et al., 1983) the microbe was able to utilize various aromatic compounds in addition to MA (Table 5.1), namely vanillin, vanillate, protocatechuate, benzoate, *p*-coumarate, guaiacol, catechol, phenol, toluene, *o*-cresol, and *m*-cresol. The broad spectrum indicated good potential to utilize the rather crude aromatic-mixtures expected from lignin hydrolysates (Antai and Crawford, 1981; Kohlstedt et al., 2018; Salvachua et al., 2015).

Table 5.1: Utilization of aromatics and catabolic intermediates by *Amycolatopsis sp.* ATCC 39116. The strain was grown in minimal medium containing 2 mM of the substrate to be tested at 37 °C. The control was carried out without substrate. Growth was measured as optical density (OD_{600nm}) after 40 hours of incubation. Growth efficiency is stated as follows: OD < 0.25, /; 0.25 < OD < 0.5, +; 0.5 < OD < 1, ++; OD > 1, +++.

Aromatics	Growth
Vanillin	+ + +
Vanillate	+ + +
Protocatechuate	+ + +
cis,cis-Muconic acid	+ + +
Benzoate	+ + +
p-Coumarate	+ + +
Guaiacol	+ +
Catechol	+ +
Phenol	+ +
Toluene	+
o-Cresol	+
m-Cresol	+
3-Methyl-catechol	+
4-Methyl-catechol	/
Control	/

5.1.2 Wild-type accumulates MA from guaiacol on a milligram scale

The utilization of guaiacol was considered particularly important, as guaiacol is the predominant building block of softwood lignin (Pandey and Kim, 2011), and was therefore investigated further. The wild-type tolerated guaiacol up to 25 mM (Figure 5.1 B).

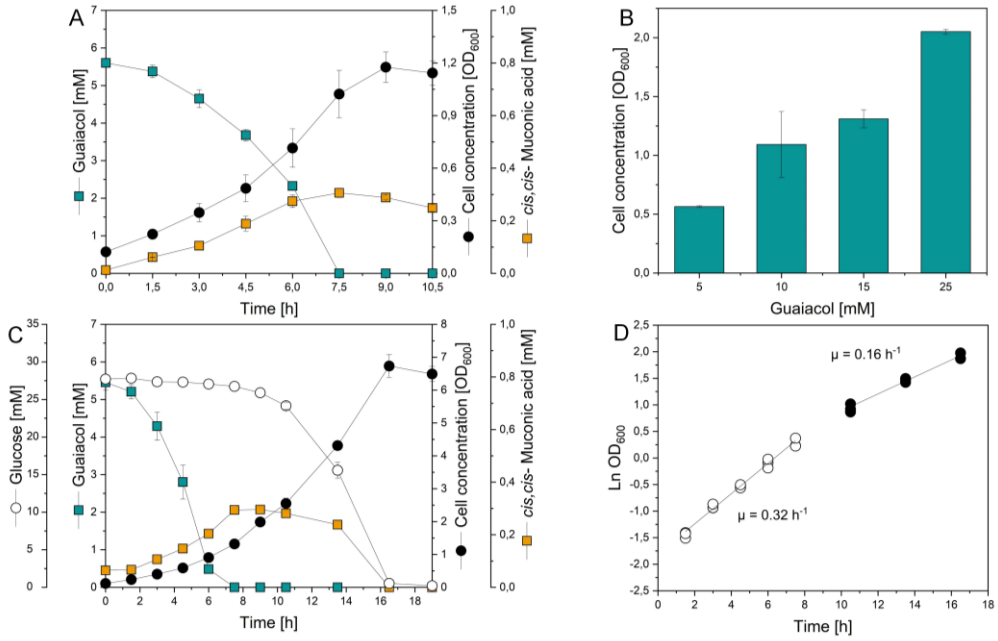

Figure 5.1: Growth physiology of *Amycolatopsis sp.* ATCC 39116 on guaiacol. *Amycolatopsis sp.* ATCC 39116 was grown in minimal medium containing 5 mM guaiacol as C-source (A). After 24 hours, the cell concentration was compared. All cultures were inoculated to an initial OD of 0.1, but the media contained different amounts of guaiacol (B). Growth dynamics of *Amycolatopsis sp.* ATCC 39116 in minimal medium containing 5 mM guaiacol and 5 mM glucose (C). The data shown in A, B, and C reflect mean values and deviations from three biological replicates, whereas the subfigure D, illustrating the specific growth rate during different phases, shows all individual data points from the corresponding experiment.

Amycolatopsis sp. ATCC 39116 immediately started to grow and consume guaiacol (Figure 5.1 A). Notably, a slight but significant accumulation of MA was observed, reflecting approximately 5%. The cells exhibited an exponential specific growth rate of 0.30 h^{-1}. Guaiacol was completely consumed within 7 h, which then triggered the reuptake of MA. Considering the goal to convert guaiacol to MA in later stages, which would require a second substrate for growth (van Duuren et al., 2011), glucose was added in a second experiment (Figure 5.1 C). Here, too, the cells began to grow immediately, with guaiacol being preferred to glucose. In this experiment, the specific growth rate was slightly increased (μ = 0.32 h^{-1}). This could indicate a synergistic use of the two substrates (Figure 5.1 D). Interestingly, *Amycolatopsis sp.* ATCC 39116 exhibited a higher specific growth rate on guaiacol than on glucose 0.16 h^{-1}. A slight accumulation of MA was also observed here (Figure 5.1 C). After guaiacol was depleted, MA and glucose were metabolized together, with glucose being the preferred substrate.

5.1.3 Low-temperature hydrothermal conversion of softwood lignin

In order to enable the production of MA from real lignin using *Amycolatopsis sp*. ATCC 39116, depolymerization of softwood kraft lignin into small aromatics should be coupled with the biotransformation. For this purpose, hydrothermal conversion (HTC) of lignin was carried out under different conditions (Figure 5.2). HTC was conducted by Sören Starck (Saarland University) (Starck, 2020).

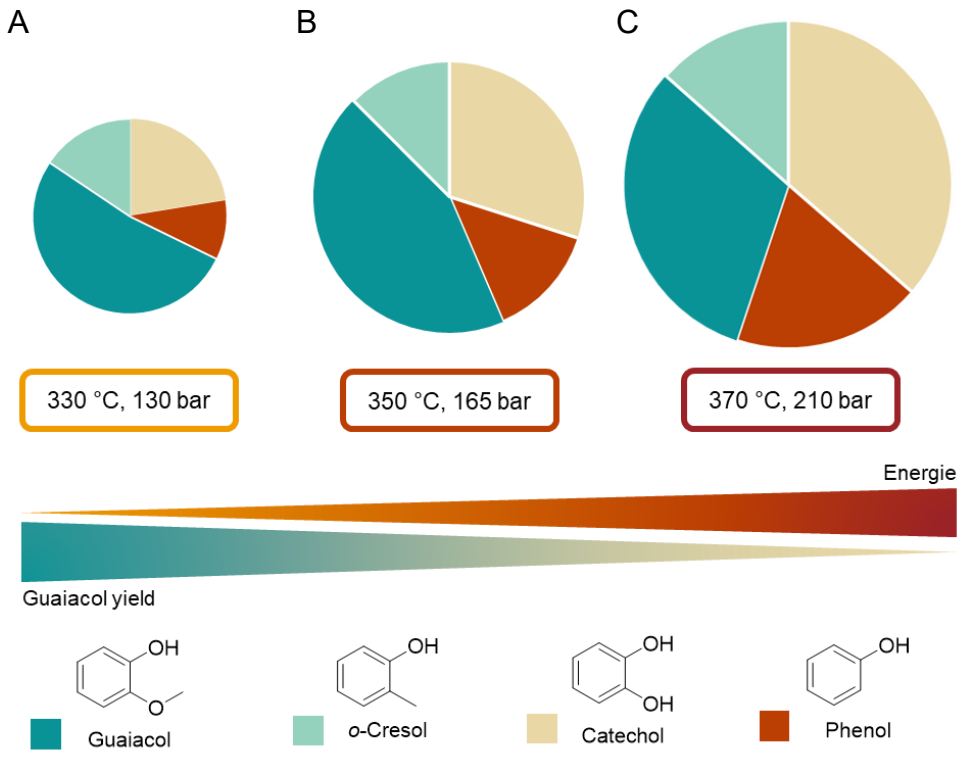

Figure 5.2: Hydrothermal conversion of lignin into small aromatic compounds. Softwood lignin was suspended in water and depolymerized in a pressure vessel for 20 min at 330 °C and 130 bar, 350 °C and 165 bar, 370 °C and 210 bar. Subsequently, debris was removed from the hydrolysate. HPLC analysis revealed that the hydrolysate contains guaiacol, catechol, phenol, and *o*-cresol. The composition of the hydrolysates can be seen in the cake diagram for each condition. The size of the circle illustrates the total amount obtained. Hydrothermal conversion at 370 °C (C) yielded in 12% aromatic monomers. The yields at 350 °C (B) and 330 °C (A) relate to the size of the corresponding circles, respectively 8% and 4%. HTC was conducted by Sören Starck (Saarland University) (Starck, 2020).

First, HTC of lignin was carried out at 350 °C and 165 bar, resulting in a total yield of aromatic monomers of 8%. The hydrolysate contained large amounts of guaiacol (44%), as well as catechol (30%), phenol (14%) and *o*-cresol (12%). A further test at a lower temperature (330 °C, 130 bar) increased the guaiacol yield up to 52% but reduced the overall yield to 4%. The highest yield of aromatics (12%) was achieved at 370 °C and 210 bar, and the hydrolysate obtained contained only the 4 aromatic monomers. The product spectrum shifted slightly towards phenol and catechol. The guaiacol yield dropped to 31%, but is still significant. The total yield of aromatics varied with temperature. The higher the temperature, the higher the aromatic yield. For future experiments, these conditions were chosen to produce lignin hydrolysate. For further use, the hydrolysate was freed from debris by centrifugation, and the supernatant was concentrated by steam distillation. During subsequent steam distillation, catechol was removed. Overall, the entire process resulted in an aqueous solution that contained 7 g L^{-1} guaiacol, 3 g L^{-1} *o*-cresol, and traces of phenol (0.2 g L^{-1}).

5.1.4 Wild-type metabolizes aromatics contained in depolymerized lignin

It was important to see if *Amycolatopsis sp.* ATCC 39116 was able to utilize the depolymerized lignin. In a growth study, the bacterium was grown in a minimal medium, containing the obtained softwood lignin hydrolysate and glucose (Figure 5.3).

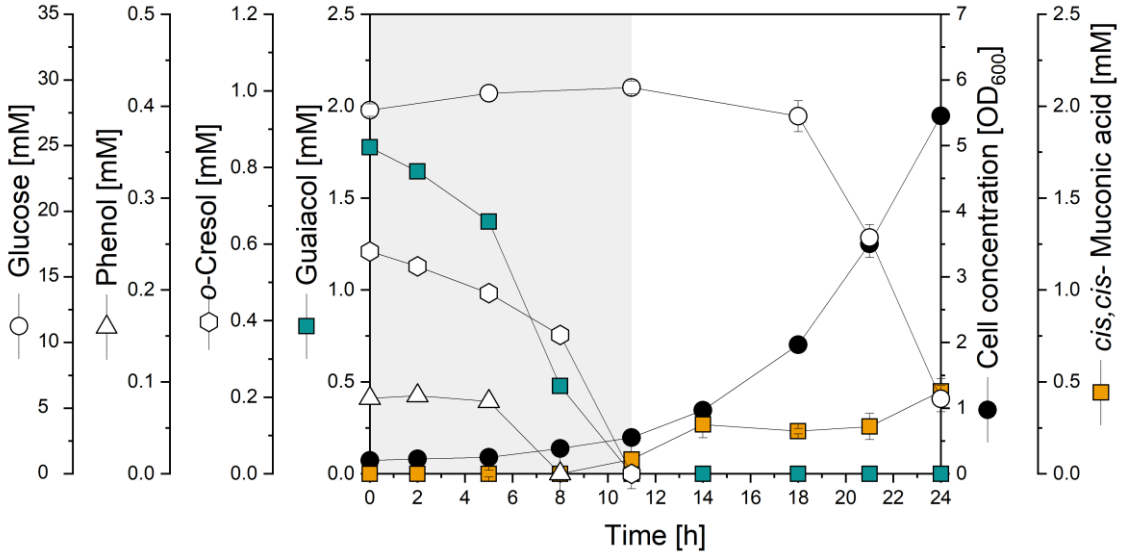

Figure 5.3: *Amycolatopsis sp.* ATCC 39116 utilizes the softwood lignin hydrolysate. It was grown in a minimal medium with glucose and lignin hydrolysate. The hydrolysate was produced through hydrothermal conversion, followed by aromatic enrichment by distillation. The incubation temperature was 37 °C. (n=3)

As shown in Figure 5.3, the microbe began to convert guaiacol and *o*-cresol immediately without lag-phase. Interestingly, all aromatics were co-consumed, whereas glucose remained almost unaffected. Guaiacol was degraded faster than phenol and *o*-cresol. After 10 hours, all aromatics were degraded, and a small amount of about 0.25 mM MA could be observed.

This proof of concept demonstrated that the chemical conversion of lignin into aromatics can be combined with the microbe's conversion of aromatics. Admittedly, MA's formation was only weak, necessitating metabolic engineering efforts.

5.2 Metabolic engineering for high-yield MA-production

The resistance to guaiacol and the accumulation of MA (Section 5.1.2) indicate that *Amycolatopsis sp.* ATCC 39116 is capable of accumulating and secreting MA from lignin-based feed stocks. The next step was to develop a strain with enhanced MA production. However, genetic engineering of *Amycolatopsis sp.* ATCC 39116 is challenging (Meyer et al., 2017). Therefore, a new genetic engineering approach was developed.

5.2.1 Development of genetic tools for Amycolatopsis sp. ATCC 39116

To improve the genetic engineering of *Amycolatopsis sp.* ATCC 39116, the plasmid pKG1132 was used, which enables a combination of conjugation and blue-white screening (Myronovskyi et al., 2011). The cloning host *E. coli* ET12567/pUZ8002 was used for conjugal transfer of DNA from *E. coli* to *Amycolatopsis sp.* ATCC 39116. After conjugation (Section 4.4.7), the cell mixture was plated on GYM agar plates, and after 24 hours at 30 °C, the plates were overlaid with nalidixic acid and apramycin. Nalidixic acid was used to eliminate the *E. coli* helper strain ET12567, but this proved to be inefficient due to the low resistance of *Amycolatopsis sp*. ATCC 39116 to nalidixic acid. To enhance the efficiency, a hygromycin resistance gene was introduced into the microbe, which then allowed to eliminate *E. coli* ET12567 with hygromycin instead of nalidixic acid (Section 4.4.10). This modification was successful, and within two days, several hundred apramycin-resistant transformants were obtained from a single conjugation, growing on GYM agar plates containing apramycin (Figure 5.4 B). Approximately 50 colonies were transferred to fresh apramycin selection plates in small squares measuring 5 × 5 mm and incubated for 24 hours. A blue-white screening was performed to confirm successful first recombination. X-Gluc was added dropwise onto each colony to allow clear differentiation. Within 20 minutes, the colonies produced a clear blue color, indicating the successful genomic integration of the *gusA* gene *(uidA)*. All tested colonies turned blue, demonstrating efficient selection with apramycin. One of the blue colonies was picked and incubated in liquid culture without selection pressure overnight at 37 °C to promote the second recombination event. The grown cells were diluted (10^6 -fold) and then plated on $GYM^{X\text{-}Gluc}$ agar to prescreen colonies that had excised the plasmid. After 24 hours, about 50 colonies per plate were grown. Colonies that appeared white were streaked out on GYM agar plates and subjected to another blue-white screening. The frequency of the second recombination event was approximately 15%, these colonies remained white. Colony PCR was performed to distinguish between wild-type and mutant. Notably, about 50% of the white colonies contained the desired deletion. This method enabled efficient genetic engineering of *Amycolatopsis sp.* ATCC 39116 in approximately 10 days.

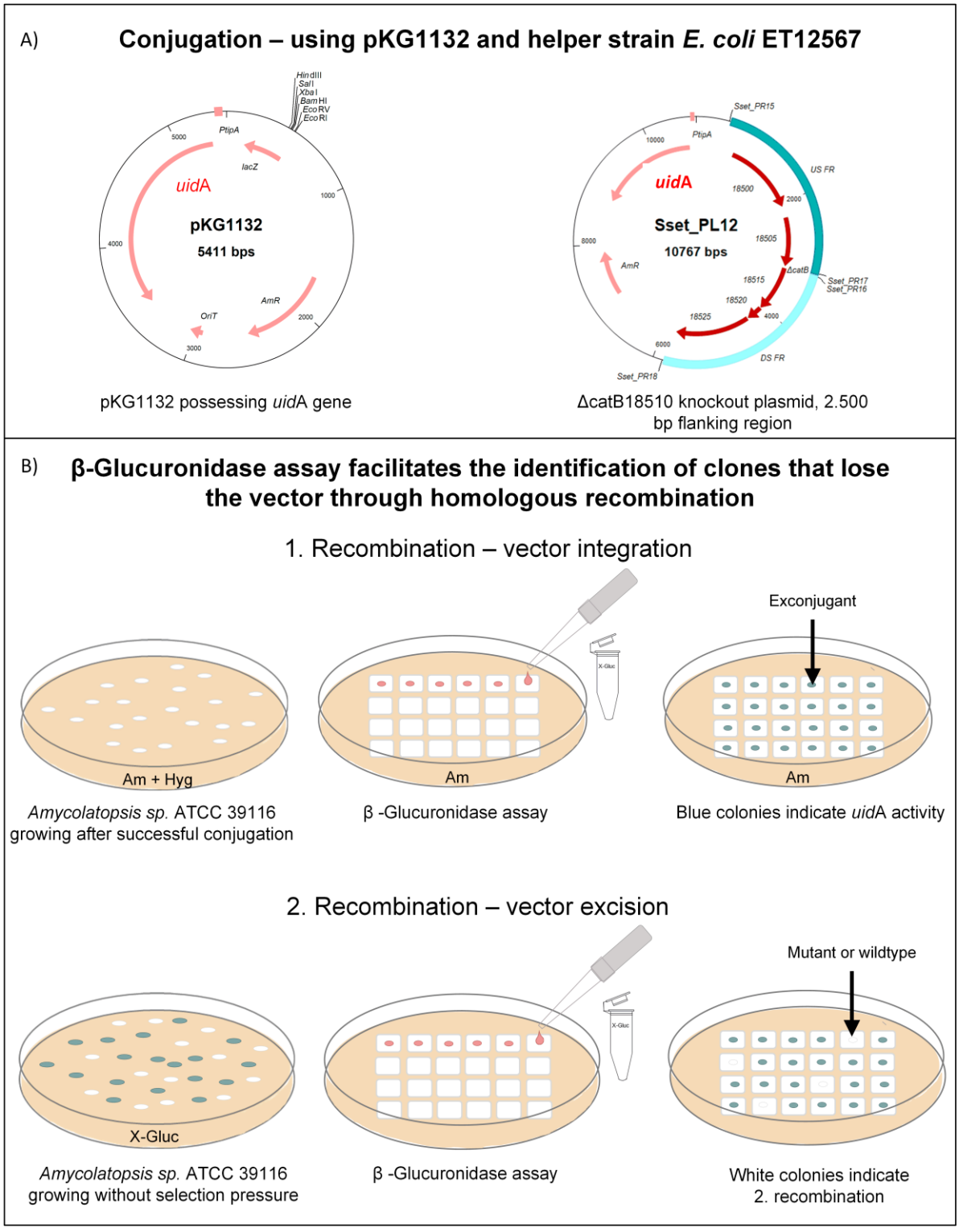

Figure 5.4: Theoretical background for the new genetic approach of *Amycolatopsis sp.* ATCC 39116, it involves the use of conjugation and blue-white screening. For blue-white screening, the *uidA* gene, which encodes the β-glucuronidase protein (GusA; NP_416134) from *E. coli*, was cloned into the BglII site of pKC1132 as a BglII fragment and placed under the control of the *tipA* promoter (Myronovskyi et al., 2011). The new plasmid was designated pKG1132. Genetic modifications were achieved via homologous recombination, utilizing 2,500 bp-long flanking regions. The plasmid was introduced into *Amycolatopsis sp.* ATCC 39116 through conjugation, using the *E. coli* helper strain ET12567. Successful genomic integration of the plasmid was confirmed by the activity of the GusA enzyme, which produced a blue color

upon incubation with X-Gluc. The second recombination event was induced by cultivating a single colony at 37°C for 24 hours without selection pressure. After this second recombination event, mutants (or wild-type cells) appeared white due to the excision of the plasmid. β-Glucuronidase assay was once again used to identify clones that had lost the plasmid through homologous recombination. Finally, PCR was performed to distinguish between wild-type and mutant clones.

5.2.2 Deletion of the catB-9302 gene does not enable efficient MA production

To enable MA production, the β-ketoadipate pathway must be disrupted at the level of CatB, the enzyme responsible for converting MA to muconolactone. Through literature review and a BLAST search (Park and Kim, 2003), three putative *catB* genes were identified in the genome of *Amycolatopsis sp.* ATCC 39116.

Table 5.2: Putative *catB* genes in *Amycolatopsis sp.* ATCC 39116. The gene AATC3_020100018510 has already been studied, and it has been designated *catB* (Park and Kim, 2003), while the other two genes have not yet been examined. These genes were determined by sequence similarity to muconate lactonizing proteins and muconate cycloisomerases using BLAST search (Altschul et al., 1990).

Gene	GC content [%]	Sequence similarity, Strain
AATC3_020100001440	71.6	86 %, Saccharopolyspora erythraea NRRL2338 82 %, Nocardiopsis dassonvillei strain NOCA502F 81 %, Geodermatophilus obscurus DSM43160 80 %, Streptomyces pactum strain KLBMP 5084
AATC3_020100009302	70.8	96 %, Amycolatopsis methanolica 239 81 %, Saccharopolyspora erythraea NRRL2338
AATC3_020100018510	70.5	96 %, Amycolatopsis methanolica 239 90 %, Saccharopolyspora erythraea NRRL2338

The knockout of the *catB*-9302 gene was achieved using the suicide plasmid Sset_PL6 (Figure 8.2). The newly established method facilitates the detection of recombination events. Single crossover clones, in which Sset_PL6 had integrated into the genome, were selected under apramycin pressure and confirmed through blue-white screening (Figure 5.5, A). As expected, all tested clones were positive. One colony was then picked and incubated without selection pressure to allow for a double crossover event (Figure 5.5, B).

All white clones were subsequently analyzed by colony PCR to differentiate between mutant and wild-type, revealing a 50% frequency of successful knockouts.

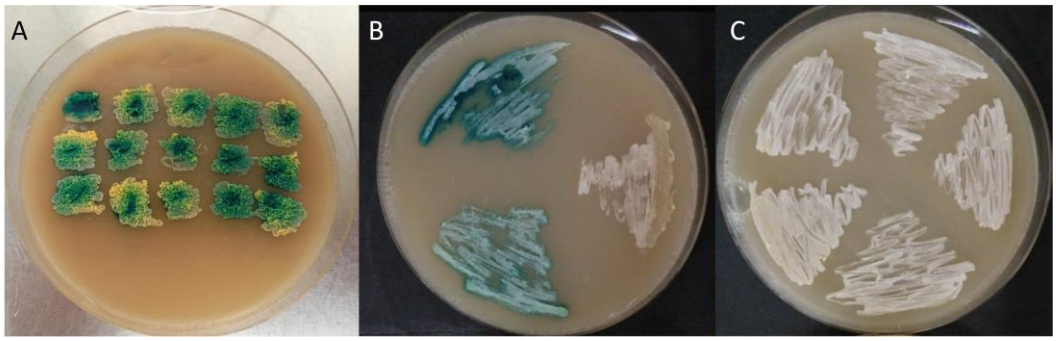

Figure 5.5: Blue-white screening for verification of desired mutations in *Amycolatopsis sp*. ATCC 39116. For deletion of AATC3_020100009302, the deletion plasmid Sset_PL6 was introduced via conjugation using *E. coli* ET12567. To confirm the first recombineering event, transformants were transferred to a fresh plate containing apramycin, cultivated overnight, and overlaid with X-Gluc. Positive clones are blue (A), indicating that Sset_PL6 had been integrated into the genome by a single crossover event. To induce the second double crossover event, the cells were incubated without selection pressure. Positive clones now appeared white (B and C), indicating successful excision of the plasmid.

The first deletion mutant *Amycolatopsis sp.* ATCC 39116 MA-1 did not produce MA from guaiacol at high yield. No significant change in production physiology and growth was observed compared to the wild-type (Figure 5.6).

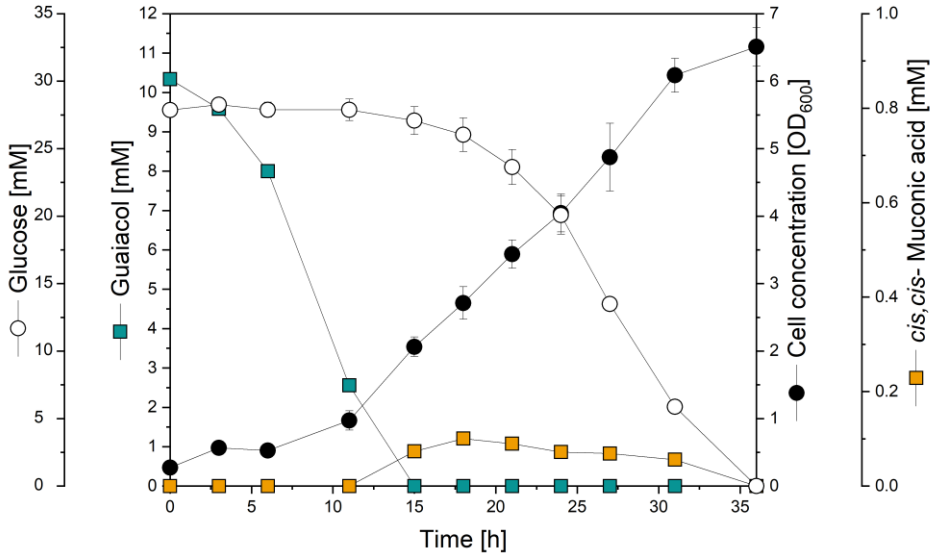

Figure 5.6 Growth physiology of *Amycolatopsis sp.* ATCC 39116 MA-1 on guaiacol and glucose. *Amycolatopsis sp*. ATCC 39116 MA-1 *ΔcatB-9302::hyg*^{R} was grown in minimal medium that contained a mixture of sugar and guaiacol. The incubation temperature was 37 °C. (n=3)

5.2.3 Deletion of catB-18510 gene enables efficient MA production from guaiacol

The first knockout (*ΔcatB*-9302) did not result in the desired high-efficiency production strain. This gene likely plays only a minor role, if any, in MA degradation, though compensatory effects cannot be ruled out. Consequently, a second deletion targeting the *catB*-18510 gene was performed in the MA-1 background using the plasmid Sset_PL12 (Figure 8.3). The genomic modification was straightforward.

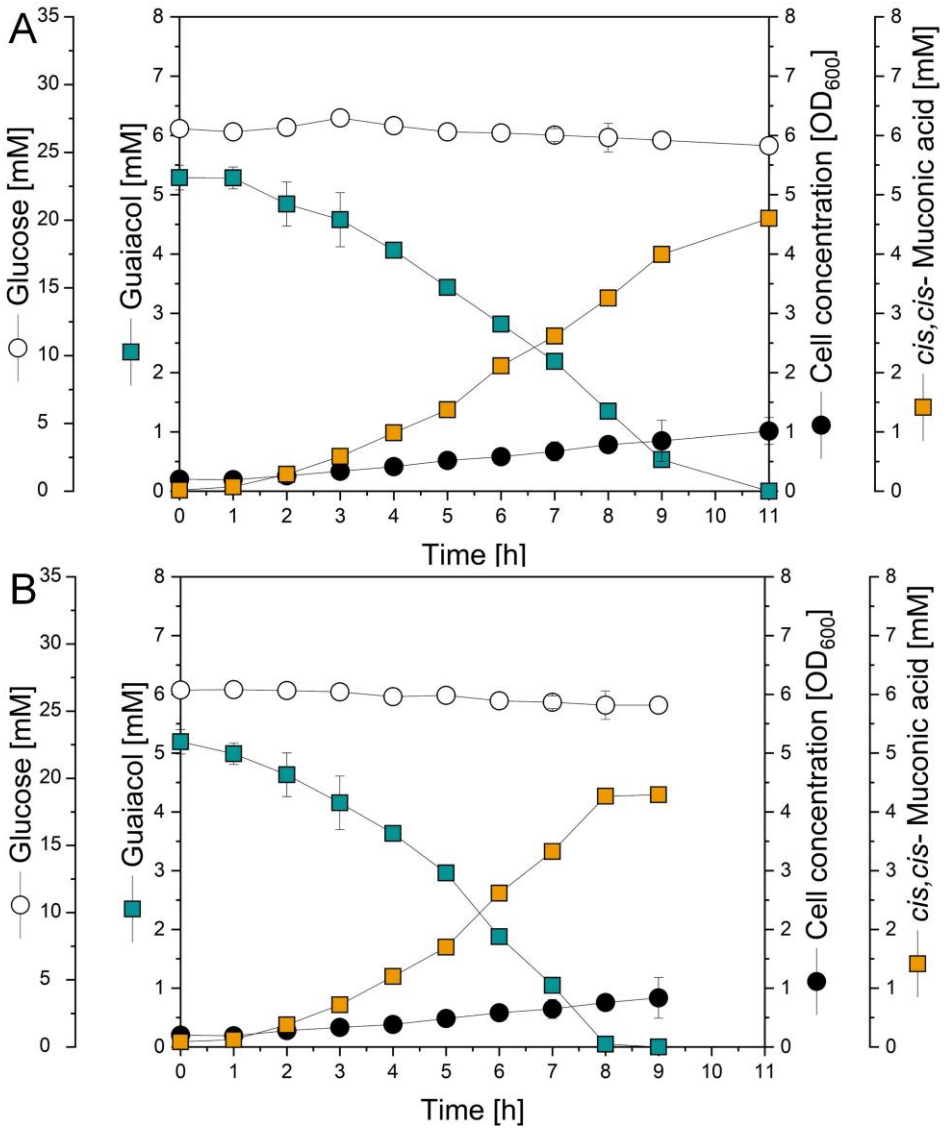

Figure 5.7: Production performance of *Amycolatopsis sp.* ATCC 39116 MA-2. Deletion of *catB*-18510 gene and *catB*-9302 enabled the production of *cis,cis*-muconic acid from guaiacol. Cells were grown at 37 °C (A) and at 42 °C (B). To support growth, the medium contained glucose. (n=3)

The new strain was designated MA-2 and verified by PCR and sequencing. It had lost the ability to grow on aromatics, e.g., guaiacol or benzoate as sole carbon source. This was confirmed by growing MA-2 on plate cultures containing the aromatics as a single carbon source. As shown in Figure 5.7 A, *Amycolatopsis sp.* ATCC 39116 MA-2 accumulated high levels of MA from guaiacol in liquid culture. Specifically, 4.6 mM of MA was produced from 5.2 mM of guaiacol within 10 hours, corresponding to a yield of 0.88 mol mol^{-1} - an 18-fold improvement over the wild type. Interestingly, this yield did not reach 100%, as might have been expected.

The cells exhibited steady growth with a specific growth rate of 0.13 h^{-1}. The exponential, glucose-based growth phase began only after the depletion of the aromatic source (data not shown). During the initial culture phase, while the aromatic compound was being converted, glucose levels remained almost constant, and cell concentration increased only slightly. This indicates that *Amycolatopsis sp*. ATCC 39116 clearly preferred the aromatic compound over glucose as a carbon source. The conversion process accelerated when the cultivation temperature was increased to 42 °C (Figure 5.7 B). Within 8 hours, 4.3 mM out of 5.2 mM guaiacol was converted to MA, yielding 0.82 mol mol^{-1}. The cells grew faster at 42 °C, with a specific growth rate of 0.16 h^{-1}, compared to growth at 37 °C. However, the yield was slightly lower at around 80%. As a result, further cultivation experiments were conducted at 37 °C to optimize yield.

Deletion of the third *cat*B-1440 gene does not improve production performance. To eliminate compensatory effects, the third putative *catB*-1440 gene was also targeted for deletion. However, a marker-less deletion of *catB*-1440 was not possible, as the plasmid could not be assembled *in vitro*, likely due to inhibitory secondary DNA structures (data not shown). As a result, a new plasmid, designated Sset_PL13 (Figure 8.4), was constructed. This plasmid contained a copy of the *catA*-18515 gene and its native promoter, between the flanking regions of *catB*-1440. Sset_PL13 was designed to remove *catB*-1440 while simultaneously enhancing production performance.

The obtained strain *Amycolatopsis sp*. MA-3, was verified by PCR and sequencing for correctness of the genetic modification. For evaluation, it was grown on guaiacol and glucose (Figure 8.6). After 55 hours, no more guaiacol was detectable. Only 2.5 mM MA was formed from 7.2 mM guaiacol. Less than half of the guaiacol was converted into MA. The additional *catA*-18515 gene did not result in an improved conversion. The yield dropped from 90% to 39% and it took 5 times longer to consume the guaiacol. The new strain was not better than MA-2, markerless deletion of *catB*-1440 from the genome was not possible, so further experiments were carried out with *Amycolatopsis sp.* ATCC 39116 MA-2.

5.2.4 Single deletion of catB-18510 enables MA production

Finally, only the *catB*-18510 gene was deleted from the wild-type to confirm it is the sole active gene involved. For this purpose, the plasmid Sset_PL12 from Section 5.2.3 was used, but in the wild-type background. After extensive screening, a correct conjugant was identified, and the resulting strain was designated *Amycolatopsis sp*. ATCC 39116 MA-4. To demonstrate MA production, MA-4 was grown on guaiacol (Figure 5.8).

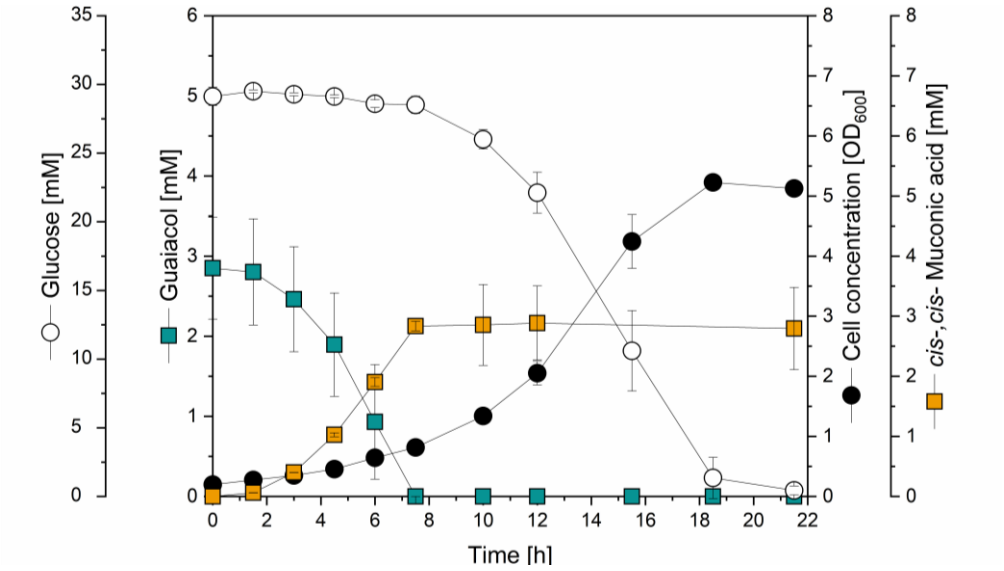

Figure 5.8: Production performance of *Amycolatopsis sp.* ATCC 39116 MA-4 Single deletion of the *catB*-18510 gene enabled the production of *cis,cis*-muconic acid from guaiacol. Cultivation was carried out at 37 °C. To support growth, the medium additionally contained glucose. (n=3)

After 7 hours, a titer of 2.82 mM MA was reached, corresponding to 99% of the initially added guaiacol. The cells exhibited exponential growth on glucose after guaiacol depletion, with a specific growth rate of 0.19 h^{-1}. During guaiacol conversion, glucose levels remained nearly unaffected. While *Amycolatopsis sp.* ATCC 39116 MA-4 showed great potential for MA production, further genetic engineering of this mutant strain proved inefficient due to the absence of the hygromycin resistance gene. As a result, it was decided to continue experiments with MA-2.

5.2.5 Production of MA from guaiacol on a gram scale

The next step was to evaluate the production performance of *Amycolatopsis sp.* MA-2 in a bioreactor. The experiment was conducted in fed-batch mode, starting with a first batch containing 5 mM guaiacol, followed by repeated feeding phases where additional guaiacol was added. Glucose present in the initial batch medium served as the growth substrate, with a small additional amount of glucose added after 7 hours. Figure 5.9 shows the MA production of *Amycolatopsis sp.* ATCC 39116 MA-2 in the fed-batch experiment. Over 24 hours, 3.1 g L^{-1} of MA was produced from guaiacol, with a consistent growth rate of 0.057 h^{-1}. The cells began producing MA immediately after the process started, achieving a high yield of 0.96 mol mol^{-1}. The initial guaiacol was fully converted within 5 hours, and additional guaiacol was then added in pulses.

Guaiacol, catechol (intermediate), and glucose concentrations were monitored at-line by HPLC, allowing precise control throughout the process. This prevented substrate limitations and minimized catechol accumulation. As shown in Figure 5.9, a small portion of the pathway intermediate catechol accumulated in the medium, which reached a concentration of about 2 mM after 10 hours. Due to catechol's toxicity, subsequent feeding intervals were slightly extended to prevent further buildup. The catechol concentration quickly decreased and remained negligible. Notably, the temporary rise in catechol concentration did not negatively impact cell growth or productivity.

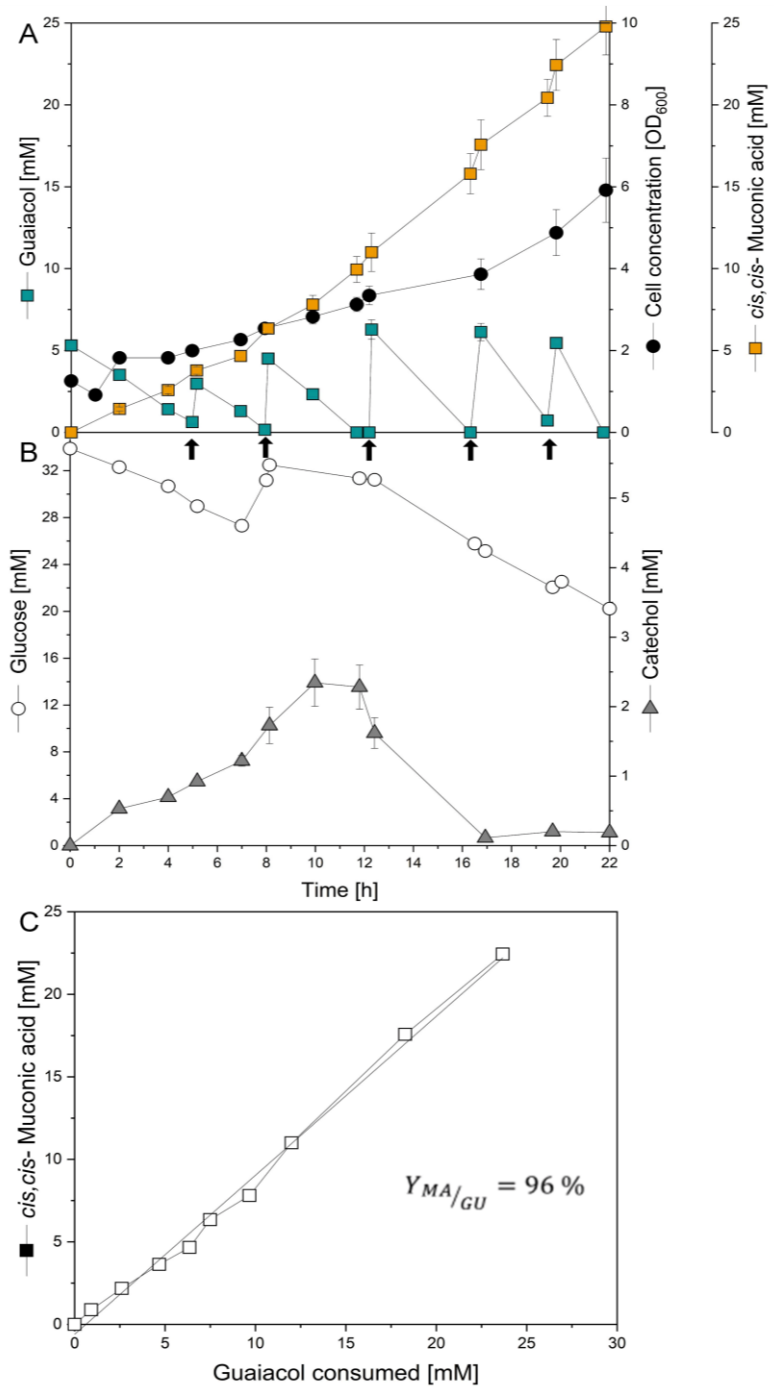

Figure 5.9: Production of MA in a fed-batch process, using *Amycolatopsis sp.* MA-2 (*ΔcatB-9302::hyg*^{R}*, ΔcatB-18510).* Cultivation was carried out in a monitored and stirred bioreactor at 37 °C. The initial batch contained glucose and 5 mM guaiacol. Guaiacol was added repeatedly after it had been consumed by the cells (highlighted by arrows). (n=3)

5.2.6 Production of MA from softwood lignin hydrolysate

Next, the production performance of the engineered strain MA-2 on lignin hydrolysate was evaluated (Figure 5.10). For this experiment, lignin was depolymerized as described in Section 4.5 and used as a substrate in a minimal medium containing glucose. As shown in Figure 5.10, *Amycolatopsis sp.* ATCC 39116 MA-2 has converted approximately 70% of the lignin hydrolysate (which contained 2.3 mM of aromatic compounds) into MA. A final MA concentration of 1.8 mM was achieved within 10 hours, corresponding to a yield of 0.72 mol mol^{-1}. The three aromatics' concentrations decreased simultaneously, indicating that they were co-consumed. However, cell growth of MA-2 was weaker compared to the wild-type (Figure 5.3) since the engineered strain could no longer utilize the aromatics for growth. Overall, the novel strain demonstrated more than a six-fold increase in production efficiency in terms of final MA titer, and importantly, it successfully produced MA from lignin hydrolysate.

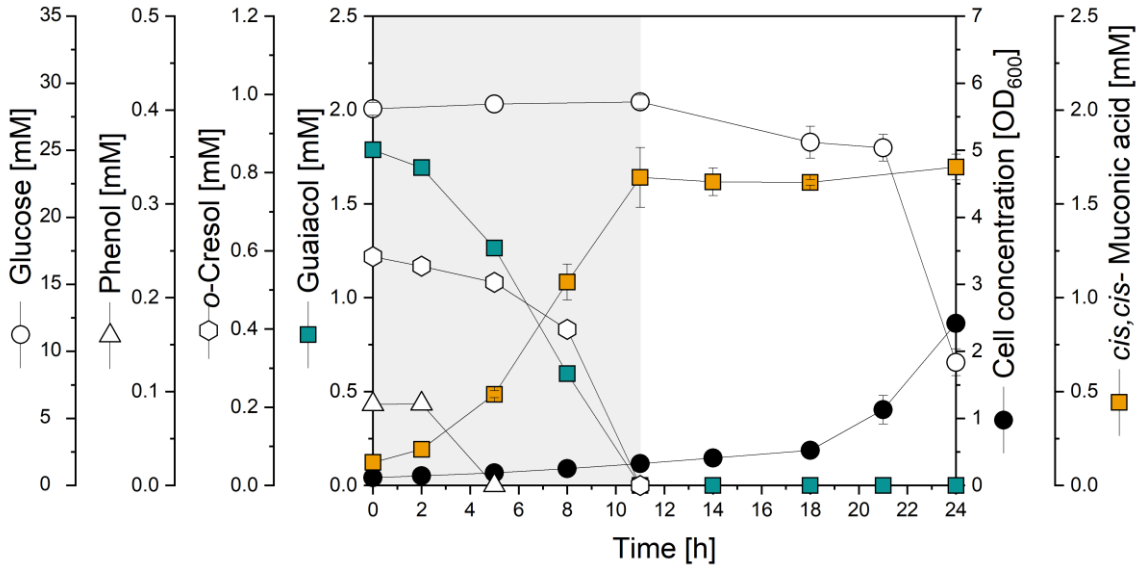

Figure 5.10: Production of MA from real lignin hydrolysate, derived from hydrothermal conversion of softwood lignin (370 °C, 210 bar, 20 min) using *Amycolatopsis sp.* ATCC 39116 MA-2 (*ΔcatB-9302::hyg^R, ΔcatB-18510*). Cultivation was performed at 37°C. Glucose was present in the medium to support growth. (n=3)

It should be noted that a yield of around 90% was expected based on preliminary tests (Section 5.2.3). This suggests that one of the aromatic compounds may not have been fully converted to MA. Indeed, HPLC analysis revealed the presence of an unknown substance.

5.2.7 Production of methyl-MA from o-cresol

The conversion of lignin hydrolysate using *Amycolatopsis sp.* ATCC 39116 MA-2 resulted in an unknown product detected by HPLC analysis (data not shown). This new metabolite was produced during the experiment and was not detectable at the beginning. The new product peak eluted after MA, indicating a slightly hydrophobic nature. The unknown product revealed a higher UV absorption at 260 nm than at 210 nm, indicating a non-aromatic compound.

As shown in Section 5.2.6, *Amycolatopsis sp*. ATCC 39116 MA-2 was capable of utilizing phenol and *o*-cresol from the lignin hydrolysate. *Amycolatopsis sp.* ATCC 39116 is able to convert phenol to catechol, from which MA is formed, this has been confirmed by before (Antai and Crawford, 1983). Unlike phenol, *o*-cresol has a methyl group on the aromatic ring, possibly resulting in a methylated product. Therefore, a cultivation of *Amycolatopsis sp.* ATCC 39116 MA-2 was conducted using *o*-cresol as substrate to confirm the production of an unknown substance. This experiment revealed that *Amycolatopsis sp.* ATCC 39116 MA-2 did not accumulate MA from *o*-cresol but an unknown product, which was confirmed again by HPLC analysis (data not shown). To identify it, pure MA and the unknown product produced by *Amycolatopsis sp*. ATCC 39116 MA-2 from *o*-cresol were subjected to GC-MS analysis.

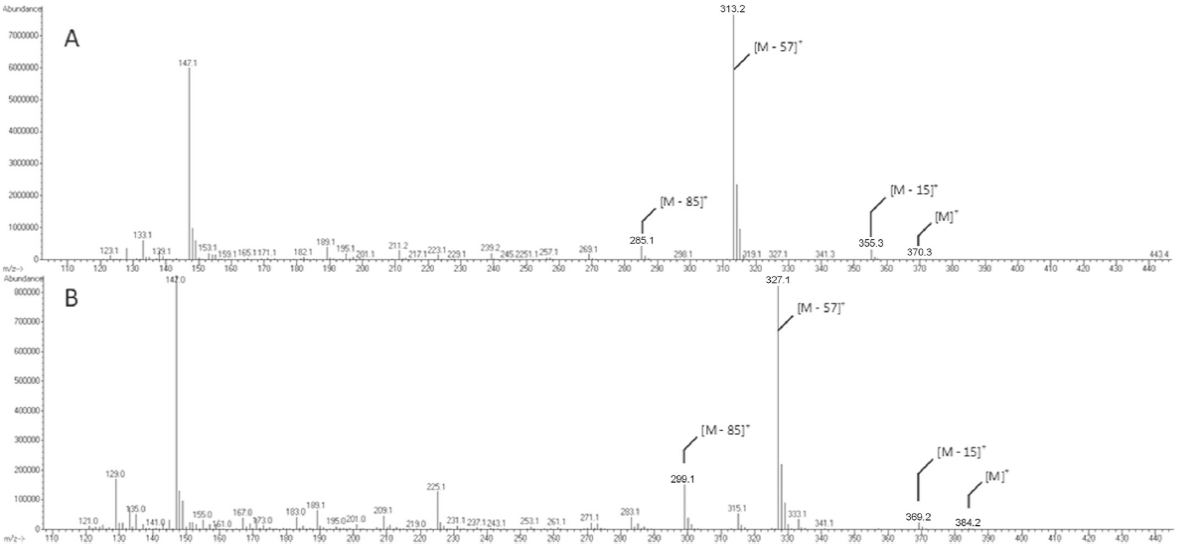

Figure 5.11: Structural GC-MS analysis of the unknown product, which is produced from *o*-cresol by *Amycolatopsis sp.* ATCC 39116 MA-2 (*ΔcatB-9302::hyg*^{R}*, ΔcatB-18510*). GC-MS mass spectrum of t-butyldimethylsilyl derivatized pure MA (A). MA eluted after 9.5 min. The ion at m/z 355 represents a $[M-15]^+$ fragment, obtained by losing a methyl group from the derivatization residue. The loss of t-butyl-dimethylsilyl group also from the derivatization residue results in an ion at m/z 313 represents a $[M-57]^+$ fragment. The loss of a t-butyl-dimethylsilyl group from the derivatization residue in combination with the loss of a CO group from one of the MA carboxylic groups leads to ion at m/z 285 represents an $[M-85]^+$ fragment. This ion pattern is typically for t-butyldimethylsilyl derivatized products (Wittmann, 2007). GC-MS mass spectrum of t-butyldimethylsilyl derivatized unknown product (B). The metabolite, produced from *o*-cresol, was eluted after 9.7 min. It exhibits the same fragmentation pattern as MA, whereby a mass shift of 14 was observed. From this analysis, it was concluded that the unknown product is methyl-muconate, probably 2-methyl muconate, considering the position of the corresponding methyl group in *o*-cresol.

The substances were derivatized with t-butyl-dimethylsilyl. The pure MA eluted after 9.5 min and showed ions at m/z 370 $[M]^+$, 355 $[M-15]^+$, 313 $[M-57]^+$, and 285 $[M-85]^+$ (Figure 5.11 A). The unknown product eluted after 9.7 min and exhibits the same fragmentation pattern but with a mass shift of 14 (Figure 5.11 B). This result suggests that the unknown product is very similar to MA but carries an additional CH_2 group, which explains the mass shift of 14. The unknown product was found derivatized at both carboxyl groups, indicating that the methyl group was positioned in the inner carbon skeleton. From these results, it can be deduced that the unknown product was methyl-MA, or more precisely, 2-methyl MA, since the methyl group and the hydroxyl group in *o*-cresol are next to each other.

To understand how this product was formed, the substrate specificity of catechol-dioxygenase (c*at*A-18515) was studied by an enzyme assay. This enzyme is responsible for the conversion of catechol into MA.

Table 5.3: Substrate specificity of catechol dioxygenase (CatA-18515) was measured in the crude cell extract of *Amycolatopsis sp.* ATCC 39116 MA-2 (*ΔcatB-9302::hyg^R, ΔcatB-18510*), containing catechol. In further experiments, catechol was substituted by equimolar amounts of 3- and 4-methyl catechol. (n=3)

Substrate	Specific activity [mU mg^{-1}]
Catechol	640±19
3-Methyl catechol	470±9
4-Methyl catechol	380±5

The assay was first performed with catechol as control, revealing an activity of 640 mU mg^{-1} (Table 5.3). Subsequently, catechol was replaced by 3-methylcatechol. 3-Methylcatechol is the methylated intermediate formed when *o*-cresol is degraded and subsequently converted to methyl-MA. The cell extract was able to convert 3-methylcatechol with a high activity of 470 mU mg^{-1}. Furthermore, the enzyme CatA also accepted 4-catechol as substrate (380 mU mg^{-1}). Altogether, the engineered producer was able to produce 2-methyl MA from *o*-cresol.

5.3 Promising production of MA from vanillin and vanillate

As demonstrated, *Amycolatopsis sp.* ATCC 39116 MA-2 is capable of producing MA from small aromatic compounds such as guaiacol, catechol, and benzoate via the β-ketoadipate pathway. To further enhance its potential as a cell factory, expanding its substrate range is essential. Interestingly, vanillin, a by-product of the pulp and paper industry, can be obtained through the alkaline oxidation of softwood lignin (Fache et al., 2016). It is already known that *Amycolatopsis sp*. ATCC 39116 possesses the *vanAB* genes, enabling the degradation of vanillin (Fleige et al., 2013). In addition, it possesses the *vdcBCD* genes, which catalyze the decarboxylation of vanillate to guaiacol and CO_2 (Pometto et al., 1981). This means that *Amycolatopsis sp*. ATCC 39116 MA-2 should already be able to produce MA from vanillin or vanillate.

5.3.1 Production of MA from vanillic acid as sole C-source

Initial experiments were conducted using vanillic acid, including a fed-batch process to simulate a more industrially relevant setup (Figure 5.12 B). These experiments (Figure 5.12 A and B) were performed by Bianca Stephan during her bachelor's thesis (Saarland University). The conversion was carried out in shake flasks, starting with an initial batch phase containing 5 mM vanillate. After inoculation (1 OD_{600nm}), pulses of 5 mM were added after every 12 hours. After 36 hours, the feed was increased to 10 mM vanillate.

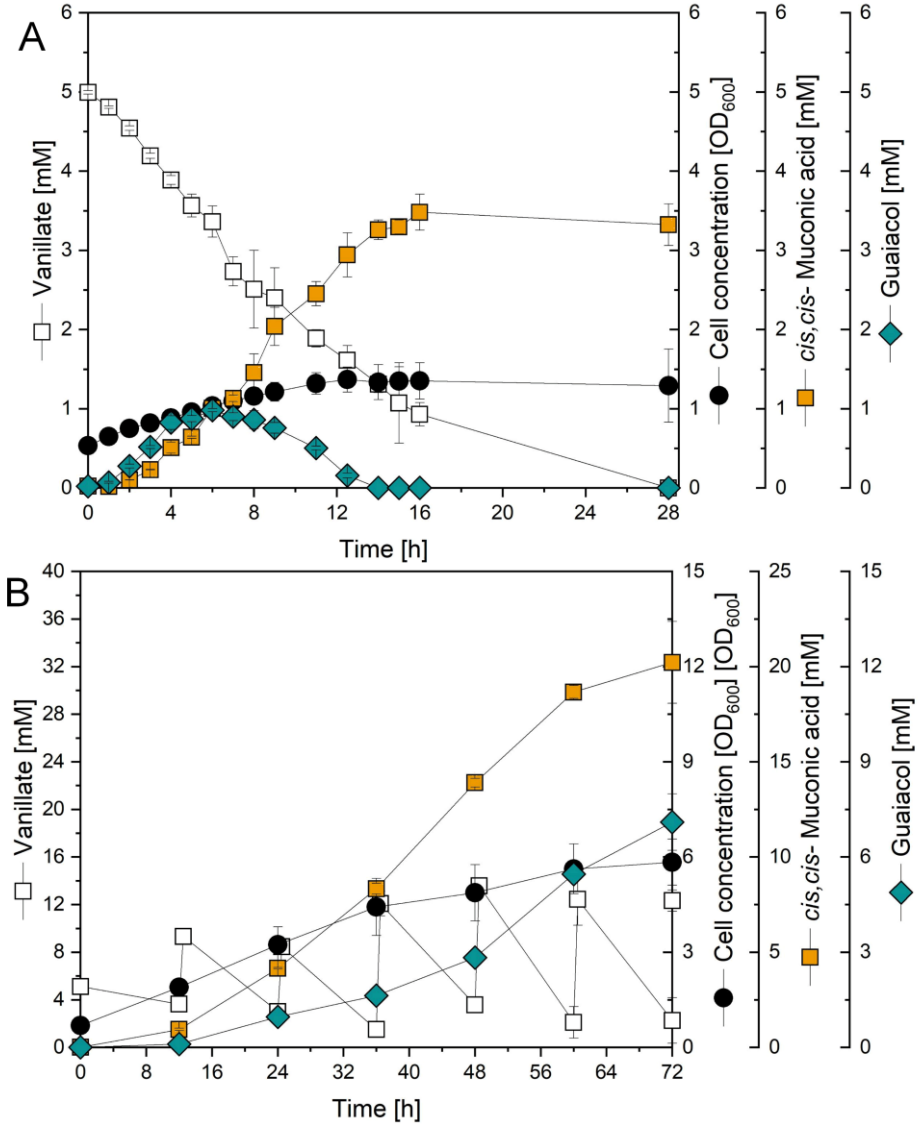

Figure 5.12: MA production from vanillate in a batch (A) and fed-batch process (B) using *Amycolatopsis sp.* ATCC 39116 MA-2 (*ΔcatB-9302::hyg*^{R}, *ΔcatB-18510*). The first batch contained 5 mM vanillate, followed by a feeding phase in which vanillate was added in pulses every 12 h. Cultivations were carried out at 37 °C in shake flasks. (n=3)

Figure 5.12 A shows that *Amycolatopsis sp.* ATCC 39116 MA-2 successfully utilized vanillate as the sole C-source for cell growth and MA production. From 5 mM vanillate, 3.4 mM MA was produced, corresponding to a yield of 68%. The strain grew exponentially with a specific growth rate of 0.06 h^{-1}, reaching a final cell concentration of 1.3 OD_{600nm}.

In the fed-batch cultivation (Figure 5.12 B), the strain produced 3 g L^{-1} MA within 72 hours. The total MA accumulation (20.2 mM) from 47.12 mM vanillate added, resulted in a yield of 43%. As shown in Figure 5.12 B, part of the vanillate was converted into the pathway intermediate guaiacol, which accumulated during the process. Overall, the strain demonstrated excellent potential as a MA producer, efficiently utilizing vanillate as the sole substrate.

5.3.2 Native vdcBCD genes enables MA production from vanillin and vanillate

It was hypothesized that *Amycolatopsis sp*. ATCC 39116 MA-2 produces MA from vanillin and vanillate due to the presence of its native *vdc*BCD genes. To investigate this, strain MA-2 was cultured in minimal medium containing glucose plus vanillin, vanillate, or protocatechuate, respectively.

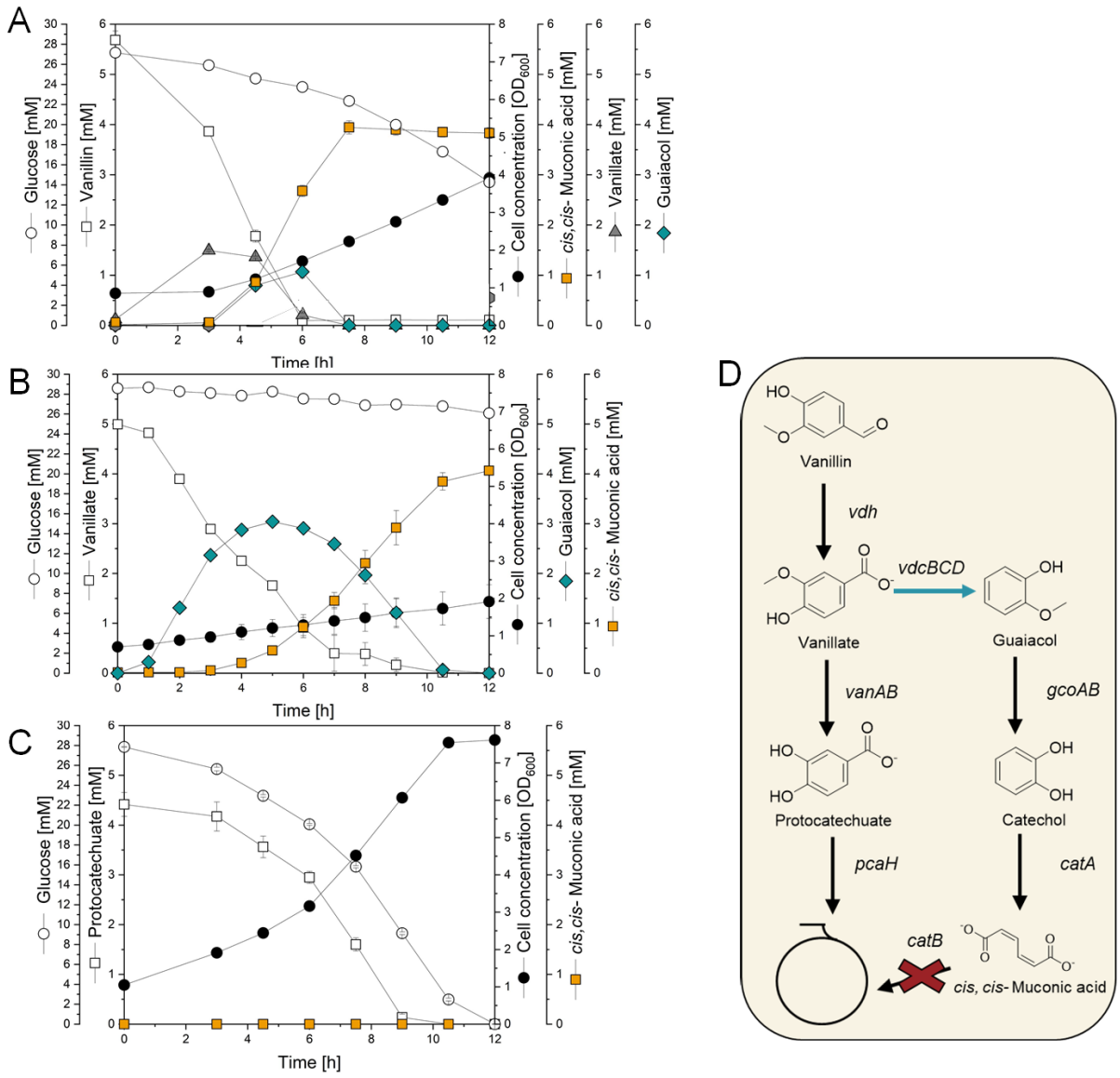

Figure 5.13: Production of MA from vanillin (A) and vanillate (B) using *Amycolatopsis sp.* ATCC 39116 MA-2 (*ΔcatB-9302::hyg*^{R}*, ΔcatB-18510*) at 37 °C. MA-2 was found unable to produce MA from protocatechuate (C). Overview of the metabolic pathway (D). The blue arrow highlights the *vdc*BCD genes that lead to MA production. Glucose was present in the medium to support growth. (n=3)

As shown in Figure 5.13 A and B, *Amycolatopsis sp*. ATCC 39116 MA-2 produced MA from vanillin and vanillate but not from protocatechuate (Figure 5.13 C). When vanillin (5.6 mM) was used as substrate, 3.9 mM MA was formed within 7 hours, representing a yield of 0.69 mol mol^{-1}. This yield was approximately 20% lower in comparison to the MA production from guaiacol (90%). During the conversion process, small amounts of pathway intermediates, including vanillate and guaiacol, were detected.

The MA yield from vanillate was approximately 10% higher than that observed from vanillin (Figure 5.13 B). From 5 mM of vanillate, 3.9 mM of MA was produced within 10 hours, resulting in a yield of 0.78 mol mol^{-1}. Throughout the conversion of vanillin and vanillate, glucose levels declined gradually, and the cell concentration increased only slightly compared to growth in a mixture of protocatechuate and glucose. Despite the good growth in this mixture (Figure 5.13 C), no MA was formed. A potential solution to this challenge is to convert protocatechuate into catechol.

5.3.3 Integration of the aroY gene enables MA-production from protocatechuate

To enable MA production from protocatechuate and increase the overall MA yield, the PCA 3,4-ortho-cleavage pathway was interrupted by deleting the *pcaG* gene, redirected to the CAT 1,2-*ortho*-cleavage route. This modification was achieved in a single step using the plasmid Sset_PL20 (Figure 8.5), which replaced the *pcaG* gene with the *aroY* gene. The genomic modification was performed on the *Amycolatopsis sp*. ATCC 39116 MA-2 background and was carried out smoothly. The newly engineered strain was designated *Amycolatopsis sp*. ATCC 39116 MA-5, and its modifications were confirmed by PCR and sequencing (Plasmid was cloned by technical assistant Mirjam Selzer, Saarland University). The strain lost its ability to grow on vanillin, vanillate, and protocatechuate as sole C-source. This was verified by growing MA-5 on plates containing the aromatics as the sole carbon source. As shown in Figure 5.14 A, *Amycolatopsis sp.* ATCC 39116 MA-5 accumulated large amounts of MA from protocatechuate.

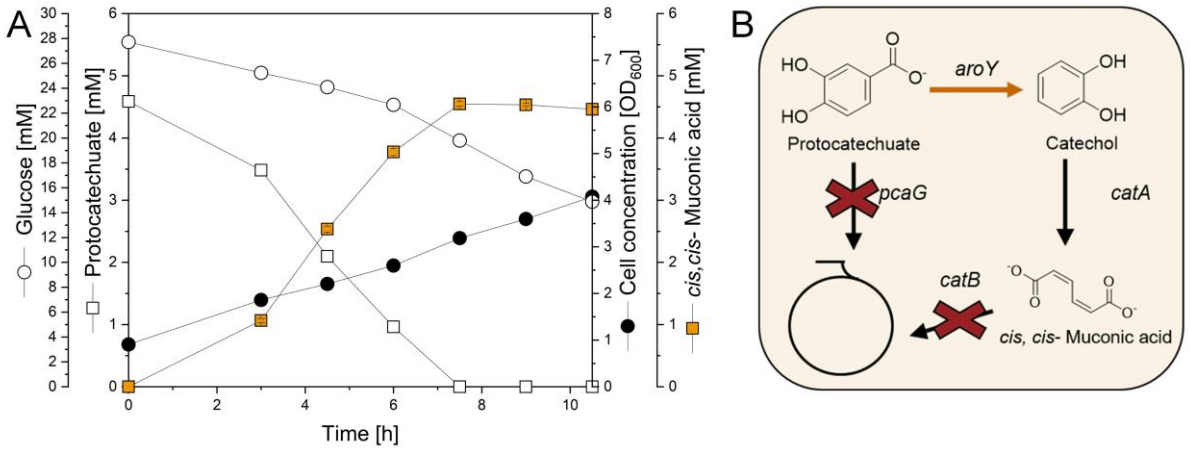

Figure 5.14: Production of MA from protocatechuate (A) using metabolically modified *Amycolatopsis sp.* ATCC 39116 MA-5 (*ΔcatB-9302::hyg*^{R}*, ΔcatB-18510, ΔpcaG-37543::aroY*) at 37 °C. A brief overview of the engineered protocatechuate pathway (B). Glucose was present in the medium to support growth. (n=3)

After 8 hours, no more protocatechuate was detectable, and 4.5 mM of MA was produced from 4.5 mM of protocatechuate, representing a 100% yield. Remarkably, the new strain immediately grew exponentially on glucose (μ= 1.4 h^{-1}), indicating that protocatechuate does not inhibit glucose utilization. Thanks to the introduction of the *aroY* gene, *Amycolatopsis sp.* ATCC 39116 MA-5 is now capable of producing large amounts of MA from protocatechuate.

5.3.4 Comparison of Amycolatopsis sp. ATCC 39116 MA-2 and MA-5

It was now interesting to compare the two producers MA-2 and MA-5. The data for *Amycolatopsis sp.* ATCC 39116 MA-5, grown on vanillin and vanillate, are given in the appendix (Figure 8.7).

Table 5.4: Comparison of MA yield. In order to ensure comparability, both strains were grown in minimal medium with glucose and protocatechuate, vanillin or vanillate.

Yield	MA-2 [%]	MA-5 [%]
Vanillin	70	88
Vanillate	78	96
Protocatechuate	0	100

Amycolatopsis sp. ATCC 39116 MA-5 demonstrated higher yields across all three substrates. The MA yield from vanillate and protocatechuate reached nearly 100 %. However, a 100% yield from vanillin could not be achieved. Further HPLC analysis revealed the presence of an additional product peak in the supernatant, which was identified as vanillyl alcohol (data not shown).

Next, softwood-based vanillin (Eurovanillin, Borregaard) used as feedstock for MA production. *Amycolatopsis sp.* ATCC 39116 MA-2 was grown in minimal medium containing 5.3 mM softwood-based vanillin as substrate. The strain successfully grew and produced MA. From 5.3 mM vanillate, 3.1 mM MA was formed, corresponding to a yield of 58%. However, intermediates such as guaiacol and vanillate accumulated during the experiment. Interestingly, the conversion of vanillin into MA lasted over 77 hours, which is more than four times longer compared to the conversion of vanillate (Section 5.3.1).

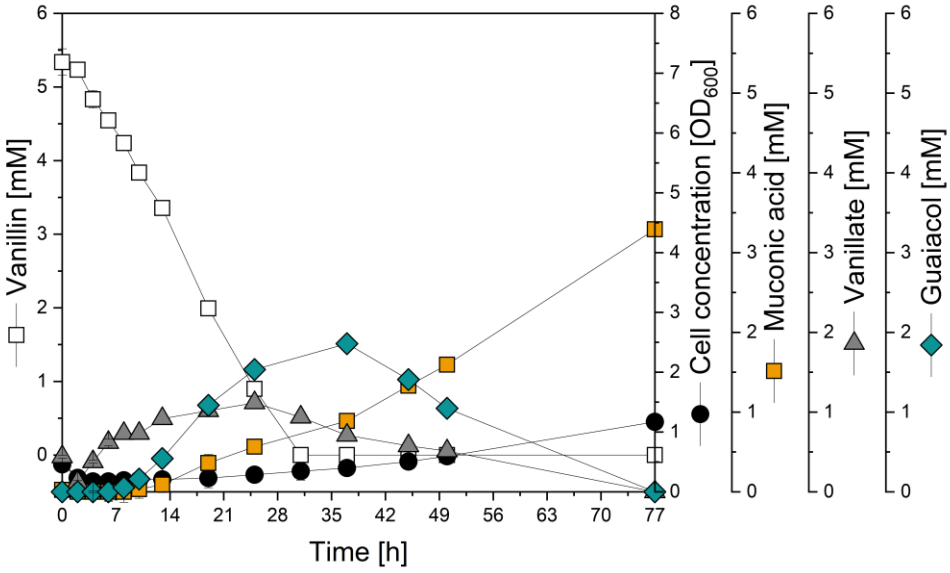

Figure 5.15: MA production from vanillin using *Amycolatopsis sp.* ATCC 39116 MA-2 (*ΔcatB-9302::hyg*^{R}*, ΔcatB-18510*) at 37 °C. Vanillin was ordered from Borregaard. (n=3)

Despite the slower conversion, *Amycolatopsis sp.* ATCC 39116 MA-5 remains an excellent candidate for MA production using vanillin, vanillate, and its intermediate, protocatechuate.

5.4 Using side streams from pulp and paper industry as C-source

As shown above, *Amycolatopsis sp.* ATCC 39116 successfully converted various aromatic monomers and corresponding lignin-derived aromatics into MA. In these processes, glucose was used as the growth substrate, since the disruption of the CAT 1,2-*ortho*-cleavage pathway that allows MA accumulation does not allow the cell factories to grow on the aromatics. As glucose is a first-generation sugar derived from e.g. corn and competes unfavorably with food production, it appeared interesting to replace it with more sustainable alternatives.

5.4.1 Metabolization of xylose, rhamnose, galactose, arabinose and mannose

Amycolatopsis sp. ATCC 39116 was grown on minimal medium agar plates, containing either glucose, mannose, rhamnose, galactose, arabinose, or xylose as sole source of carbon (Figure 5.16). The microbe was able to utilize all six sugars.

Figure 5.16: *Amycolatopsis sp.* ATCC 39116 growing on agar plates containing various sugars. Plates consist of minimal medium and glucose, mannose, rhamnose, galactose, arabinose or xylose as a sole C-source. Glucose was used as reference. The experiment was conducted by Bianca Stephan during her bachelor's thesis (Saarland University), and the picture was taken from her work.

Subsequent experiments in shake flasks then investigated the kinetics and stoichiometry of growth on the different sugars. To this end, the buffer of the liquid medium was switched from phosphate to MOPS to prevent salts from precipitating.

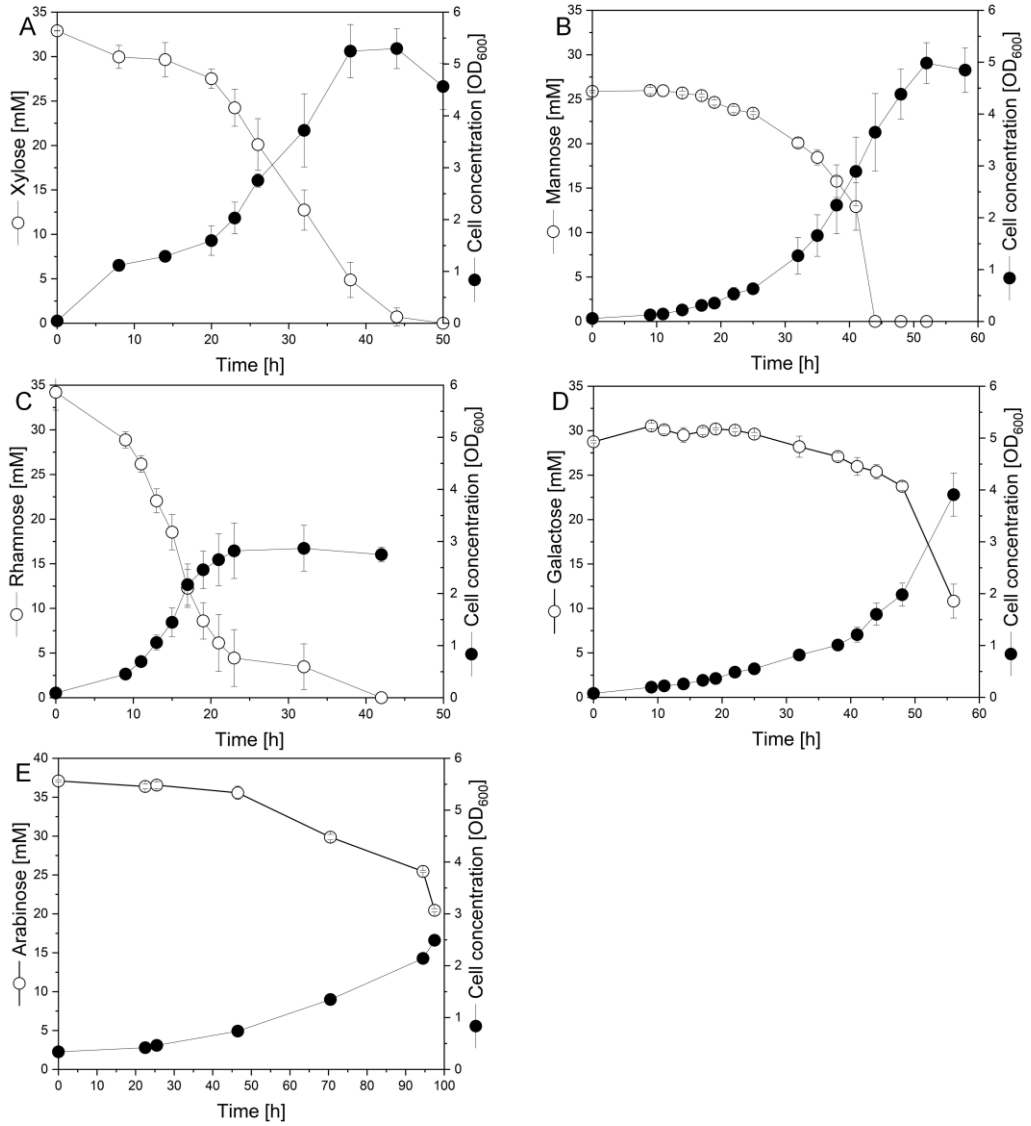

Figure 5.17: *Amycolatopsis sp.* ATCC 39116 growing in shake flasks on different sugars. The microbe was grown in shake flasks in in minimal medium at 37 °C using (A) xylose, (B) arabinose, (C) rhamnose, (D) galactose, and (E) mannose as the sole carbon source, respectively. (n=3)

Amycolatopsis sp. ATCC 39116 consumed 35 mM of xylose within 45 hours (Figure 5.17 A). It grew exponentially ($\mu = 0.067\ h^{-1}$) and reached a final cell concentration of 4.5 OD_{600nm}. The microbe was also able to degrade mannose (Figure 5.17 B). After a lag phase of 20 hours, it grew exponentially ($\mu = 0.094\ h^{-1}$) up to a cell concentration of 5 OD_{600nm}.

On rhamnose, *Amycolatopsis sp.* ATCC 39116 exhibited a biphasic growth profile (Figure 5.17 C). After a short lag phase of 10 hours, the strain consumed 30 mM of the initially added 35 mM rhamnose within 20 hours. Then, growth suddenly slowed down, it took additional 20 hours to deplete the last 5 mM rhamnose. Arabinose and galactose utilization was significantly slower (Figure 5.17 D and E). All in all, all sugars could be used, although at different specific growth rates (Figure 5.18). The specific growth rate for arabinose could not be determined.

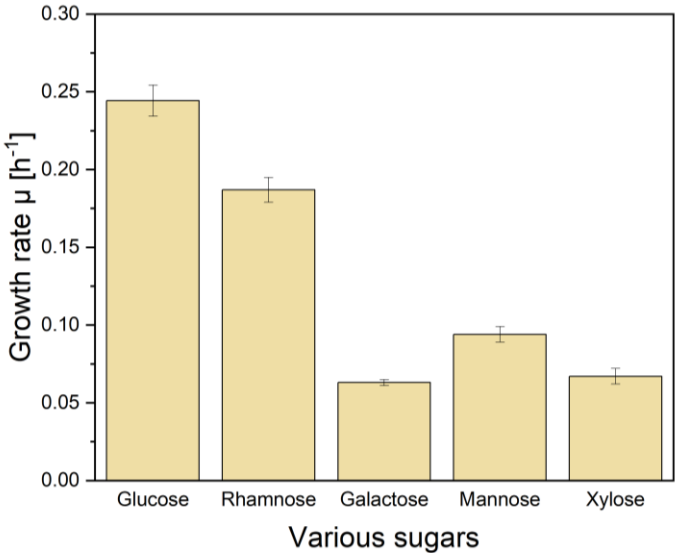

Figure 5.18: Specific growth rate of *Amycolatopsis sp.* ATCC 39116 on different sugars. The cells were grown at 37°C in minimal medium with glucose, rhamnose, galactose, mannose or xylose as sole C-source. (n=3)

5.4.2 Utilization of depolymerized hemicellulose as substrate for growth

As shown*, Amycolatopsis sp.* ATCC 39116 MA-2 was capable of utilizing different sugars. Towards a more sustainable feedstock, depolymerized hemicellulose, containing xylose and glucose, was tested next. Hemicellulose is a commercially relevant side-stream from the pulp and paper industry. Prior to the cultivation, the polymer was processed as described above (Section 4.6).

As shown in Figure 5.19, *Amycolatopsis sp.* ATCC 39116 preferred glucose over xylose and depleted the hexose first. Afterwards, the strain started to grow on xylose (μ=0.026 h^{-1}).

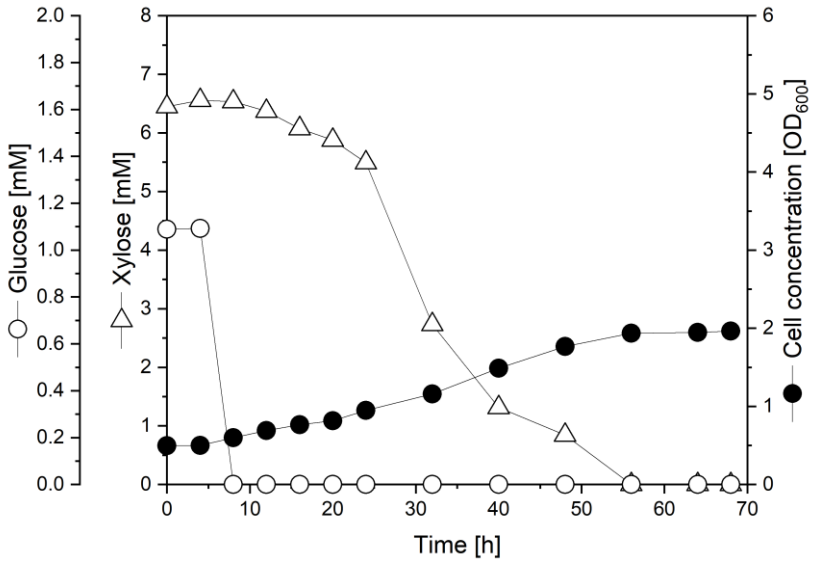

Figure 5.19: *Amycolatopsis sp.* ATCC 39116 MA-2 utilize depolymerized hemicellulose. The mutant (*ΔcatB-9302::hyg^R, ΔcatB-18510*) was grown in a minimal medium containing depolymerized hemicellulose. The substrate was produced by hydrothermal conversion, followed by steam distillation to remove furfural. The incubation temperature was 37 °C. (n=3)

5.4.3 Production of MA from guaiacol growing on depolymerized hemicellulose

Next, the production performance of the engineered strain MA-2 on xylose was to be investigated (Figure 5.20). In a first attempt, the model compound xylose was used as a growth substrate and guaiacol as precursor for MA production.

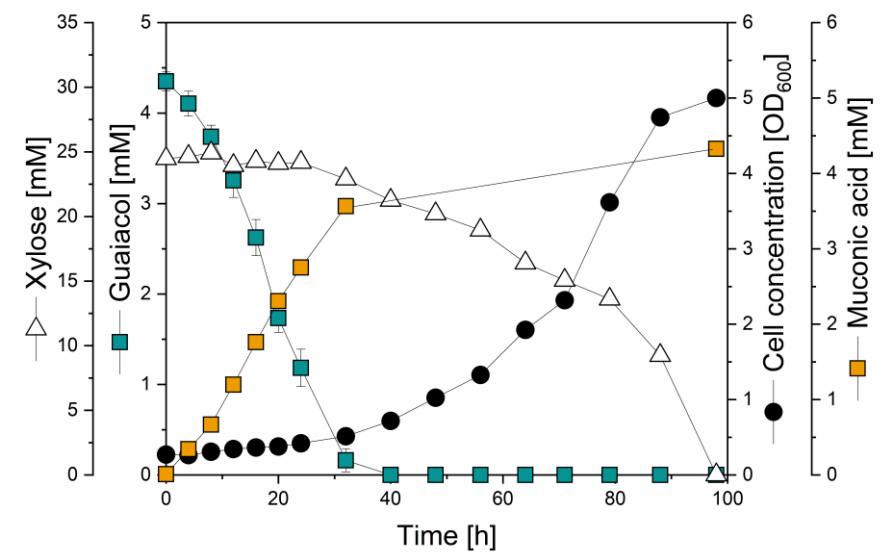

Figure 5.20: Production of MA from guaiacol while growing xylose. *Amycolatopsis sp*. ATCC 39116 MA-2 (*ΔcatB-9302::hyg*^{R}*, ΔcatB-18510*) was grown in a minimal medium containing pure xylose and guaiacol. The incubation temperature was 37 °C. (n=3)

Within 30 hours, *Amycolatopsis sp*. ATCC 39116 MA-2 produced 3.5 mM MA from 4.3 mM guaiacol. At the end of cultivation, the titer of muconic acid increased to 4.3 mM, including *cis-, cis* and *cis-, trans* muconic acid. The product formation corresponded to a yield of 1 mol mol^{-1}. During the conversion, the level of xylose remained almost stable and the cell concentration increased only slightly. Obviously, *Amycolatopsis sp*. ATCC 39116 preferred to utilize the aromatic compound over the sugar.

In a further experiment, depolymerized hemicellulose was used as substrate for growth and guaiacol as precursor for MA production (Figure 5.21).

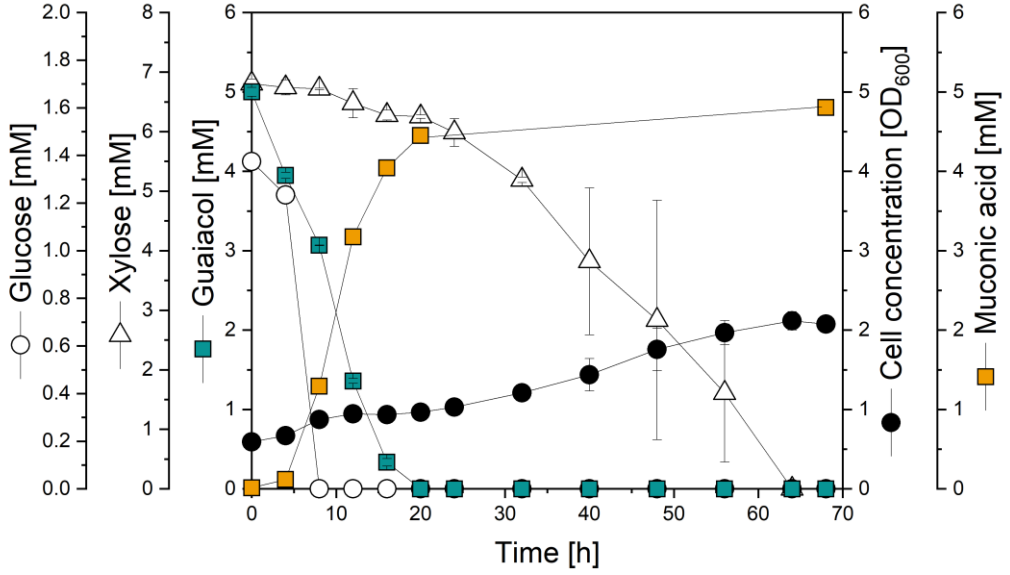

Figure 5.21: Production of MA from guaiacol while growing on depolymerized hemicellulose. *Amycolatopsis sp*. ATCC 39116 MA-2 (*ΔcatB-9302::hyg*^{R}*, ΔcatB-18510*) was grown in a minimal medium containing depolymerized hemicellulose and guaiacol. The substrate was produced by hydrothermal conversion, followed by steam distillation to remove furfural. The incubation temperature was 37 °C. (n=3)

Amycolatopsis sp. ATCC 39116 MA-2 was found capable of producing MA from guaiacol while growing on hemicellulose hydrolysate. Within 20 hours, the strain produced 4.4 mM MA from 5 mM guaiacol. The final MA titer of 4.8 mM, including *cis-, cis* and *cis-, trans* muconic acid derivates, was obtained after 70 hours, when xylose was depleted. The product formation corresponded to a yield of 0.96 mol mol^{-1}. Depolymerized hemicellulose appears to be an appropriate growth substrate for *Amycolatopsis sp*. ATCC 39116 MA-2.

5.4.4 Utilization of spent sulfite liquor as substrate for growth

Amycolatopsis sp. ATCC 39116 was able to grow on different types of sugars, present in spent sulphite liquor (SSL), another major byproduct from the pulp and paper industry (Section 5.4.1). Beneficially, the microbe grew well on medium, containing spent sulfite liquor ultrafiltration permeate (SSL UF, Borregaard, Snarpsborg, Norway) as sole carbon source (Figure 5.22).

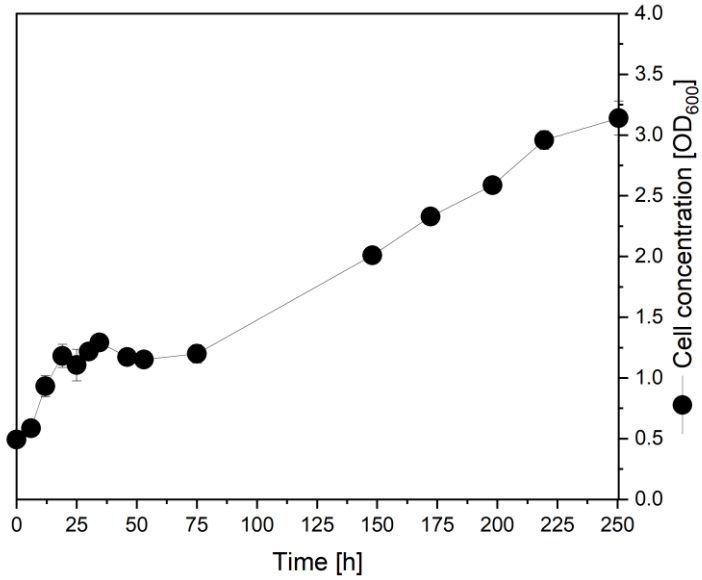

Figure 5.22: Growth physiology of *Amycolatopsis sp.* ATCC 39116 MA-5 on spent sulphite liqour (SSL UF, Borregaard, Snarpsborg, Norway). The strain MA-5 (*ΔcatB-9302::hyg^R, ΔcatB-18510, ΔpcaG-37543::aroY*) was grown in a minimal medium containing 10% SSL as C-source at 37 °C. (n=3)

To further evaluate SSL as the growth substrate, vanillin was added as precursor for MA production (Figure 5.23). The vanillin level decreased immediately after the start of the cultivation. About 80 % of the vanillin was initially converted to vanillate and guaiacol. The rest was reduced to vanillyl alcohol. The alcohol peaked after about 25 h at 1.3 mM. Afterwards its concentration slightly decreased over time. Low levels of vanillate (0.2 mM) remained in the medium until the end of cultivation.

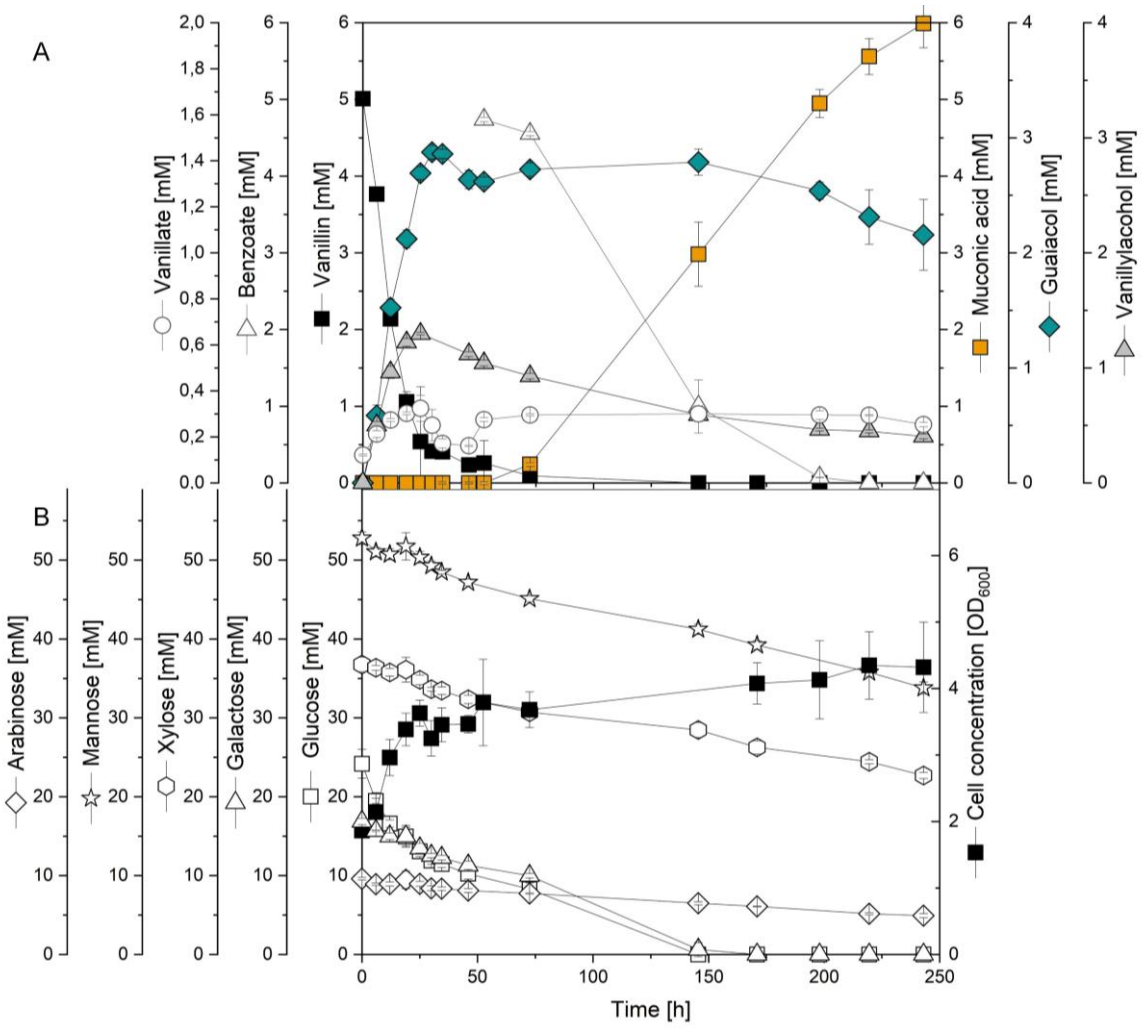

Figure 5.23: Production performance of *Amycolatopsis sp.* ATCC 39116 MA-5. The strain MA-5 (*ΔcatB-9302::hyg*^{R}*, ΔcatB-18510, ΔpcaG-37543::aroY*) was grown in minimal medium with 10% SSL (SSL UF, Borregaard, Snarpsborg, Norway) as C-source (B) and 5 mM Vanillin as precursor for MA production (A). After 50 hours, benzoate was added as an additional precursor für MA production. The cultivation was carried out at 37 °C. (n=3)

After 50 hours, 5 mM benzoate was added to further promote MA production. Benzoate was converted to MA within 150 hours. After benzoate was consumed, the MA titer increased further, indicating that vanillin was also converted into the target product MA. In total, 6 mM MA (*cis-,cis-* and *cis-, trans-*muconic acid) was formed after 250 hours, revealing that *Amycolatopsis sp*. ATCC 39116 MA-5 produced MA from aromatics, while growing on SSL. Regarding the sugars, glucose and galactose were depleted after 150 hours. Arabinose, mannose, and xylose decreased uniformly over time but were not completely consumed during the process time.

5.4.5 Inhibiting effects of different sugars on the production of MA from vanillin

Finally, the different sugars were compared, regarding their effects on the production of MA from vanillin. For this purpose, *Amycolatopsis sp*. ATCC 39116 MA-5 was cultivated in minimal medium containing about 4 mM vanillin plus one sugar (glucose, arabinose, xylose, galactose, mannose, or rhamnose). In addition, a combination of all SSL-based sugars was tested as synthetic mixture. All cultures were incubated for six days and analyzed for the final concentration of the formed MA and aromatic pathway intermediates (Figure 5.24).

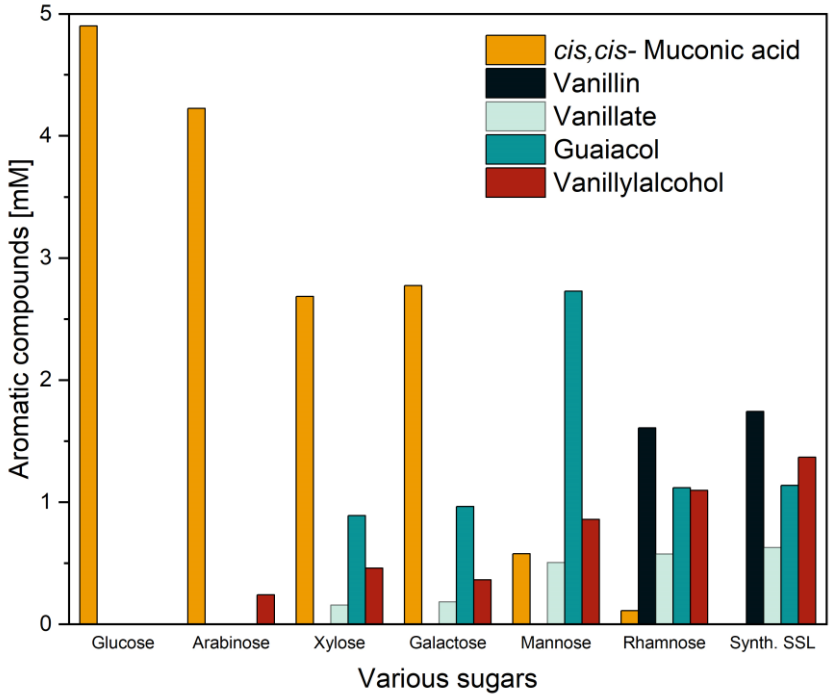

Figure 5.24: Inhibiting effects of different sugars on MA production from vanillin. The strain MA-5 (*ΔcatB-9302::hyg*^{R}*, ΔcatB-18510, ΔpcaG-37543::aroY*) was grown in minimal medium with 5 mM Vanillin as precursor for MA production and one sugar (glucose, arabinose, xylose, galactose, mannose, or rhamnose) or a combination of all sugars present in SSL After 6 days, the concentrations of MA and aromatics were measured by HPLC. The cultivation was carried out at 37 °C.

Amycolatopsis sp. ATCC 39116 MA-5 produced MA from vanillin at a stoichiometric yield of 100 % (1 mol mol^{-1}), only when glucose was used as the growth substrate. If the growth substrate was switched to arabinose, a yield of 93% was observed, while 7% of vanillin was converted to vanillylalcohol instead of vanillic acid.

Xylose and galactose have a moderate inhibiting effects on the aromatic degradation pathways. After 6 days of cultivation, a yield of 67% MA from vanillin was obtained for xylose, while a yield of 63 % was found for galactose. Next to MA, vanillylalcohol, vanillate, and guaiacol were still present in the medium. For mannose and rhamnose, a high inhibiting effect on the aromatic degradation pathways and high yields of vanillylalcohol were observed. Only 0.6 mM MA was produced from vanillin if mannose was used as C-source, corresponding to a yield of 14%. In the case of rhamnose, the yield dropped to 2.5% MA from vanillin after 6 days. Vanillin was still detectable in the medium.

6 Discussion

As shown, this work demonstrates the integrated chemical and biochemical production of *cis,cis*-muconic acid (MA) from real lignin (Figure 7.2) and vanillin (Figure 5.15). The innovative aspects of this new process include the usage of metabolically modified *Amycolatopsis* sp. ATCC 39116 strains, which enable the conversion of guaiacol and guaiacol-rich hydrolysates into the platform chemical MA. MA is a chemical of recognized industrial value, particularly for the production of commercial plastics (Zhang et al., 2015).

Remarkably, the guaiacol-rich hydrolysate was not artificially prepared but obtained from softwood lignin through a hydrothermal conversion process at high pressure and temperature (Section 5.1.3). Lignin is considered as a low-value by-product from the pulp and paper industry, and efficient valorization strategies are still missing (Bandounas et al., 2011; Rinaldi et al., 2016).

The production of MA is enhanced by the successful disruption of the β-ketoadipate pathway, a convergent pathway for the degradation of aromatics in the microbe (Harwood and Parales, 1996; Park and Kim, 2003). Naturally, this pathway degrades aromatics to β-ketoadipate and directs them to the citric acid cycle (Harwood and Parales, 1996). In this study, we disrupted the metabolic pathway at the muconate cycloisomerase step, which is downstream of the target product MA. This disruption leads to the accumulation of MA from various aromatic compounds such as guaiacol, *o*-cresol, or vanillate, and lignin hydrolysates (Figure 5.10 and Figure 5.13).

Furthermore, the integration of the protocatechuate decarboxylase gene (*aroY*) enables the use of protocatechuate as precursor substrates for MA production (Figure 5.14).

6.1 *Amycolatopsis sp.* ATCC 39116 has ideal properties as a cell factory for MA production from lignin-based aromatics

Amycolatopsis sp. ATCC 39116 is an advantageous candidate for lignin valorization due to its unique properties. This strain is naturally able to depolymerize lignin (Antai and Crawford, 1981) and metabolizes a wide range of aromatic compounds (Antai and Crawford, 1983; Antai and Crawford, 1981; Pometto et al., 1981; Sutherland et al., 1981a; Sutherland et al., 1983). It tolerates guaiacol in increased concentrations up to 25 mM (Table 8.2), and shows a preference for aromatics over sugars (Figure 5.7). In addition, the microbe exhibits natural thermotolerance, performing optimally at 42 °C (Figure 5.7). This is highly advantageous for industrial applications, as it reduces cooling costs and contamination risks (Abdel-Banat et al., 2010).

These characteristics, along with our findings, highlight *Amycolatopsis sp.* ATCC 39116 as a highly promising host for future lignin valorization efforts.

6.2 The successful bioconversion of guaiacol into MA sets a milestone in lignin valorization

For the biotechnological production of MA from pure aromatics, a wide range of substrates is available, including benzoate (Bang and Choi, 1995; Becker et al., 2018; Mizuno et al., 1988; van Duuren et al., 2012), catechol (Becker et al., 2018; Kohlstedt et al., 2018; Maxwell Peter, 1983), phenol (Becker et al., 2018; Vardon et al., 2015), vanillate (Sonoki et al., 2018) and vanillin (Sonoki et al., 2018). Here, we described a novel strain of *Amycolatopsis sp.* ATCC 39116 that produced 3.1 g L^{-1} MA from guaiacol in a fed-batch process. *Amycolatopsis sp*. ATCC 39116 is one of the few microbes that can utilize guaiacol (Pometto et al., 1981), alongside *Acetobacterium woodii* DSM 1030 (Kalil et al., 2002) or *Rhodococcus rhodochrous* (Garcia-Hidalgo et al., 2019). The metabolic pathway involves the demethylation of guaiacol to catechol, the immediate precursor of MA (Sutherland, 1986). Recently, the cytochrome P450-reductase gene *gcoAB*, responsible for the conversion of guaiacol, was characterized and introduced via plasmid-based expression into *P. putida* KT2440 (Mallinson et al., 2018; Tumen-Velasquez et al., 2018).

However, chromosomal integration of the native *gcoAB* in *A. baylyi* or *P. putida* did not result in strains capable of using guaiacol as the sole carbon source, unlike *Amycolatopsis sp.* ATCC 39116 (Tumen-Velasquez et al., 2018). Evolution by Amplification and Synthetic Biology (EASy) was necessary to make these genes accessible to other microbes (Tumen-Velasquez et al., 2018). This highlights the challenges of using *gcoAB* in other hosts and underscores the potential of the strains developed in this work. Additionally, guaiacol has been shown to be a crucial target for lignin valorization (Beckham et al., 2016). Lignin from softwoods is predominantly composed of guaiacyl units, and in hardwoods, the proportion of guaiacyl and syringyl units is approximately equal (Gullichsen et al., 1999). Therefore, guaiacol is a major building block of lignin. This explains why significant amounts of guaiacol are produced during the thermochemical degradation of lignin, as observed in this work and documented in the literature (Pińkowska et al., 2012). Recently, a mild formic acid-induced treatment of lignin yielded substantial amounts of guaiacol (Rahimi et al., 2014), describing the highest yield of structurally identified monomeric aromatics. Furthermore, a pure guaiacol solution (25.5 wt%) was produced using Lewis acid ($La(OTf)^3$) as a catalyst in a methanol-water solvent (Shen et al., 2019). This process results in a highly attractive aromatic feedstock for further upgrading and perfectly aligning with the strains developed in this study.

6.3 Efficient production of MA using metabolically engineered *Amycolatopsis sp.* ATCC 39116 MA-2

As demonstrated in this work, the engineered strain *Amycolatopsis sp.* ATCC 39116 MA-2, with deletions of the *catB* genes AATC3_0201000018510 and AATC3_020100009302, successfully converts guaiacol to MA. This study revealed that deleting all three predicted gene candidates is not required for efficient MA production. The single knockout of the *catB* gene AATC3_0201000018510 is sufficient for MA production (Section 5.2.4). This active *catB* gene is located in the *cat*-operon, adjacent to *catA* and *catC* (Park and Kim, 2003).

However, compared to the construction of *Amycolatopsis sp.* ATCC 39116 MA-2, it took longer to remove the *catB* 18510 gene from the genome of the wild-type and create *Amycolatopsis sp.* ATCC 39116 MA-4. Without the use of the antibiotic hygromycin, it was more challenging to eliminate *E. coli* ET12567, leading to a screening issue during the first recombineering event as agar plates were overgrown with *E. coli* ET12567. Consequently, further experiments were carried out with MA-2, which has a similar performance but is easier to manipulate due to its hygromycin resistance. The knockout of the third *catB*-1440 gene could not be achieved in a markerless manner due to the sequence of the flanking regions containing repeating elements, which made it impossible to assembly a markerless knockout plasmid. As an alternative, we attempted to remove the third *catB* gene by simultaneous integration of an additional *catA* gene, under control of its native promoter. Unfortunately, this did not result in an improved conversion. Instead, the yield dropped from around 90% to 40%. The additional copy of the *catA* gene appears to have had a negative impact on the production rate, perhaps the chosen promoter was too strong. This suggests that the regulation of the *cat*-operon is highly complex and sensitive.

The chosen producer strain, *Amycolatopsis sp.* ATCC 39116 MA-2, forms MA even at gram scale and achieves yields of up to 96% (mol mol $^{-1}$), representing an 18-fold improvement compared to the wild-type. Although a perfect stoichiometric conversion (100%) was expected (van Duuren et al., 2011), it turned out that isomerization of *cis,cis*-muconic acid to *cis,trans*-muconic acid occurred. This isomerization is well-documented (Carraher et al., 2017) and can be detected by HPLC (Soni et al., 2018). Indeed, the HPLC diagram revealed a second peak, with the highest absorbance at 260 nm, eluting slightly later than *cis,cis*-muconic acid. Considering this extra amount, closed the balance to 99%.

Additionally, the created strains produced MA from true lignin hydrolysates derived from hydrothermal conversion, achieving a yield of 72%. This is a significant step towards sustainable MA production and the valorization of pulp side streams. Similar experiments with lignin hydrolysates containing large amounts of catechol or *p*-coumarate have been conducted (Becker et al., 2018; Kohlstedt et al., 2018; Vardon et al., 2015). However, this study is the first to use a guaiacol-rich hydrolysate (Weiland et al., 2022).

This proof of concept further demonstrates the feasibility of combining chemical lignin depolymerization with biological conversion by *Amycolatopsis sp.* ATCC 39116. Until this work, the use of guaiacol as a substrate for MA production has remained a challenge (Weiland et al., 2022). Compared to other aromatic substrates, the titer achieved from guaiacol is still relatively low, requesting further efforts for improvement in the future (Becker et al., 2018).

6.4 New toolbox for genome editing appears useful for streamlined metabolic engineering of *Amycolatopsis sp*. ATCC 39116

Genetic modification of *Amycolatopsis sp*. ATCC 39116 has proven extremely challenging, similar to other actinomycetes (Fleige et al., 2016; Fleige and Steinbüchel, 2014; Siegl and Luzhetskyy, 2012). This difficulty is reflected in the rarity of reported genomic deletion and integration mutants of this microbe (Meyer et al., 2017). The challenges in genetic engineering are related to its high GC content of 71.9% (Davis et al., 2012; Frey et al., 2008). Non-homologous DNA integration frequently occurs after plasmid transformation (Fleige et al., 2016), and the overall rate of homologous recombination events, required to remove the plasmid backbone, is very low (Fleige et al., 2013). Recently, an improved deletion system has been developed that overcomes these problems, representing a significant achievement (Meyer et al., 2017). This system requires the artificial introduction of a streptomycin resistance into the host genome. However, this is a drawback for industrial applications, which requires efficient genetic biocontainment strategies to protect against potential escape mechanisms of genetically modified organisms from large-scale cultivation and strongly prefer the use of strains without antibiotic resistance (Mandell et al., 2015). In contrast, our approach relies on blue-white screening for strain selection, which is simpler and does not inherently involve antibiotic resistance genes. However, to facilitate the removal of *E. coli,* used for plasmid transformation, we introduce an antibiotic resistance gene. Fortunately, this resistance gene is flanked by *loxP* sites so that it can subsequently be removed (Myronovskyi et al., 2011). The system also works without this antibiotic resistance but requires a slightly higher screening effort.

The implementation of blue-white screening has significantly reduced experimental efforts and expedited the generation of new mutants. A new strain can now be constructed within 10 days, which is 30–40% faster than the current state of the art and involves less experimental effort (Meyer et al., 2017). Elaborate steps, such as repeated strain transfers during selection, are now obsolete. While previous studies reported difficulties in distinguishing between white and blue colonies using the β-glucuronidase system (Fleige et al., 2013), our new approach enables clear differentiation (Figure 5.5). Furthermore, the discrimination of conjugants was highly effective on X-Gluc selection agar. This success is likely due to the use of the *tipA* promoter, which results in higher *gusA* expression and sufficient β-glucuronidase reporter activity (Myronovskyi et al., 2011). In previous studies, the β-glucuronidase gene was used under the control of the *ermE* promoter (Fleige et al., 2016). The method developed in this work, utilizing the *tipA* promoter for higher *gusA* expression, opens new possibilities for future strain development. This advancement provides a more efficient and reliable tool for distinguishing between blue and white clones, facilitating quicker and more precise genetic modifications.

6.5 The capability of *Amycolatopsis sp*. ATCC 39116 to convert methylated aromatics extends the spectrum of chemicals accessible from lignin

Amycolatopsis sp. ATCC 39116 has demonstrated the capability to convert methylated aromatics, thereby extending the range of chemicals accessible from lignin. In this study (Section 5.2.7), it was observed that *Amycolatopsis sp*. ATCC 39116 forms 2-methyl-MA from *o*-cresol instead of MA (Figure 5.11). It is assumed that the *gcoAB* gene, which converts guaiacol into catechol (Mallinson et al., 2018), can also convert *o*-cresol into 3-methylcatechol. This presents a new area for further exploration. 3-Methylcatechol can be cleaved by catechol 1,2-dioxygenase (CatA), as demonstrated before (An et al., 2001) and in this work, channeling it through the *ortho*-cleavage pathway to produce the new methylated product. From the results in this work, it can be inferred that the unknown product is 2-methyl MA. The ability of catechol 1,2-dioxygenase to accept methylated catechol underscores the enzyme's promiscuity (Tawfik and S., 2010), which is crucial for converting structurally different aromatics into valuable products.

Lignin hydrolysates typically contain various cresols and methylated forms of guaiacol, such as methoxymethylphenols (Pińkowska et al., 2012). This opens up new research possibilities and promising approaches (Henson et al., 2022). The production of MA with a single, stereochemically defined methyl group in the inner hydrocarbon chain is challenging through chemical mean, likely explaining why such a chemical is not commercially available (Rinkel, 2019). Additionally, blends of MA and its methylated derivates from lignin feedstocks could lead to plastics with new properties (Henson et al., 2022; Rinkel, 2019; Rorrer, 2016). The presence of methyl groups in MA has an impact on the molecular architecture of the resulting polymers and the properties of the composite produced from them (Rinkel, 2019; Rorrer, 2016). Advanced downstream purification could also aim to separate the different MA variants for specific applications.

6.6 Valorization of alkaline-oxidized softwood lignin

The catabolism of vanillin and vanillate via guaiacol and catechol is well documented (Pometto et al., 1981; Sutherland et al., 1983). Consequently, it is not surprising that the mutant *Amycolatopsis sp.* ATCC 39116 MA-2 is capable of producing MA from vanillin and vanillate (Section 5.3.2). Unlike phenolics from lignin, which have been thoroughly studied (Becker et al., 2018; Kohlstedt et al., 2018; van Duuren et al., 2011) these two lignin-based aromatics have not yet been studied in detail (Weiland et al., 2023). In this regard, this work highlights the potential of using these less-studied aromatics for MA production, expanding the scope of lignin valorization.

In previous studies, e.g., vanillin was converted to β-ketoadipate using *Pseudomonas putida* (Suzuki et al., 2021), and 2-pyrone-4-6-dicarboxylic acid was produced from vanillate and vanillin by *Novosphingobium aromaticivorans* (Perez et al., 2019). Moreover, MA has been produced from vanillate, using *P. putida* (Shinoda et al., 2019), and *Corynebacterium glutamicum* (Weiland et al., 2023). Vanillin and vanillate can be produced by alkaline oxidation of softwood lignin, an industrial process, already yielding in 3,000 tons of vanillin (Fache et al., 2016; Kratzl et al., 1974). However, the global market for flavoring vanillin is rather small at 16,000 tons ($ 230 million in 2011) (Ponnusamy et al., 2018). This indicates a substantial potential for further valorization. This work describes the new strain MA-2 that forms MA from vanillate even at gram scale (3 g L^{-1}) within 72 hours in a fed-batch culture.

This finding offers enormous potential for the valorization of large streams of softwood lignin, showcasing the strain's capability to contribute to sustainable and efficient lignin utilization.

6.7 Efficient production of MA from vanillate and vanillin

As demonstrated in this work, the engineered strain *Amycolatopsis sp.* ATCC 39116 MA-2 (Δ *catB* AATC3_0201000018510, Δ *catB* AATC3_020100009302) successfully converts vanillin and vanillate into MA. Given that glucose is a staple food and its use for chemical production competes with the food industry (Buschke et al., 2013), it is advantageous to use *Amycolatopsis sp*. ATCC 39116 MA-2 as a producer of MA from vanillin or vanillate, as no additional carbon source is required. To proof this concept, an experiment was conducted using only vanillate as substrate. Vanillate was chosen because it is expected to produce less vanillyl alcohol as a byproduct (Meyer et al., 2018). The microbe produced 3.4 mM MA, corresponding to a yield of 68%, indicating that more vanillate is converted into guaiacol than protocatechuate. This is supported by the *vdcBCD* genes studied previously (Meyer et al., 2017), which were found to be very efficient. Consequently, more vanillate is converted to guaiacol rather than being channeled into the PCA 3,4- ortho-cleavage pathway. In an additional fed-batch experiment, *Amycolatopsis sp.* ATCC 39116 MA-2 produced 20.2 mM MA, corresponding to a yield of 43%. This performance is comparable to studies by Shinoda, who produced 3.2 g L^{-1} MA from vanillate using *P. putida* (Shinoda et al., 2019). As shown in Figure 5.12 B, only part of the vanillate was converted into the intermediate guaiacol, which reached a final concentration of about 7 mM after 72 hours. If one includes the guaiacol and excludes the excess vanillate in the calculation, the yield increases to 60%. Thus, approximately 40% of the substrate was used for growth and 60% for MA production. This suggests that optimizing the conversion pathways and reducing substrate usage for growth could further enhance the yield of MA production.

Further studies focused on the metabolization of vanillin, vanillate, and protocatechuate. In order to shift the flux towards MA production, glucose was added as an additional substrate for growth.

The strain achieves yields of up to 70 % MA from vanillin and furthermore 78% MA from vanillate. Although a stoichiometric conversion with 100% yield (mol mol $^{-1}$) was not observed, these results are promising. *Amycolatopsis sp.* ATCC 39116 MA-2 can still convert vanillic acid to protocatechuate (Meyer et al., 2018). Additionally, the microbe can convert vanillin to the dead-end product vanillyl alcohol (Meyer et al., 2018). The formation of vanillyl alcohol is a well-known detoxification mechanism (Fleige et al., 2016; Meyer et al., 2018).

Further work is needed to determine how much vanillin is being diverted to the dead-end product, vanillyl alcohol. Additional metabolic engineering, such as the deletion of the 3,4-ortho-cleavage pathway and the oxidoreductase gene (*ytf*G), could potentially improve the yield. Furthermore, MA was not formed from protocatechuate, as protocatechuate was converted to acetyl-CoA and succinyl-CoA via the PCA 3,4-*ortho*-cleavage pathway (Meyer et al., 2018). A simple solution to overcome this problem would be the conversion of protocatechuate to catechol, using protocatechuate decarboxylase (AroY) (Vardon et al., 2015).

6.8 Further metabolic engineering towards highly efficient MA production from vanillin, vanillate and protocatechuate

In this work, *Amycolatopsis sp*. ATCC 39116 MA-2 was enhanced to a high-efficiency production host for *cis, cis*-muconic acid production from vanillin, vanillate, and protocatechuate. This was achieved by deleting the gene *pcaG* and redirecting protocatechuate to the CAT 1,2-ortho-cleavage pathway through the introduction of the protocatechuate decarboxylase gene (*aroY*).

Amycolatopsis sp. ATCC 39116 MA-5 produced MA from protocatechuate for the first time, with a stochiometric yield of 100%. The yield of MA from vanillin and vanillate could be increased by approximately 25%. Closer HPLC analysis revealed an additional product peak in the supernatant, identified as vanillyl alcohol (data not shown), consistent with previous reports (Fleige et al., 2016; Meyer et al., 2018). It is interesting to note that *Amycolatopsis sp*. ATCC 39116 MA-5 only accumulates about 10% of vanillylalcohol when it is used as a host for MA production from vanillin, while *Corynebacterium glutamicum* accumulates about 50% of it (Weiland et al., 2023).

Notably, the genetic engineering of *Corynebacterium glutamicum* enhanced the yield to 100%, indicating that the deletion of the oxidoreductase gene (*ytfG*) is a promising target for improvement.

As shown in Figure 5.13 B, guaiacol accumulated in large amounts, indicating that the VdcBCD enzymes work faster than GcoAB (Meyer et al., 2017). This suggests that the expression of *gcoAB* is a bottleneck in MA production. Further studies to fine-tune the expression of *gcoAB* could potentially improve the yield. This work demonstrates that *Amycolatopsis sp.* ATCC 39116 has been successfully upgraded for high-efficiency production of MA from vanillin, vanillate, and especially protocatechuate. Consequently, this microbe offers promising potential for utilizing the large streams of softwood lignin that are currently underutilized.

6.9 *Amycolatopsis sp.* ATCC 39116: A versatile microbe for utilizing various pulp process side streams

Interestingly, *Amycolatopsis sp*. ATCC 39116 MA-2 is capable of growing on a variety of sugars, including L-arabinose, D-xylose, D-fructose, D-glucose, D-mannitol, and L-rhamnose (Shinoda et al., 2019). This capability may also enable the use of other byproducts from the pulp and paper industry, such as xylose or spent sulphite lqiuor (SSL), commonly known as brown liqour from the sulphite pulping process. After the delignification of wood chips, hemicellulose and cellulose are retained (Hamaguchi et al., 2012). Hemicellulose can be easily separated and further valorized, for example, by the conversion into xylose through hydrothermal conversion (Jing and LÜ, 2007). The pulp contains around 89% of the cellulose from wood chips (Rueda et al., 2015). The remaining cellulose, a portion of hemicellulose, and the lignin are left behind in the SSL (Rueda et al., 2015). Industrial SSL contains the following sugars: xylose (22%), glucose (2%), galactose (2%), mannose (1.5%), and arabinose (1.5%). Additionally, it includes furfural (0.15%), HMF (0.03%), acetic acid (6.12%), lignosulfonates (42%) and other unidentified organics (10%) (Rueda et al., 2015). This diverse composition makes SSL a valuable feedstock for further biotechnological processes, whereby the metabolic versatility of *Amycolatopsis sp*. ATCC 39116 MA-2 can be utilized for improved utilization.

As demonstrated in this work, the engineered strain *Amycolatopsis sp.* ATCC 39116 MA-2, with deletions of the *catB* genes AATC3_0201000018510 and AATC3_020100009302, is capable of growing on all different sugars present in SSL (Section 5.4.1). Additionally, the strain naturally depolymerizes lignin (Antai and Crawford, 1981) and metabolizes a wide range of lignin-derived aromatic compounds (Table 3.1) (Antai and Crawford, 1983; Antai and Crawford, 1981; Pometto et al., 1981; Sutherland et al., 1981a; Sutherland et al., 1983). These properties make *Amycolatopsis sp.* ATCC 39116 a promising organism for further valorization strategies.

6.10 Utilization of sugar-containing side streams from the pulp industry enables an entirely lignocellulose-based production process

Given that xylose is predominant in spent sulfite liquor (SSL) and can easlily be produced by the conversion of hemicellulose, initial studies in this work focused on xylose utilization. *Amycolatopsis sp.* ATCC 39116 metabolized 5 g L^{-1} of xylose within 45 hours, reaching a final cell concentration of 4.5 $OD_{600.}$ Moreover, further experiments with the engineered strain *Amycolatopsis sp.* ATCC 39116 MA-2 revealed that the microbe could also grow on xylose, derived from hemicellulose hydrolysates, and produce MA from guaiacol while growing on the hydrolysate (Section 5.4.3).

To further improve the sustainability of pulp mills, lignocellulosic by-product streams, e.g., SSL, can be used as alternative feedstocks (Sinner et al., 2022). Every year, around 90 billion liters of SSL accumulate from the sulfite digestion of wood (Lawford and Rousseau, 1993). SSL contains a complex mixture of carbohydrates, making it an attractive substrate stream for industrial biotechnology (Sinner et al., 2022).

In the next approach, *Amycolatopsis sp*. ATCC 39116 was grown successfully in SSL (Section 5.4.4). Since minimal substrate is needed for the production of MA for growth (Section 5.2.3), it was expected that MA production would proceed smoothly. In a further experiment, vanillin was added as a precursor. However, some issues arose with using vanillin for MA production. Vanillin was immediately converted via vanillic acid into guaiacol or channeled into vanillyl alcohol, with no MA being formed from vanillin. Instead, guaiacol remained in the medium.

To test if MA production from other aromatics is possible, benzoate was added after 50 h and converted to MA, albeit very slowly (over 150 hours). The MA titer continued to increase even after benzoate was consumed, indicating that a small portion of vanillin was also being converted to MA. The observed regulatory effects that prevent the degradation of guaiacol appear to limit the use of SSL as a substrate for cell growth. Further studies (Section 5.4.5) revealed that rhamnose and mannose exert strong regulatory effects on the vanillin catabolism. Additionally, the combination of all sugars present in SSL completely inhibits the production of MA from vanillin. After 6 days, no MA was detected, and large amounts of vanillin and vanillyl alcohol remained in the medium.

These results highlight the challenge of using SSL (Sinner et al., 2022). We observed inhibition effects that cannot easily be circumvented. To address this problem, the expression of the *gcoAB* gene must be optimized. However, this is also challenging, as demonstrated by our own results (data not shown) and previous studies (Mallinson et al., 2018; Tumen-Velasquez et al., 2018), who expressed these genes in *Pseudomonas putida* KT2440.

7 Conclusion and Outlook

This work provides innovative ideas for the use of various side streams from the pulp and paper industry, specifically using *Amycolatopsis species* ATCC 39116 (Figure 6.1). The metabolically engineered organism can produce *cis,cis*-muconic acid (MA) from guaiacol-rich lignin hydrolysate, and from vanillin obtained by alkaline oxidation of softwood lignin. Moreover, it is able to grow on xylose, which can be derived from hemicellulose. By turning these waste streams into valuable resources, this approach enhances the sustainability of lignocellulose processing, demonstrating how side streams from the pulp and paper industry can be efficiently utilized in a bio-based economy.

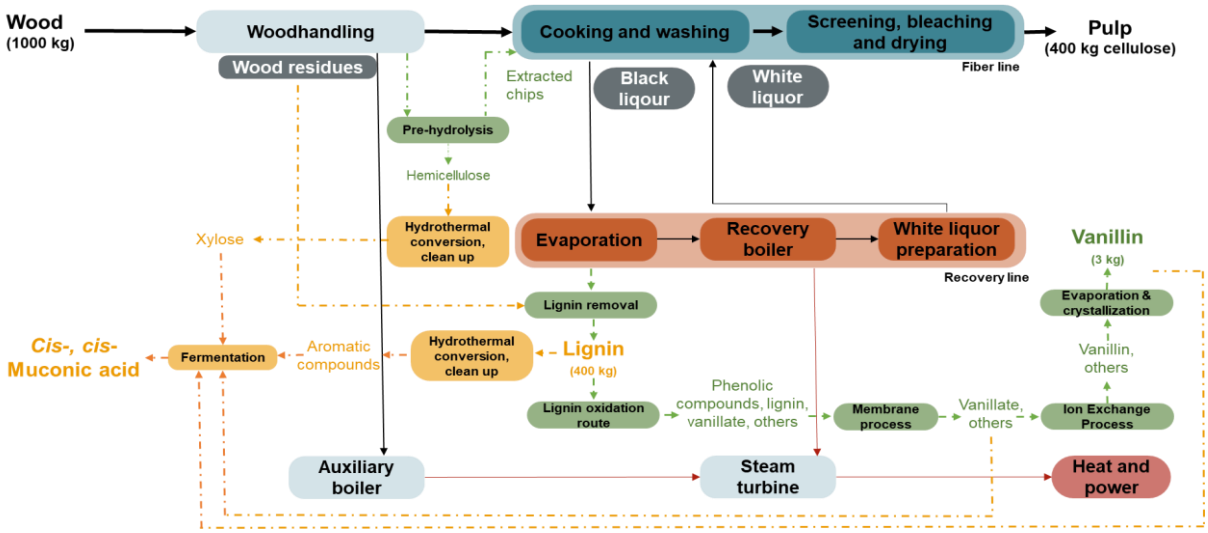

Figure 7.1: Industrial Kraft pulp processes. Advanced kraft pulping, offering a high potential for valorization strategies, using *Amycolatopsis sp.* ATCC 39116 (yellow). The figure is adapted from previous work (Hamaguchi et al., 2012; Silva et al., 2009).

Notably, this work has been demonstrated for the first time that guaiacol-rich lignin hydrolysates can be efficiently converted to MA (Figure 7.2) (Weiland et al., 2022). The ability to metabolize guaiacol is particularly significant, as a pure guaiacol solution was recently produced from lignin (Shen et al., 2019). The integrated chemical and biochemical production of MA using metabolically engineered *Amycolatopsis sp.* ATCC 39116, opens new routes for the bio-based production of adipic acid and terephthalic acid, which are important monomers for the manufacturing of commercial plastics, e.g. nylon and PET (Kohlstedt et al., 2018; Kohlstedt et al., 2022).

In this regard, the strains and workflows created display a promising start for future applications in industrial settings, but further optimization efforts are needed to achieve this goal.

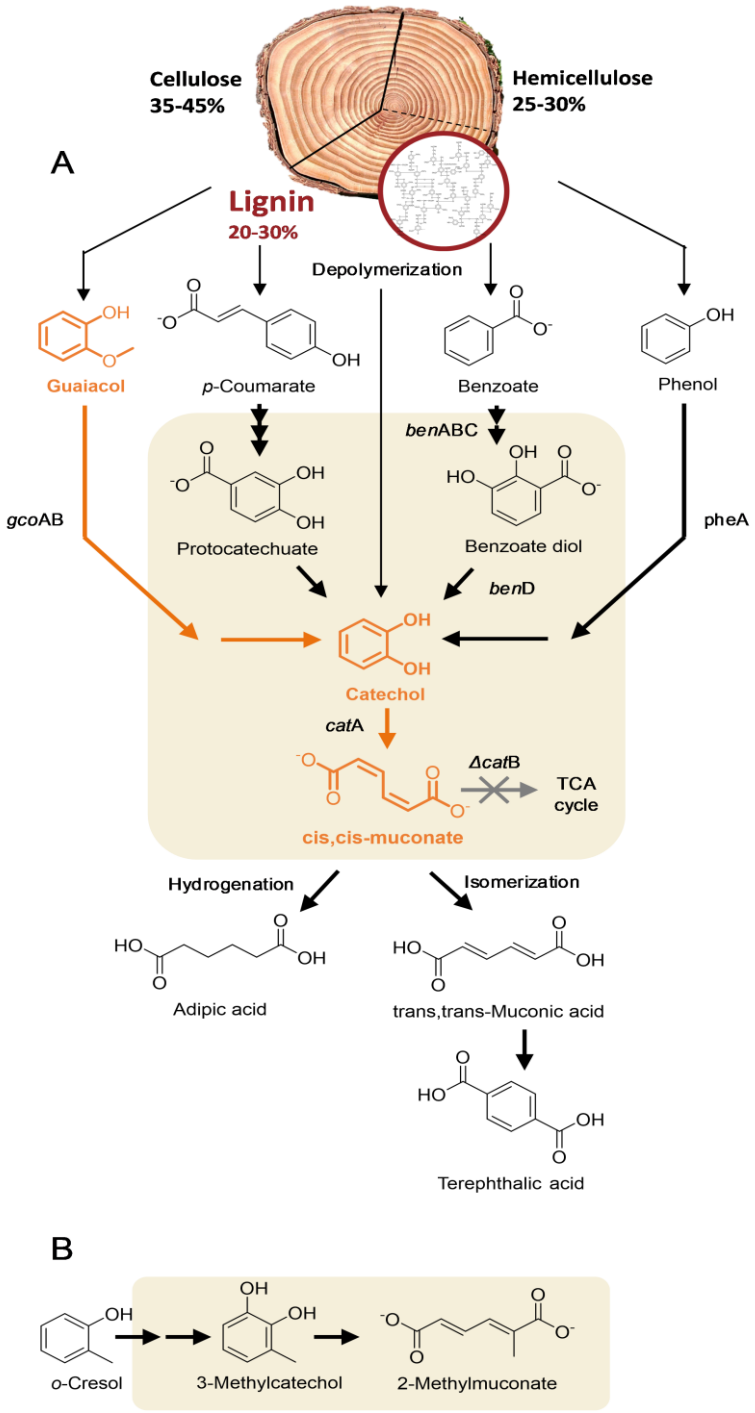

Figure 7.2: From lignin to plastics, using *Amycolatopsis sp.* ATCC 39116 MA-2. This process integrates chemical and biochemical processes to produce *cis,cis*-muconic acid (MA) from lignin. Hydrothermal conversion depolymerized lignin into small aromatics, that can be used as feedstock for MA production (A). *Amycolatopsis sp.* ATCC 39116 MA-2 (represented by the square) accumulates MA because the β-ketoadipate pathway is interrupted at the level of muconate cycloisomerase (CatB). This was achieved by the deletion of the following two *catB* AATC3_020100009302 and AATC3_020100018510. *Amycolatopsis sp.* ATCC 39116

MA-2 is able to utilize guaiacol in particular for MA production (highlighted by the orange color). In addition, the mutant converts benzoate, phenol, catechol and lignin hydrolysate to MA (An et al., 2000); (Park and Kim, 2003); (An et al., 2001); (Sutherland, 1986; Tumen-Velasquez et al., 2018). MA can be readily hydrogenated to adipic acid, an important building block for industrial nylons and polyurethanes (Rosini et al., 2023; Xie et al., 2014). In addition, isomerization of MA, followed by a Diels-Alder reaction with ethylene, and dehydrogenation, leads to terephthalic acid, one of the two constitutive monomers of industrial polymer polyethylene terephthalate (PET) (Ravindranath et al., 1986). Furthermore, the engineered producer converts *o*-cresol into 2-methyl MA via 3-methyl-catechol as intermediate (B). The position of the methyl group arises from the cleavage of catechol (Park and Kim, 2003), which is also used for methylated variants (An et al., 2001). The figure is adapted from (Beckham et al., 2016).

As shown, *Amycolatopsis sp.* ATCC 39116 produced up to 3.1 g L^{-1} MA from guaiacol. Compared to other processes, which have demonstrated titers up to 85 g L^{-1}, its potential seems to be still at the beginning (Becker et al., 2018). To increase the performance of *Amycolatopsis sp.* ATCC 39116 as production host, the relevant metabolic pathways should be further investigated. As an example, the regulation of key genes, especially that of *catA* and *gcoAB*, should be optimized. Stronger expression of *catA*, would help to prevent the transient accumulation of catechol, which is toxic to the cell (Van Duuren, 2011). Furthermore, a better understanding of the regulation of the *gcoAB* genes is needed. Their expression is repressed by some sugars, such as mannose or rhamnose. It would be desirable to replace the native promoter with a constitutive promoter. Unluckily, a proper expression of these genes seems to be challenging (Mallinson et al., 2018; Tumen-Velasquez et al., 2018).

8 Appendix

8.1 Primers

Table 8.1: Primers used for genetic engineering of *Amycolatopsis sp.* ATCC 39116 and the validation of plasmids and strains for correctness of the genetic modifications performed. Overhangs for Gibson Assembly are underlined.

Sset_PR#	5'-Sequence-3'	Plasmid and target
1	CGACCACGCTCAGCGCCTTCAG	Sset_PL4 US *catB-9302*
2	CACGAACCGGCGGATCAGCTCGTG	Sset_PL4 DS *catB-9302*
3	TGGAGCTGGGCATCAGCATC	Sequencing *cat*B *9302* locus/ Sset_PL6
4	GATCCGCGGCCGCGCGCGATCACGAACCGGCG GATCAG	Sequencing *cat*B *9302* locus/ Sset_PL6
5	AAGGGAGTGGGTCCGTGTGAGGTTCCGGGCCCG TTCGCG	Sequencing *cat*B *9302* locus/ Sset_PL6
6	CGAACGGGCCCGGAACCTCACACGGACCCACTC CCTTG	Sequencing *cat*B *9302* locus/ Sset_PL6
7	GACATGATTACGAATTCGATCGACCACGCTCAGC GCCTTC	Sequencing *cat*B *9302* locus/ Sset_PL6
8	AGCGCTGGTTGGCGTCCAC	Sequencing *cat*B *9302* locus/ Sset_PL6
9	GTGACCAGCCGCAGGTAGG	Sequencing *cat*B *9302* locus/ Sset_PL6
10	GACGTGCCGATCATGTTCC	Sequencing *cat*B *9302* locus/ Sset_PL6
11	GTGCGGGTCGACGTGAGTG	Sequencing *cat*B *9302* locus/ Sset_PL6
12	ACGCGGTGGTCTACCTGGCGAG	Sequencing *cat*B *9302* locus/ Sset_PL6
13	CTCGTCGCTCATCGGCGCGTACAGGTTGCCCAG GTTCGCGGCGCCGAGCGCGAACGGGCCCGGAA CCTCAATTTGCTATAACGAGCCTTTTATC	Sset_PL6 *Hyg* pKHint31
14	CCTTGACGGCGCAGACATCGGATCTCTATCGTCG GCGTCGTCACCGAGGCGTACAAGGGAGTGGGTC CGTGTGTAGGTTATATCCTAGCCATTTG	Sset_PL6 *Hyg* pKHint31
15	GATCCGCGGCCGCGCGCGATCGCCCTTGTTCGG GTAGTAG	Sset_PL12 US *cat*B *18510*
16	CTTGATATCCGGGGGAGTTTCACATCGGCTGACC TCGTGTGGTTG	Sset_PL12 US *cat*B *18510*
17	CCCCCAACCACACGAGGTCAGCCGATGTGAAACT CCCCCGGATATCAAGG	Sset_PL12 DS *cat*B *18510*
18	GACATGATTACGAATTCGATGACGCTCCACTCGT TTC	Sset_PL12 DS *cat*B *18510*
19	CCAAGGATTCCGTGGTCAAC	Sequencing *cat*B *18510* locus/ Sset_PL12

Table 8.1: Primers used for genetic engineering of *Amycolatopsis sp.* ATCC 39116 (continued).

Sset_PR#	5'-Sequence-3'	Plasmid and target
20	GAACTTGTCGCTCTTGAACC	Sequencing *cat*B *18510* locus/ Sset_PL12
21	CGCCCTTGTTCGGGTAG	Sequencing *cat*B *18510* locus/ Sset_PL12
22	GAAGTGCCGGATCTGGG	Sequencing *cat*B *18510* locus/ Sset_PL12
23	GGGTCCTTGACCTTGAG	Sequencing *cat*B *18510* locus/ Sset_PL12
24	CGATGGAGCTGCGTCAC	Sequencing *cat*B *18510* locus/ Sset_PL12
25	AGGATTCCGTGGTCAAC	Sequencing *cat*B *18510* locus/ Sset_PL12
26	AGTGGCCGCTGTTCCTG	Sequencing *cat*B *18510* locus/ Sset_PL12
27	AGGACTCACCCATGTTG	Sequencing *cat*B *18510* locus/ Sset_PL12
28	TCGGCGAGGGACGACAC	Sequencing *cat*B *18510* locus/ Sset_PL12
29	CGAAGTAGGCGTCCTTG	Sequencing *cat*B *18510* locus/ Sset_PL12
30	CAGTACGAGGACTTCTTC	Sequencing *cat*B *18510* locus/ Sset_PL12
31	GATCCGCGGCCGCGCGCGATGAGGACATCGGTGACCTCTC	Sset_PL13 US *cat*B *1440*
32	TGAGGCCGTTGGAGGTTTCCGCGGTCTGCTCCCTGGTGTC	Sset_PL13 US *cat*B *1440*
33	GACACCAGGGAGCAGACCGCGGAAACCTCCAACGGCCTCAG	Sset_PL13 P*catA 18515*
37	GCGTGGTGGGTGGCGGTCATCGCCGGCCTCCTTCCC	Sset_PL13 P*catA 18515*
34	TGGGCGACGGAGCCGGCCCGTCAAGCCGGGTCGAG	Sset_PL13 *catA 18515*
38	GAGCGGGAAGGAGGCCGGCGATGACCGCCACCCACCAC	Sset_PL13 *catA 18515*
35	TCGTGCTCGACCCGGCTTGACGGGCCGGCTCCGTC	Sset_PL13 DS *cat*B *1440*
36	GACATGATTACGAATTCGATAGAAGGGAGCACACCATGAGG	Sset_PL13 DS *cat*B *1440*
39	GATCCGCGGCCGCGCGCGATCGGTGCCGCTGGAGATCG	Sset_PL19 *pcaH-375388*
40	CGAAAAGGGCCAAGTGTCGCAGCACGGTTTCCTTTCTCCTCAC	Sset_PL19 US *pcaH-375388*
41	AGGAGAAAGGAAACCGTGCTGCGACACTTGGCCCTTTTCGC	Sset_PL19 *pcaH-375388*
42	GACATGATTACGAATTCGATGTCGAGCCCGGCGATGG	Sset_PL19 *pcaH-375388*
43	GGCGATTAAGTTGGGTAACG	Sset_PL1
44	TTATGCTTCCGGCTCGTATG	Sset_PL1
45	CGAGTGAGCGACACTTG	Sequencing *aro*Y/ Sset_PL20
46	AAACCGCTGCCGGTAAC	Sequencing *aro*Y/ Sset_PL20

Table 8.1: Primers used for genetic engineering of *Amycolatopsis sp.* ATCC 39116 (continued).

Sset_PR#	5'-Sequence-3'	Plasmid and target
47	GAACTTCCCGTCACGAG	Sequencing *aro*Y/ Sset_PL20
51	TGGCGTTCGAGTTCGAC	Sequencing *pcaH 37538 locus*/ Sset_PL20
52	GAACTTCCCGTCACGAG	Sequencing *pcaH 37538 locus*/ Sset_PL19/PL20
53	CGTCGATCGTGAACGTCAAC	Sequencing *pcaH 37538 locus*/ Sset_PL20
54	TGTGTTCTGCGGGACACC	Sequencing *pcaH 37538 locus*/ Sset_PL19/PL20
55	GATCCGCGGCCGCGCGCGATGGCGCAGCTGGACAAGTTC	Sset_PL20 US *pcaG-37543*
56	TCGTTGATGGGGTTTTGCATTCGTCTTCCTCTGTGTTCTGCG	Sset_PL20 US *pcaG-37543*
57	CAGAACACAGAGGAAGACGAATGCAAAACCCCATCAACGATCTC	Sset_PL20 *aro*Y
58	CTATTTTTTATCGCTGAACAGCTCCG	Sset_PL20 *aro*Y
59	TTCAGCGATAAAAAATAGCCTGTTCGACCCGATTCTC	D Sset_PL20 DS *pcaG-37543*
60	GACATGATTACGAATTCGATGACGGGCGGGATTAGTG	Sset_PL20 DS *pcaG-37543*
61	GGCGATTAAGTTGGGTAACG	Sset_PL20 US *pcaG-37543*
62	TTATGCTTCCGGCTCGTATG	Sset_PL20 DS *pcaG-37543*

8.2 Plasmid cards

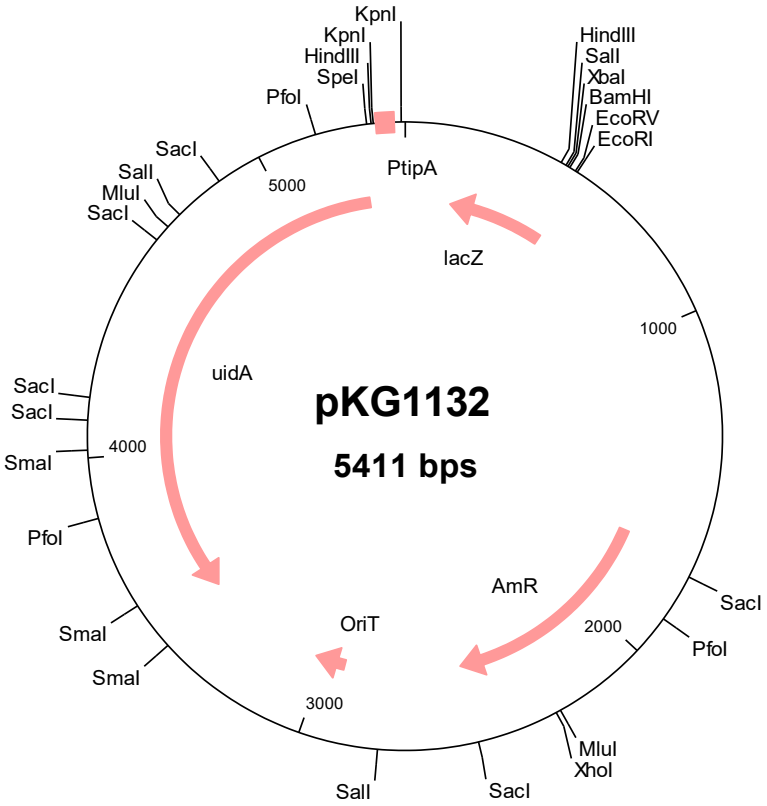

Figure 8.1: Plasmid card of pKG1132. It possesses next to an apramycin resistance gene (*amR)* the *uidA* gene, encoding β-glucuronidase for blue-white selection. This gene was set under the control of the *tipA* promoter (Murakami et al., 1989), and cloned using ligation into the BglII site of pKC1132 and designated as pKG1132 for improved genetic engineering (Myronovskyi *et al.*, 2011)

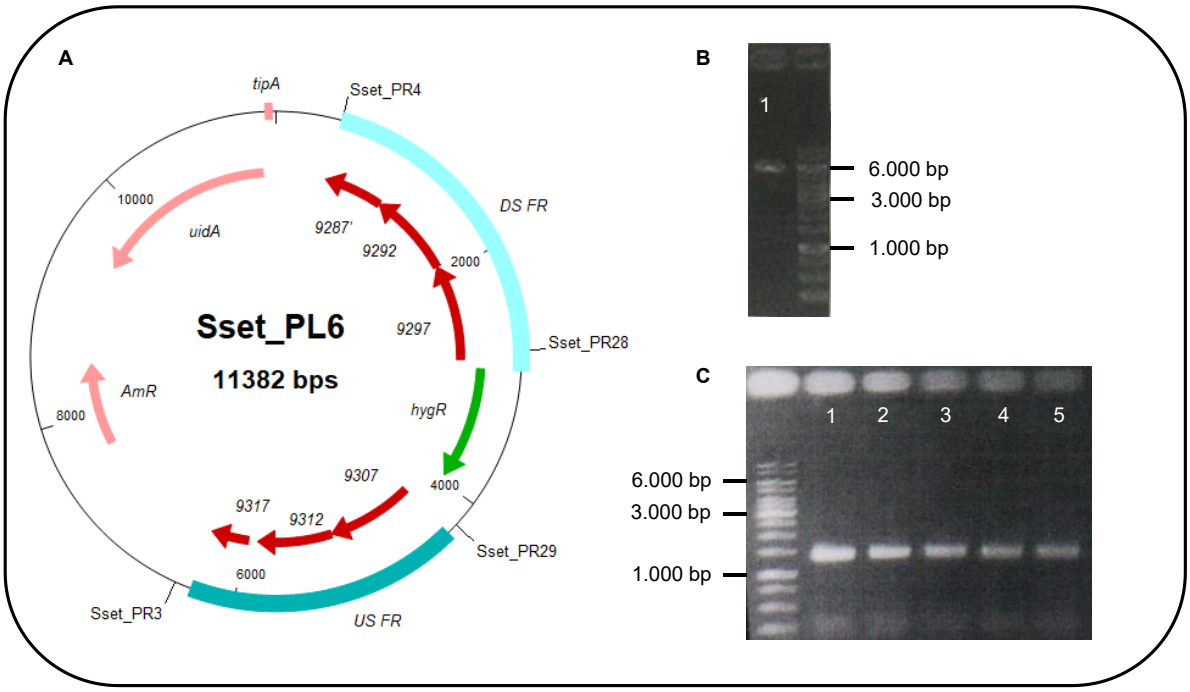

Figure 8.2: Design of the deletion plasmid Sset_PL6 for the engineering of *Amycolatopsis sp*. MA-1 (Δ*cat*B *9302::hyg*^{R}) (A). The whole locus of AATC3_020100009302 plus 2.500 bp up and downstream was amplified (B). using Sset_PR1/2 (5,846 bp). This fragment was ligated blunt end into the plasmid backbone pKG1132, which was linearized using the restriction enzyme *Eco*RV (5,411 bp). AATC3_020100009302 was replaced by a hygromycin resistance gene, using ET recombination, resulting in Sset_PL6. Therefore, the hygromycin resistance gene was amplified and 100 bp homologous overhangs were added using the primer pair Sset_PR13/14. Plasmid pKHint31 was used as template. The exchange was verified by using the primer pair Sset_PR13/14 leading to an amplicon with a size of 1,411 bp (C). Agarose gel electrophoresis was performed in a 1% gel. For the determination of product size, a 1 kb DNA ladder was used. Plasmid Sset_PL6 was sequenced using primers Sset_PR3 to Sset_PR12.

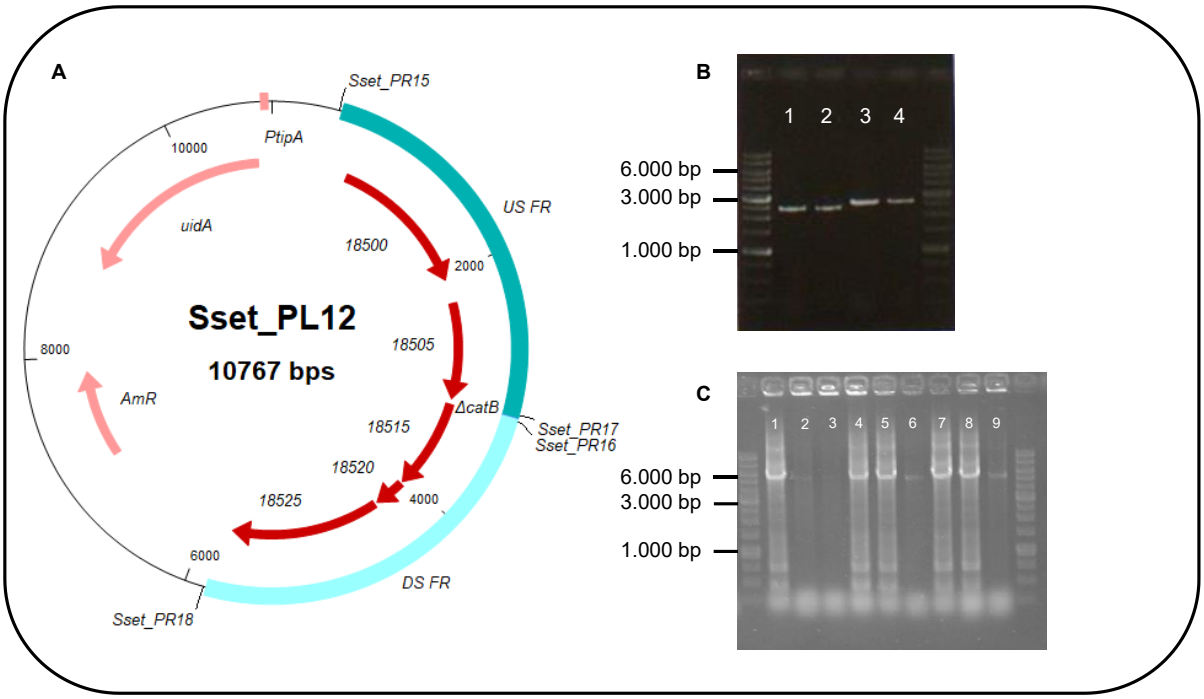

Figure 8.3: Construction of the deletion plasmid Sset_PL12 for the engineering of *Amycolatopsis sp*. MA-2 (*ΔcatB-9302::hyg*^{R}*, ΔcatB-18510*) and *Amycolatopsis sp*. MA-4 (*ΔcatB-18510*) (A). 2.500 bp long US and DS flanking regions of *catB*- 18510 were amplified, and 20 bp homologous overhangs were added using primer pairs Sset_PR15/16 and Sset_PR17/18, resulting in fragments with a size of 2,663 bp for US FR (B line 3 and 4) and 2,534 bp for DS FR (B line 1 and 2), respectively. These fragments were incorporated into the plasmid backbone pKG1132, linearized with restriction enzyme *Eco*RV (5,411 bp), using Gibson assembly. The assembly was verified using the primer pair Sset_PR15/18, resulting in an amplicon with a size of 5,396 bp (C line 1). Agarose gel electrophoresis was performed in a 1% gel. For the determination of product size, a 1 kb DNA ladder was used. Plasmid Sset_PL12 was sequenced using primers Sset_PR19 to Sset_PR30.

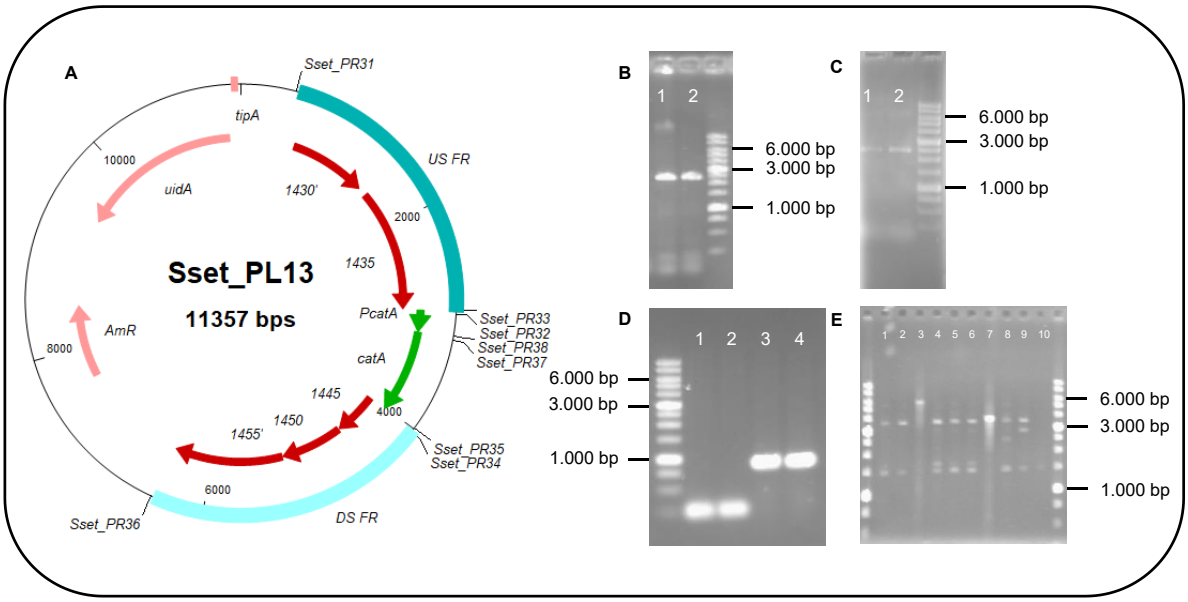

Figure 8.4: Design of the deletion plasmid Sset_PL13 for the construction of *Amycolatopsis sp*. MA-2 (*ΔcatB-9302::hyg*^{R}*, ΔcatB-18510, ΔcatB-1440::Pcat_catA-18515*) (A). US and DS flanking regions of *catB*-1440 were amplified and 20 bp homologous overhangs were added using primer pairs Sset_PR31/32 and Sset_PR35/36, resulting in fragments with a size of 2,492 bp for US FR (B line 1 and 2) and 2,466 bp for DS FR (C line 1 and 2), respectively. Furthermore, *cat*A-18515 and its promoter were amplified and overhangs were added using the primer pair Sset_PR33/34 (1,108 bp, D line 3 and 4). This fragment was used for the exchange of *catB*- 1440. All fragments were incorporated into the plasmid backbone pKG1132, linearized with restriction enzyme *Eco*RV (5,411 bp), using Gibson assembly. The assembly was verified using the primer pair Sset_PR31/36, resulting in an amplicon with a size of 5,986 bp (E line 3). Agarose gel electrophoresis was performed in a 1% gel. For the determination of product size, a 1 kb DNA ladder was used. The US and DS regions of *catB*-1440 could not be sequenced probably due to secondary structures. C*at*A-18515 and its promoter were sequenced using the construction primers.

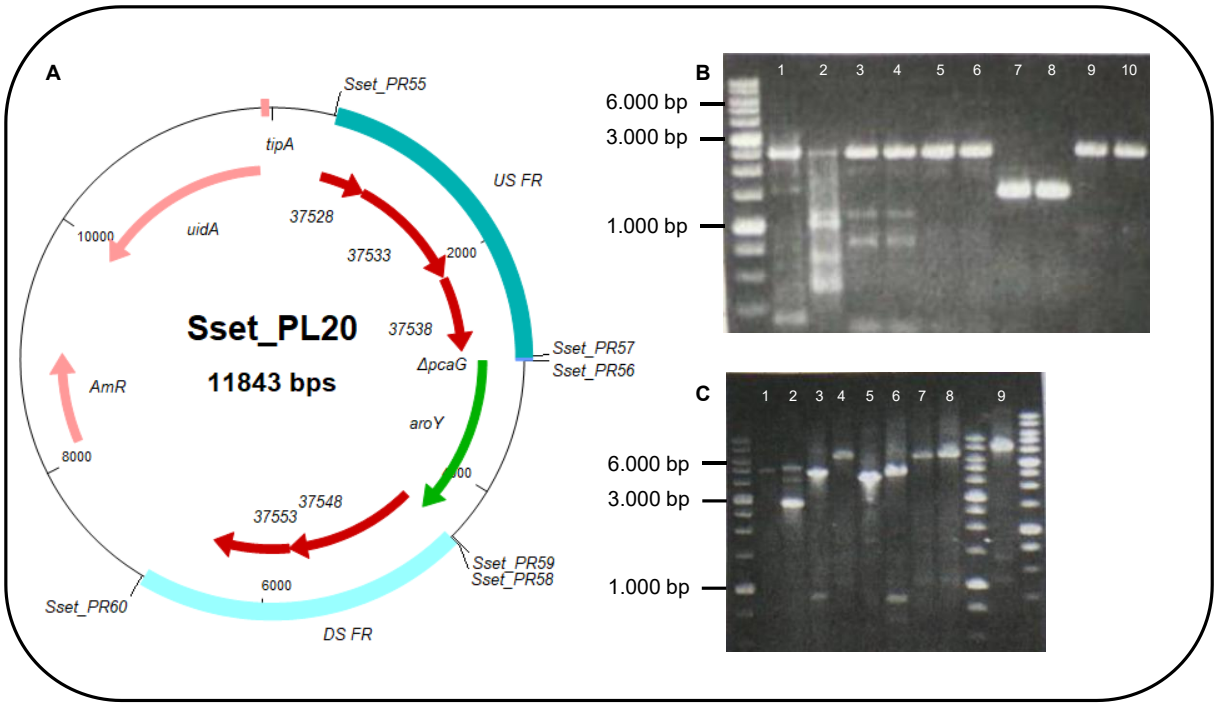

Figure 8.5: Design of the deletion plasmid Sset_PL20 for the engineering of *Amycolatopsis sp*. MA-5 (*ΔcatB-9302::hyg*^{R}*, ΔcatB-18510, ΔpcaG-37543::aroY)* (A). US and DS flanking regions of *pcaG*-37543 were amplified and 20 bp homologous overhangs were added using primer pairs Sset_PR55/56 and Sset_PR59/60, resulting in fragments with a size of 2,499 bp for US FR (B line 3 and 4) and 2,523 bp for DS FR (B line 5 and 6), respectively. Furthermore, *aroY* was amplified from the genome of *Enterococcus cloacae,* and overhangs were added using the primer pair Sset_PR57/58 (1,508 bp, D line 7 and 8). *Aro*Y was set under control of the promoter of *pcaG*-37543. All fragments were incorporated into the plasmid backbone pKG1132, linearized with restriction enzyme *Eco*RV (5411 bp), using Gibson assembly. The assembly was verified using the primer pair Sset_PR55/60, resulting in an amplicon with a size of 6,472 bp (line 4). To determine the product size, agarose gel electrophoresis was performed in a 1% gel with a 1 kb DNA ladder. Plasmid Sset_PL20 was sequenced using primers Sset_PR40 to Sset_PR44 and Sset_PR51 to PR54 and 59.

8.3 Further cultivation experiments

Table 8.2: Toxicity tests of different aromatic compounds *Amycolatopsis sp*. ATCC 39116 was grown in minimal medium at 37 °C. Each experimental set-up contained the amount of aromatic substrate indicated in the table. In addition, a control was performed without substrate addition. Growth was measured as optical density (OD_{600} nm) after 40 hours and is indicated as follows: + cells are able to grow, - no growth.

Aromatics	Concentration [mM]	Growth
cis,cis-Muconic acid	100,0	+
	200,0	+
	300,0	-
Guaiacol	25,0	+
	50,0	-
	75,0	-
Catechol	5,0	+
	10,0	-
	15,0	-
Phenol	2,5	+
	5,0	+
	7,5	+
o-Cresol	2,5	+
	5,0	-
	7,5	-
m-Cresol	2,5	+
	5,0	-
	7,5	-
Methylcatechol	5,0	-
	10,0	-
	15,0	-

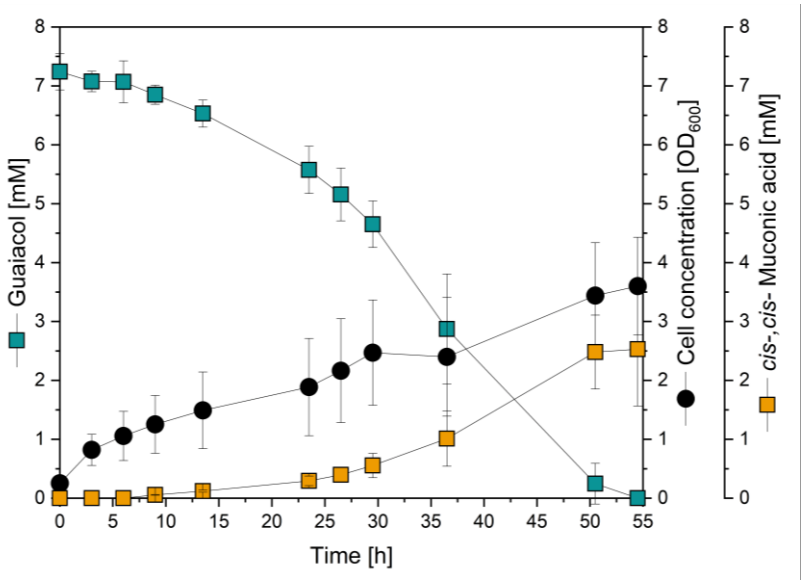

Figure 8.6: Production of MA from guaiacol using *Amycolatopsis sp*. ATCC 39116 MA-3 (*ΔcatB*-9302::hyg^R, *ΔcatB*-18510, *ΔcatB*-1440::*Pcat_catA*-18515). Cultivation was carried out at 37 °C. Glucose was present in the medium to support growth but was not measured. (n=3)

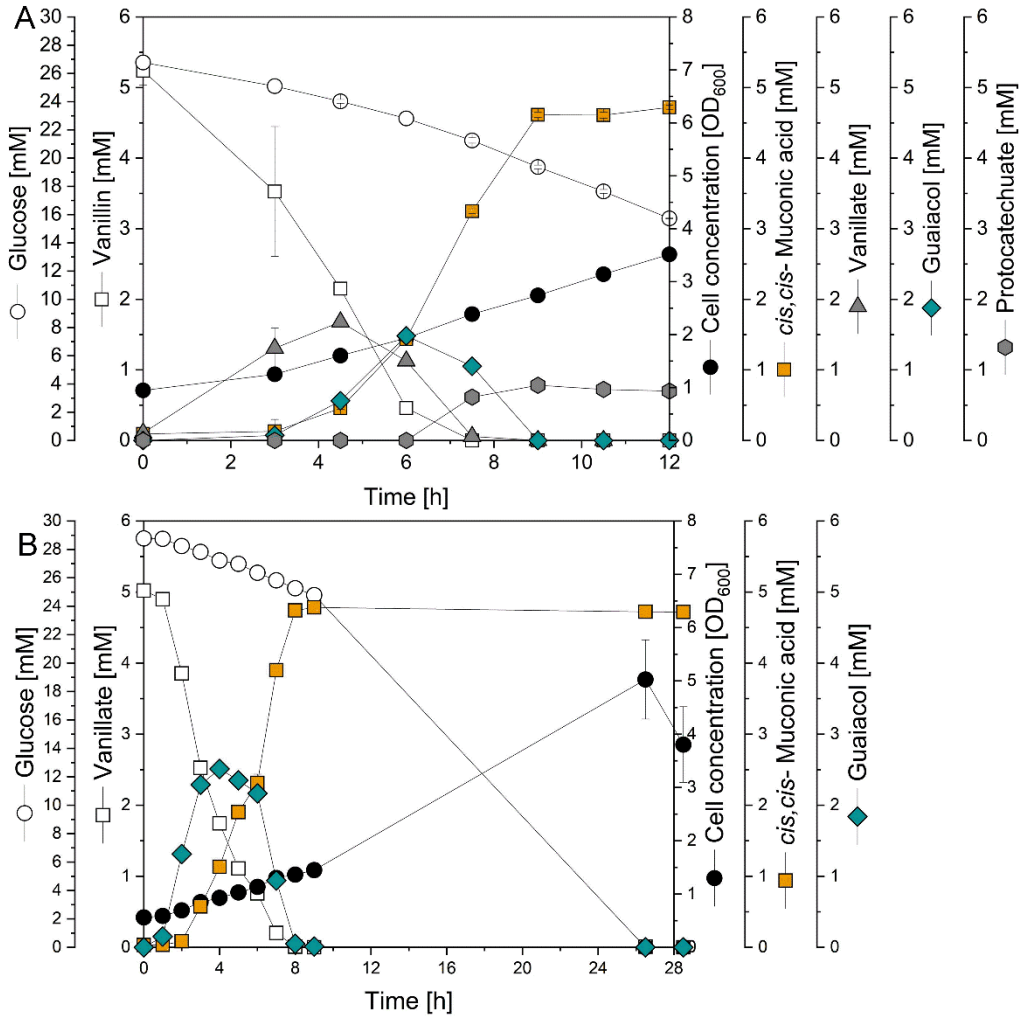

Figure 8.7 Production of MA from vanillin (A) and vanillate (B) using *Amycolatopsis sp.* ATCC 39116 MA-5 (*ΔcatB-9302::hyg*^{R}*, ΔcatB-18510, ΔpcaG-37543::aroY*) at 37 °C. Glucose was present in the medium to support growth but was not measured. (n=3)

9 References

Abdel-Banat, B. M., Hoshida, H., Ano, A., Nonklang, S., Akada, R., 2010. High-temperature fermentation: how can processes for ethanol production at high temperatures become superior to the traditional process using mesophilic yeast? Applied Microbiology and Biotechnology. 85**,** 861-7.

Abdelaziz, O. Y., Brink, D. P., Prothmann, J., Ravi, K., Sun, M., Garcia-Hidalgo, J., Sandahl, M., Hulteberg, C. P., Turner, C., Liden, G., 2016. Biological valorization of low molecular weight lignin. Biotechnology advances. 34**,** 1318-1346.

Achyuthan, K. E., Achyuthan, A. M., Adams, P. D., Dirk, S. M., Harper, J. C., Simmons, B. A., Singh, A. K., 2010. Supramolecular self-assembled chaos: polyphenolic lignin's barrier to cost-effective lignocellulosic biofuels. Molecules. 15 12**,** 8641-88.

Altschul, S. F., Gish, W., Miller, W., Myers, E. W., Lipman, D. J., 1990. Basic local alignment search tool. J Mol Biol. 215**,** 403-10.

An, H.-R., Park, H.-J., Kim, E.-S., 2000. Characterization of benzoate degradation *via* ortho-Cleavage by *Streptomyces setonii*. Journal of Microbiology and Biotechnology. 10**,** 111-114.

An, H.-R., Park, H.-J., Kim, E.-S., 2001. Cloning and expression of thermophilic catechol 1,2-dioxygenase gene (*cat*A) from *Streptomyces setonii*. FEMS microbiology letters. 195**,** 17-22.

Antai, S., Crawford, D., 1983. Degradation of phenol by *Stretomyces setonii*. Canadian Journal of Microbiology. 29**,** 142-143.

Antai, S. P., Crawford, D. L., 1981. Degradation of softwood, hardwood, and grass lignocelluloses by two streptomyces strains. Applied and Environmental Microbiology. 42**,** 378-80.

Arevalo-Gallegos, A., Ahmad, Z., Asgher, M., Parra-Saldivar, R., Iqbal, H. M. N., 2017. Lignocellulose: A sustainable material to produce value-added products with a zero waste approach-A review. Int J Biol Macromol. 99**,** 308-318.

Argyropoulos, D. D. S., Crestini, C., Dahlstrand, C., Furusjö, E., Gioia, C., Jedvert, K., Henriksson, G., Hulteberg, C., Lawoko, M., Pierrou, C., Samec, J. S. M., Subbotina, E., Wallmo, H., Wimby, M., 2023. Kraft Lignin: A Valuable, Sustainable Resource, Opportunities and Challenges. ChemSusChem. 16**,** e202300492.

Bandounas, L., Wierckx, N. J., de Winde, J. H., Ruijssenaars, H. J., 2011. Isolation and characterization of novel bacterial strains exhibiting ligninolytic potential. Bmc Biotechnology. 11**,** 94.

Bang, S.-G., Choi, C. Y., 1995. DO-stat fed-batch production of cis, cis-muconic acid from benzoic acid by Pseudomonas putida BM014. Journal of Fermentation and Bioengineering. 79**,** 381-383.

Bar-On, Y. M., Phillips, R., Milo, R., 2018. The biomass distribution on Earth. Proc Natl Acad Sci U S A. 115**,** 6506-6511.

Becker, J., Kuhl, M., Kohlstedt, M., Starck, S., Wittmann, C., 2018. Metabolic engineering of Corynebacterium glutamicum for the production of cis, cis-muconic acid from lignin. Microbial Cell Factories. 17**,** 115.

Becker, J., Reinefeld, J., Stellmacher, R., Schäfer, R., Lange, A., Meyer, H., Lalk, M., Zelder, O., von Abendroth, G., Schröder, H., Haefner, S., Wittmann, C., 2013. Systems-wide analysis and engineering of metabolic pathway fluxes in bio-

succinate producing basfia succiniciproducens. Biotechnology and Bioengineering. 110, 3013-3023.
Becker, J., Wittmann, C., 2019. A field of dreams: Lignin valorization into chemicals, materials, fuels, and health-care products. Biotechnology Advances. 37, 107360.
Beckham, G. T., Johnson, C. W., Karp, E. M., Salvachua, D., Vardon, D. R., 2016. Opportunities and challenges in biological lignin valorization. Current Opinion in Biotechnology. 42, 40-53.
Bierman, M., Logan, R., O'Brien, K., Seno, E. T., Rao, R. N., Schoner, B. E., 1992. Plasmid cloning vectors for the conjugal transfer of DNA from *Escherichia coli* to *Streptomyces spp*. Gene. 116, 43-9.
Boudet, A.-M., 1998. A new view of lignification. Trends in Plant Science. 3, 67-71.
Bruijnincx, P. C. A., Rinaldi, R., Weckhuysen, B. M., 2015. Unlocking the potential of a sleeping giant: lignins as sustainable raw materials for renewable fuels, chemicals and materials. Green Chemistry. 17, 4860-4861.
Bugg, T. D. H., Williamson, J. J., Rashid, G. M. M., 2020. Bacterial enzymes for lignin depolymerisation: new biocatalysts for generation of renewable chemicals from biomass. Curr Opin Chem Biol. 55, 26-33.
Buschke, N., Schäfer, R., Becker, J., Wittmann, C., 2013. Metabolic engineering of industrial platform microorganisms for biorefinery applications – Optimization of substrate spectrum and process robustness by rational and evolutive strategies. Bioresour. Technol. 135, 544-554.
Carraher, J. M., Pfennig, T., Rao, R. G., Shanks, B. H., Tessonnier, J.-P., 2017. cis,cis-Muconic acid isomerization and catalytic conversion to biobased cyclic-C6-1,4-diacid monomers. Green Chemistry. 19, 3042-3050.
Caspi, R., Altman, T., Dale, J. M., Dreher, K., Fulcher, C. A., Gilham, F., Kaipa, P., Karthikeyan, A. S., Kothari, A., Krummenacker, M., Latendresse, M., Mueller, L. A., Paley, S., Popescu, L., Pujar, A., Shearer, A. G., Zhang, P., Karp, P. D., 2010. The MetaCyc database of metabolic pathways and enzymes and the BioCyc collection of pathway/genome databases. Nucleic Acids Research. 38, D473-D479.
Curran, K. A., Leavitt, J. M., Karim, A. S., Alper, H. S., 2013. Metabolic engineering of muconic acid production in *Saccharomyces cerevisiae*. Metabolic Engineering. 15, 55-66.
da Costa Sousa, L., Chundawat, S. P. S., Balan, V., Dale, B. E., 2009. 'Cradle-to-grave' assessment of existing lignocellulose pretreatment technologies. Current Opinion in Biotechnology. 20, 339-347.
Davis, J. R., Goodwin, L. A., Woyke, T., Teshima, H., Bruce, D., Detter, C., Tapia, R., Han, S., Han, J., Pitluck, S., Nolan, M., Mikhailova, N., Land, M. L., Sello, J. K., 2012. Genome Sequence of *Amycolatopsis sp*. Strain ATCC 39116, a Plant Biomass-Degrading Actinomycete. Journal of Bacteriology. 194, 2396-2397.
de Gonzalo, G., Colpa, D. I., Habib, M. H., Fraaije, M. W., 2016. Bacterial enzymes involved in lignin degradation. Journal of biotechnology. 236, 110-9.
De Wild, P., Van der Laan, R., Kloekhorst, A., Heeres, E., 2009. Lignin valorisation for chemicals and (transportation) fuels via (catalytic) pyrolysis and hydrodeoxygenation. Environmental Progress & Sustainable Energy. 28, 461-469.
de Wild, P. J., Huijgen, W. J. J., Gosselink, R. J. A., 2014. Lignin pyrolysis for profitable lignocellulosic biorefineries. Biofuels. 8.
Dhingra, G., Kumari, Æ. R., Bala, Æ. S., 2003. Development of cloning vectors and transformation methods for Amycolatopsis. 195-204.

Draths, K., Frost, J. W., 1994. Environmentally compatible synthesis of adipic acid from D-glucose. Journal of the American Chemical Society. 116**,** 399-400.

Du, L., Wang, Z., Li, S., Song, W., Lin, W., 2013. A comparison of monomeric phenols produced from lignin by fast pyrolysis and hydrothermal conversions. International Journal of Chemical Reactor Engineering. 11**,** 135-145.

Fache, M., Boutevin, B., Caillol, S., 2016. Vanillin Production from Lignin and Its Use as a Renewable Chemical. ACS Sust. Chem. Eng. 4**,** 35-46.

Fleige, C., Hansen, G., Kroll, J., Steinbüchel, A., 2013. Investigation of the *Amycolatopsis sp*. strain ATCC 39116 vanillin dehydrogenase and its impact on the biotechnical production of vanillin. Applied and Environmental Microbiology. 79**,** 81-90.

Fleige, C., Meyer, F., Steinbüchel, A., 2016. Metabolic engineering of the actinomycete *Amycolatopsis sp*. strain ATCC 39116 towards enhanced production of natural vanillin. Applied and Environmental Microbiology. 82**,** 3410-9.

Fleige, C., Steinbüchel, A., 2014. Construction of expression vectors for metabolic engineering of the vanillin-producing actinomycete *Amycolatopsis sp*. ATCC 39116. Applied Microbiology and Biotechnology. 98**,** 6387-95.

Frey, U. H., Bachmann, H. S., Peters, J., Siffert, W., 2008. PCR-amplification of GC-rich regions: 'slowdown PCR'. Nature protocols. 3**,** 1312-7.

Fuchs, G., Boll M Fau - Heider, J., Heider, J., 2011. Microbial degradation of aromatic compounds - from one strategy to four.

Furszyfer Del Rio, D. D., Sovacool, B. K., Griffiths, S., Bazilian, M., Kim, J., Foley, A. M., Rooney, D., 2022. Decarbonizing the pulp and paper industry: A critical and systematic review of sociotechnical developments and policy options. Renewable and Sustainable Energy Reviews. 167**,** 112706.

Garcia-Hidalgo, J., Ravi, K., Kure, L. L., Liden, G., Gorwa-Grauslund, M., 2019. Identification of the two-component guaiacol demethylase system from Rhodococcus rhodochrous and expression in Pseudomonas putida EM42 for guaiacol assimilation. AMB Express. 9**,** 34.

Gierer, J., 1985. Chemistry of delignification. Wood Science and Technology. 19**,** 289-312.

Gu, N. X., Palumbo, C. T., Bleem, A. C., Sullivan, K. P., Haugen, S. J., Woodworth, S. P., Ramirez, K. J., Kenny, J. K., Stanley, L. D., Katahira, R., Stahl, S. S., Beckham, G. T., 2023. Autoxidation Catalysis for Carbon-Carbon Bond Cleavage in Lignin. ACS Cent Sci. 9**,** 2277-2285.

Gullichsen, J., Fogelholm, C. J., Yhdistys, S. P.-i., Pulp, T. A. o. t., Industry, P., 1999. Chemical Pulping. Fapet Oy.

Hamaguchi, M., Cardoso, M., Vakkilainen, E., 2012. Alternative Technologies for Biofuels Production in Kraft Pulp Mills—Potential and Prospects. Energies. 53390**,** 2288-2309.

Harwood, C. S., Parales, R. E., 1996. The beta-ketoadipate pathway and the biology of self-identity. Annual review of microbiology. 50**,** 553-90.

Henson, W. R., Rorrer, N. A., Meyers, A. W., Hoyt, C. B., Mayes, H. B., Anderson, J. J., Black, B. A., Jayakody, L., Katahira, R., Michener, W. E., VanderWall, T. A., Salvachúa, D., Johnson, C. W., Beckham, G. T., 2022. Bioconversion of wastewater-derived cresols to methyl muconic acids for use in performance-advantaged bioproducts††Electronic supplementary information (ESI) available. See DOI: https://doi.org/10.1039/d1gc04590c. Green Chemistry. 24**,** 3677-3688.

Hopwood, D. A., 1988. The Leeuwenhoek lecture, 1987. Towards an understanding of gene switching in Streptomyces, the basis of sporulation and antibiotic production. Proc R Soc Lond B Biol Sci. 235**,** 121-38.

Inoue, H., Nojima, H., Okayama, H., 1990. High efficiency transformation of Escherichia coli with plasmids. Gene. 96**,** 23-8.

Janusz, G., Pawlik, A., Sulej, J., Swiderska-Burek, U., Jarosz-Wilkolazka, A., Paszczynski, A., 2017. Lignin degradation: microorganisms, enzymes involved, genomes analysis and evolution. FEMS Microbiol Rev. 41**,** 941-962.

Jefferson, R. A., 1989. The GUS reporter gene system. Nature. 342**,** 837-838.

Jimenez, J. I., Perez-Pantoja, D., Chavarria, M., Diaz, E., de Lorenzo, V., 2014. A second chromosomal copy of the *cat*A gene endows *Pseudomonas putida* mt-2 with an enzymatic safety valve for excess of catechol. Environmental Microbiology. 16**,** 1767-78.

Jing, Q., LÜ, X., 2007. Kinetics of Non-catalyzed Decomposition of D-xylose in High Temperature Liquid Water* *Supported by the National Natural Science Foundation of China (No.20476089) and the Project of the Ministry of Science and Technology of China (No.2004CCA05500). Chinese Journal of Chemical Engineering. 15**,** 666-669.

Johansson, A., Aaltonen, O., Ylinen, P., 1987. Organosolv pulping — methods and pulp properties. Biomass. 13**,** 45-65.

Joseph Zakzeski, P. C. A. B., Anna L. Jongerius, and Bert M. Weckhuysen, 2009. The Catalytic Valorization of Lignin for the Production of Renewable Chemicals. Chem. Rev.

Kalil, M. S., Asyiqin, Z., Zaki, M., 2002. Catechol synthesis via demethylation of guaiacol by anaerobic bacterium *Acetobacterium woodii* DSM 1030. Pakistan Journal of Biological Science. 5**,** 1186-1188.

Kalpana, G. V., Bloom, B. R., Jacobs, W. R., Jr., 1991. Insertional mutagenesis and illegitimate recombination in mycobacteria. Proc Natl Acad Sci U S A. 88**,** 5433-7.

Kamide, K., 2005. 1 - Introduction. In: Kamide, K., (Ed.), Cellulose and Cellulose Derivatives. Elsevier, Amsterdam, pp. 1-23.

Karp, P. D., Paley, S. M., Krummenacker, M., Latendresse, M., Dale, J. M., Lee, T. J., Kaipa, P., Gilham, F., Spaulding, A., Popescu, L., Altman, T., Paulsen, I., Keseler, I. M., Caspi, R., 2010. Pathway Tools version 13.0: integrated software for pathway/genome informatics and systems biology. Brief Bioinform. 11**,** 40-79.

Kekulé, A., 1865. Sur la Constitution des substances aromatiques. Published in 1865.

Kieser, T., Bibb, M. J., Buttner, M. J., Chater, K. F., Hopwood, D. A., 2000. Practical Streptomyces genetics. John Innes Foundation, Norwich, UK.

Kohlstedt, M., Starck, S., Barton, N., Stolzenberger, J., Selzer, M., Mehlmann, K., Schneider, R., Pleissner, D., Rinkel, J., Dickschat, J. S., Venus, J., J, B. J. H. v. D., Wittmann, C., 2018. From lignin to nylon: Cascaded chemical and biochemical conversion using metabolically engineered Pseudomonas putida. Metabolic Engineering. 47**,** 279-293.

Kohlstedt, M., Weimer, A., Weiland, F., Stolzenberger, J., Selzer, M., Sanz, M., Kramps, L., Wittmann, C., 2022. Biobased PET from lignin using an engineered cis, cis-muconate-producing Pseudomonas putida strain with superior robustness, energy and redox properties. Metab. Eng. 72**,** 337-352.

Kratzl, K., Claus, P., Lonsky, W., Gratzl, J. S., 1974. Model studies on reactions occurring in oxidations of lignin with molecular oxygen in Alkaline Media. Wood Science and Technology. 8**,** 35-49.

Lawford, H. G., Rousseau, J. D., 1993. Production of ethanol from pulp mill hardwood and softwood spent sulfite liquors by genetically engineered E. coli. Appl Biochem Biotechnol. 39-40**,** 667-85.

Li, X., Xu, Y., Alorku, K., Wang, J., Ma, L., 2023. A review of lignin-first reductive catalytic fractionation of lignocellulose. Molecular Catalysis. 550**,** 113551.

Li, X., Zheng, Y., 2020. Biotransformation of lignin: Mechanisms, applications and future work. Biotechnol Prog. 36**,** e2922.

MacNeil, D. J., Gewain, K. M., Ruby, C. L., Dezeny, G., Gibbons, P. H., MacNeil, T., 1992. Analysis of Streptomyces avermitilis genes required for avermectin biosynthesis utilizing a novel integration vector. Gene. 111**,** 61-8.

Mallinson, S. J. B., Machovina, M. M., Silveira, R. L., Garcia-Borras, M., Gallup, N., Johnson, C. W., Allen, M. D., Skaf, M. S., Crowley, M. F., Neidle, E. L., Houk, K. N., Beckham, G. T., DuBois, J. L., McGeehan, J. E., 2018. A promiscuous cytochrome P450 aromatic O-demethylase for lignin bioconversion. Nature communications. 9**,** 2487.

Mandell, D. J., Lajoie, M. J., Mee, M. T., Takeuchi, R., Kuznetsov, G., Norville, J. E., Gregg, C. J., Stoddard, B. L., Church, G. M., 2015. Corrigendum: Biocontainment of genetically modified organisms by synthetic protein design. Nature. 527**,** 264.

Martani, F., Beltrametti, F., Porro, D., Branduardi, P., Lotti, M., 2017. The importance of fermentative conditions for the biotechnological production of lignin modifying enzymes from white-rot fungi. FEMS Microbiol Lett. 364.

Masai, E., Katayama Y Fau - Fukuda, M., Fukuda, M., 2007. Genetic and biochemical investigations on bacterial catabolic pathways for lignin-derived aromatic compounds. Biosci Biotechnol Biochem.

Maxwell Peter, C., Process for the production of muconic acid. CELGENE CORP, 1983.

Meyer, F., Netzer, J., Meinert, C., Voigt, B., Riedel, K., Steinbuchel, A., 2018. A proteomic analysis of ferulic acid metabolism in Amycolatopsis sp. ATCC 39116. Applied Microbiology and Biotechnology.

Meyer, F., Pupkes, H., Steinbüchel, A., 2017. Development of an Improved System for the Generation of Knockout Mutants of *Amycolatopsis sp.* Strain ATCC 39116. Applied and Environmental Microbiology. 83.

Mizuno, S., Yoshikawa, N., Seki, M., Mikawa, T., Imada, Y., 1988. Microbial production of cis, cis-muconic acid from benzoic acid. Applied Microbiology and Biotechnology. 28**,** 20-25.

Mullis, K., Faloona, F., Scharf, S., Saiki, R., Horn, G., Erlich, H., 1986. Specific enzymatic amplification of DNA in vitro: the polymerase chain reaction. Cold Spring Harb Symp Quant Biol. 51 Pt 1**,** 263-73.

Murakami, T., Holt, T. G., Thompson, C. J., 1989. Thiostrepton-induced gene expression in *Streptomyces lividans*. Journal of Bacteriology. 171**,** 1459-66.

Myronovskyi, M., Rosenkränzer, B., Luzhetskyy, A., 2014. Iterative marker excision system. Applied Microbiology and Biotechnology. 98**,** 4557-4570.

Myronovskyi, M., Welle, E., Fedorenko, V., Luzhetskyy, A., 2011. β-Glucuronidase as a sensitive and versatile reporter in Actinomycetes. Applied and Environmental Microbiology. 77**,** 5370-5383.

Nitsos, C., Rova, U., Christakopoulos, P., Organosolv Fractionation of Softwood Biomass for Biofuel and Biorefinery Applications. Energies, Vol. 11, 2018.

Pandey, M. P., Kim, C. S., 2011. Lignin depolymerization and conversion: a review of thermochemical methods. Chemical Engineering & Technology. 34**,** 29-41.

Park, H. J., Kim, E. S., 2003. An inducible *Streptomyces* gene cluster involved in aromatic compound metabolism. FEMS microbiology letters. 226**,** 151-7.

Pérez, J., Munoz-Dorado, J., De la Rubia, T., Martinez, J., 2002. Biodegradation and biological treatments of cellulose, hemicellulose and lignin: an overview. International microbiology. 5**,** 53-63.

Perez, J. M., Kontur, W. S., Alherech, M., Coplien, J., Karlen, S. D., Stahl, S. S., Donohue, T. J., Noguera, D. R., 2019. Funneling aromatic products of chemically depolymerized lignin into 2-pyrone-4-6-dicarboxylic acid with Novosphingobium aromaticivorans. Green Chemistry. 21**,** 1340-1350.

Pińkowska, H., Wolak, P., Złocińska, A., 2012. Hydrothermal decomposition of alkali lignin in sub- and supercritical water. Chemical Engineering Journal. 187**,** 410-414.

Pometto, A. L., Sutherland, J. B., Crawford, D. L., 1981. *Streptomyces setonii*: catabolism of vanillic acid via guaiacol and catechol. Canadian Jounal of Microbiology. 27**,** 636-638.

Ponnusamy, V. K., Nguyen, D. D., Dharmaraja, J., Shobana, S., Banu, R., Saratale, R. G., Chang, S. W., Kumar, G., 2018. A review on lignin structure, pretreatments, fermentation reactions and biorefinery potential. Bioresource technology. 271**,** 462-472.

Ragauskas, A. J., Beckham, G. T., Biddy, M. J., Chandra, R., Chen, F., Davis, M. F., Davison, B. H., Dixon, R. A., Gilna, P., Keller, M., Langan, P., Naskar, A. K., Saddler, J. N., Tschaplinski, T. J., Tuskan, G. A., Wyman, C. E., 2014. Lignin valorization: improving lignin processing in the biorefinery. Science. 344**,** 1246843.

Rahimi, A., Ulbrich, A., Coon, J. J., Stahl, S. S., 2014. Formic-acid-induced depolymerization of oxidized lignin to aromatics. Nature. 515**,** 249-52.

Ravindranath, V., McMenamin, M. G., Dees, J. H., Boyd, M. R., 1986. 2-Methylfuran toxicity in rats--role of metabolic activation in vivo. Toxicology and Applied Pharmacology. 85**,** 78-91.

Renders, T., Van den Bossche, G., Vangeel, T., Van Aelst, K., Sels, B., 2019. Reductive catalytic fractionation: state of the art of the lignin-first biorefinery. Curr. Opin. Biotechnol. 56**,** 193-201.

Rinaldi, R., Jastrzebski, R., Clough, M. T., Ralph, J., Kennema, M., Bruijnincx, P. C., Weckhuysen, B. M., 2016. Paving the Way for Lignin Valorisation: Recent Advances in Bioengineering, Biorefining and Catalysis. Angew Chem Int Ed Engl. 55**,** 8164-215.

Rinkel, J., Establishing a Comprehensive Toolboxfor Isotopic Labelling Studieson Terpene Synthases. Mathematisch-Naturwissenschaftlichen Fakultät der Rheinischen Friedrich-Wilhelms-Universität Bonn. Friedrich-Wilhelms-Universität Bonn, Bonn, 2019.

Rodriguez, A., Salvachúa, D., Katahira, R., Black, B. A., Cleveland, N. S., Reed, M. L., Smith, H., Baidoo, E. E. K., Keasling, J. D., Simmons, B. A., Beckham, G. T., Gladden, J. M., 2017. Base-Catalyzed Depolymerization of Solid Lignin-Rich Streams Enables Microbial Conversion. ACS Sustainable Chemistry & Engineering. 5**,** 8171-8180.

Rohles, C. M., Gießelmann, G., Kohlstedt, M., Wittmann, C., Becker, J., 2016. Systems metabolic engineering of Corynebacterium glutamicum for the production of the carbon-5 platform chemicals 5-aminovalerate and glutarate. Microb. Cell Fact. 15**,** 154.

Rorrer, A. S., 2016. An evaluation capacity building toolkit for principal investigators of undergraduate research experiences: A demonstration of transforming theory into practice. Evaluation and program planning. 55**,** 103-11.

Rosini, E., Molinari, F., Miani, D., Pollegioni, L., 2023. Lignin Valorization: Production of High Value-Added Compounds by Engineered Microorganisms. Catalysts. 13**,** 555.

Rothmel, R. K., Aldrich Tl Fau - Houghton, J. E., Houghton Je Fau - Coco, W. M., Coco Wm Fau - Ornston, L. N., Ornston Ln Fau - Chakrabarty, A. M., Chakrabarty, A. M., 1990. Nucleotide sequencing and characterization of Pseudomonas putida catR: a positive regulator of the catBC operon is a member of the LysR family.

Rueda, C., Calvo, P. A., Moncalián, G., Ruiz, G., Coz, A., 2015. Biorefinery options to valorize the spent liquor from sulfite pulping. Journal of Chemical Technology & Biotechnology. 90**,** 2218-2226.

Salvachua, D., Karp, E. M., Nimlos, C. T., Vardon, D. R., Beckham, G. T., 2015. Towards lignin consolidated bioprocessing: simultaneous lignin depolymerization and product generation by bacteria. Green Chemistry. 17**,** 4951-4967.

Salvachúa, D., Karp, E. M., Nimlos, C. T., Vardon, D. R., Beckham, G. T., 2015. Towards lignin consolidated bioprocessing: simultaneous lignin depolymerization and product generation by bacteria. Green Chem. 17**,** 4951-4967.

Sasaki, M., Goto, M., 2011. Thermal decomposition of guaiacol in sub-and supercritical water and its kinetic analysis. Journal of Material Cycles and Waste Management. 13**,** 68-79.

Schmiedl, D., Endisch, S., Pindel, E., Rückert, D., Reinhardt, S., Unkelbach, G., Schweppe, R., 2012. Base Catalyzed Degradation of Lignin for the Generation of oxy-Aromatic Compounds – Possibilities and Challenges. Erdöl Erdgas Kohle. 128**,** 357-363.

Schutyser, W., Renders, T., Van den Bosch, S., Koelewijn, S. F., Beckham, G. T., Sels, B. F., 2018. Chemicals from lignin: an interplay of lignocellulose fractionation, depolymerisation, and upgrading. Chem Soc Rev. 47**,** 852-908.

Shen, X., Meng, Q., Mei, Q., Liu, H., Yan, J., Song, J., Tan, D., Chen, B., Zhang, Z., Yang, G., Han, B., 2019. Selective catalytic transformation of lignin with guaiacol as the only liquid product. Chemical Science. 11**,** 1347 - 1352.

Shindo, H., Kuwatsuka, S., 1977. BEHAVIOR OF PHENOLIC SUBSTANCES IN THE DECAYING PROCESS OF PLANTS : VII. Characteristics of Phenolic Substances in the Humic Acids of Decayed Rice Straw and Compost-Supplied Field Soil. Soil Science and Plant Nutrition. 23**,** 333-340.

Shinoda, E., Takahashi, K., Abe, N., Kamimura, N., Sonoki, T., Masai, E., 2019. Isolation of a novel platform bacterium for lignin valorization and its application in glucose-free cis,cis-muconate production. J Ind Microbiol Biotechnol. 46**,** 1071-1080.

Shinoda, E., Takahashi, K., Abe, N., Kamimura, N., Sonoki, T., Masai, E. A.-O., Isolation of a novel platform bacterium for lignin valorization and its application in glucose-free cis,cis-muconate production.

Siegl, T., Luzhetskyy, A., 2012. *Actinomycetes* genome engineering approaches. Antonie Van Leeuwenhoek International Journal of General and Molecular Microbiology. 102**,** 503-516.

Silva, E. A. B. d., Zabkova, M., Araújo, J. D., Cateto, C. A., Barreiro, M. F., Belgacem, M. N., Rodrigues, A. E., 2009. An integrated process to produce vanillin and

lignin-based polyurethanes from Kraft lignin. Chemical Engineering Research and Design. 87, 1276-1292.
Sinner, P., Stiegler, M., Goldbeck, O., Seibold, G. M., Herwig, C., Kager, J., 2022. Online estimation of changing metabolic capacities in continuous Corynebacterium glutamicum cultivations growing on a complex sugar mixture. Biotechnol Bioeng. 119, 575-590.
Soni, S. K., Sharma, A., Soni, R., 2018. Cellulases: Role in Lignocellulosic Biomass Utilization. In: Lübeck, M., (Ed.), Cellulases: Methods and Protocols. Springer New York, New York, NY, pp. 3-23.
Sonoki, T., Takahashi, K., Sugita, H., Hatamura, M., Azuma, Y., Sato, T., Suzuki, S., Kamimura, N., Masai, E., 2018. Glucose-Free cis,cis-Muconic Acid Production via New Metabolic Designs Corresponding to the Heterogeneity of Lignin. ACS Sustainable Chemistry & Engineering. 6, 1256-1264.
Starck, S., Microbial production of cis,cis-muconic acid from hydrothermally converted lignocellulose. Naturwissenschaftlich-Technischen Fakultät

der Universität des Saarlandes. Saarland University, Saarbrücken, 2020.
Steinbüchel, H. P. S. A. A., 2002. Transformation of the Pseudonocardiaceae Amycolatopsis sp . strain HR167 is highly dependent on the physiological state of the cells. 454-460.
Subbotina, E., Rukkijakan, T., Marquez-Medina, M. D., Yu, X., Johnsson, M., Samec, J. S. M., 2021. Oxidative cleavage of C-C bonds in lignin. Nat Chem. 13, 1118-1125.
Sutherland, J. B., 1986. Demethylation of veratrole by cytochrome P-450 in *Streptomyces setonii*. Applied and Environmental Microbiology. 52, 98-100.
Sutherland, J. B., Crawford, D. L., Pometto, A. L., 1981a. Catabolism of substituted benzoic acids by streptomyces species. Applied and Environmental Microbiology. 41, 442-8.
Sutherland, J. B., Crawford, D. L., Pometto, A. L., 1981b. Catabolism of substituted benzoic acids by streptomyces species. Appl Environ Microbiol. 41, 442-8.
Sutherland, J. B., Crawford, D. L., Pometto, A. L. r., 1983. Metabolism of cinnamic, *p*-coumaric, and ferulic acids by *Streptomyces setonii.* Canadian Jounal of Microbiology. 29, 1253-1257.
Suzuki, Y., Otsuka, Y., Araki, T., Kamimura, N., Masai, E., Nakamura, M., Katayama, Y., 2021. Lignin valorization through efficient microbial production of β-ketoadipate from industrial black liquor. Bioresour. Technol. 337, 125489.
Tawfik, O. K., S., D., 2010. Enzyme Promiscuity: A Mechanistic and Evolutionary Perspective. Annual Review of Biochemistry. 79, 471-505.
Toledano, A., Serrano, L., Labidi, J., 2012. Organosolv lignin depolymerization with different base catalysts. Journal of Chemical Technology & Biotechnology. 87, 1593-1599.
Tuck, C. O., Pérez, E., Horváth, I. T., Sheldon, R. A., Poliakoff, M., 2012. Valorization of biomass: deriving more value from waste. Science. 337, 695-9.
Tumen-Velasquez, M., Johnson, C. W., Ahmed, A., Dominick, G., Fulk, E. M., Khanna, P., Lee, S. A., Schmidt, A. L., Linger, J. G., Eiteman, M. A., Beckham, G. T., Neidle, E. L., 2018. Accelerating pathway evolution by increasing the gene dosage of chromosomal segments. Proceedings of the National Academy of Sciences of the United States of America. 115, 7105-7110.
Van den Bosch, S., Koelewijn, S.-F., Renders, T., Van den Bossche, G., Vangeel, T., Schutyser, W., Sels, B., 2018. Catalytic strategies towards lignin-derived chemicals. Topics in Current Chemistry. 376, 129-168.

Van Duuren, J. B., Optimization of *Pseudomonas putida* KT2440 as host for the production of cis, cis-muconate from benzoate. Wageningen University, 2011.

van Duuren, J. B., Wijte, D., Karge, B., dos Santos, V. A., Yang, Y., Mars, A. E., Eggink, G., 2012. pH-stat fed-batch process to enhance the production of *cis, cis*-muconate from benzoate by *Pseudomonas putida* KT2440-JD1. Biotechnology Progress. 28**,** 85-92.

van Duuren, J. B., Wijte, D., Leprince, A., Karge, B., Puchalka, J., Wery, J., Dos Santos, V. A., Eggink, G., Mars, A. E., 2011. Generation of a catR deficient mutant of *P. putida* KT2440 that produces cis, cis-muconate from benzoate at high rate and yield. Journal of Biotechnology. 156**,** 163-72.

Vardon, D. R., Franden, M. A., Johnson, C. W., Karp, E. M., Guarnieri, M. T., Linger, J. G., Salm, M. J., Strathmann, T. J., Beckham, G. T., 2015. Adipic acid production from lignin. Energy & Environmental Science. 8**,** 617-628.

Vyas, P., Kumar, A., Singh, S., 2018a. Biomass breakdown: A review on pretreatment, instrumentations and methods. Front Biosci (Elite Ed). 10**,** 155-174.

Vyas, P., Kumar, A., Singh, S., 2018b. Biomass breakdown: a review on pretreatment, instrumentations and methods. Frontiers In Bioscience. 10**,** 155-174.

Waksman, S. A. L., H. A.;, 1953. Guide to the Classification and Identification of the Actinomycetes and Their Antibiotics. Williams & Wilkins, Baltimore.

Wang, H., Li, Z., Jia, R., Yin, J., Li, A., Xia, L., Yin, Y., Müller, R., Fu, J., Stewart, A. F., Zhang, Y., 2017. ExoCET: exonuclease in vitro assembly combined with RecET recombination for highly efficient direct DNA cloning from complex genomes. Nucleic Acids Research. 46**,** e28-e28.

Weiland, F., Barton, N., Kohlstedt, M., Becker, J., Wittmann, C., 2023. Systems metabolic engineering upgrades Corynebacterium glutamicum to high-efficiency cis, cis-muconic acid production from lignin-based aromatics. Metab. Eng. 75**,** 153-169.

Weiland, F., Kohlstedt, M., Wittmann, C., 2022. Guiding stars to the field of dreams: Metabolically engineered pathways and microbial platforms for a sustainable lignin-based industry. Metabolic Engineering. 71**,** 13-41.

Wittmann, C., 2007. Fluxome analysis using GC-MS. Microbial Cell Factories. 6**,** 6.

Xie, N. Z., Liang, H., Huang, R. B., Xu, P., 2014. Biotechnological production of muconic acid: current status and future prospects. Biotechnology advances. 32**,** 615-22.

Zakzeski, J., Bruijnincx, P. C., Jongerius, A. L., Weckhuysen, B. M., 2010. The catalytic valorization of lignin for the production of renewable chemicals. Chemical reviews. 110**,** 3552-3599.

Zhang, H., Li, Z., Pereira, B., Stephanopoulos, G., 2015. Engineering *E. coli–E. coli* cocultures for production of muconic acid from glycerol. Microbial Cell Factories. 14**,** 134.

Zhang, Y., Buchholz, F., 1998. A new logic for DNA engineering using recombination in Escherichia coli. Nature …. 20**,** 123-128.